

NT₅ Research Project

Assessing the impact of Network Exchanger (NEx) on power quality in distribution networks

Final Report



Final report

RACE for Networks

Project code: 24.NT5.R.o838

Research Theme NT5: Assessing the impact of Network Exchanger (NEx) on power quality in distribution networks

ISBN: 978-1-922746-78-8

October 2025

Citations

Razzaghi, R., Bahrani, B., Kumarawadu, A., Asbafkan, A., Blackburn, P. and Moreno, V. (2025). Assessing the impact of Network Exchanger (NEx) on power quality in distribution networks. Prepared for RACE for 2030

Project team

Monash University

- A/Prof Reza Razzaghi
- Prof Behrooz Bahrani
- Dr Ali Asbafkan
- Achala Kumarawadu

Third Equation Ltd

- Paul Blackburn
- Dr Veimar Moreno

Project partners





Acknowledgements

The authors would like to thank the stakeholders involved in the development of this report, in particular the industry reference group members who have given so generously of their time, including Ausnet Services, Energy Queensland and Essential Energy. Whilst their input is very much appreciated, any views expressed here are the responsibility of the authors alone.

Acknowledgement of Country

The authors of this report would like to respectfully acknowledge the Traditional Owners of the ancestral lands throughout Australia and their connection to land, sea and community. We recognise their continuing connection to the land, waters, and culture and pay our respects to them, their cultures and to their Elders past, present, and emerging.

What is RACE for 2030?

Reliable, Affordable Clean Energy for 2030 (RACE for 2030) is an innovative cooperative research centre for energy and carbon transition. We were funded with \$68.5 million of Commonwealth funds and commitments of \$280 million of cash and in-kind contributions from our partners. Our aim is to deliver \$3.8 billion of cumulative energy productivity benefits and 20 megatons of cumulative carbon emission savings by 2030. racefor2030.com.au

Disclaimer

The authors have used all due care and skill to ensure the material is accurate as at the date of this report. The authors do not accept any responsibility for any loss that may arise by anyone relying upon its contents.

Executive Summary

This report presents a comprehensive evaluation of the Network Exchanger (NEx)—an advanced solution developed by Third Equation Ltd—designed to enhance the hosting capacity of low-voltage (LV) distribution networks. NEx improves network performance through voltage regulation, current balancing, and power factor correction at the secondary side of distribution transformers. The project was structured into two primary workstreams: a simulation-based analysis and an experimental validation of NEx's performance. A high-fidelity distribution network model developed using the DIgSILENT PowerFactory simulation platform was utilised in the study, reflecting a representative suburban area in Queensland. The model captures both medium-voltage (11 kV) and low-voltage layers and includes detailed representations of distribution transformers, lines, customer loads, and consumer energy resources (CERs). Baseline calibration was achieved on the model using actual measurements from the network, ensuring the model's realism and accuracy. The study incorporated projected photovoltaic (PV) and electric vehicle (EV) penetration scenarios based on the Australian Energy Market Operator's (AEMO) Integrated System Plan (ISP) 2024 and EV projections released by CSIRO, from 2025 to 2050 under both the Progressive Change and Step Change pathways, to create future versions of the network model. PV systems were modelled with Volt-Var and Volt-Watt control functionalities in line with AS 4777.2:2020, following current compliance standards. No export limitations were imposed on future PV systems to reflect best-case hosting potential.

Network performance was assessed using performance indicators including voltage profiles, PV curtailment levels, thermal loading of network assets, and voltage imbalance. The study primarily focused on the noon period in spring to evaluate the highest impact from PVs (worst case scenario from network hosting capacity perspective). Results demonstrate that increasing CER uptake intensifies operational constraints on LV networks, with PVs significantly contributing to voltage violations. By 2050, under the Step Change scenario, up to 23.4% of LV buses experienced voltage violations at noon in spring within the modelled network. The study also highlights an emerging fairness issue that DNSPs will face under AS:4777.2:2020, as unequal curtailment among prosumers becomes more prevalent due to locational disparities.

In terms of total energy curtailed through Volt-Watt and Volt-Var control, 0.551 MWh and 1.96 MWh were curtailed during the spring noon half-hour period in 2050 under the Progressive Change and Step Change scenarios, respectively. These curtailments equated to 2.1% and 4.39% of the total PV energy produced during that interval. To accommodate the anticipated CER growth, transformer upgrades will be necessary. Approximately 29% and 68% of transformers in the network exceeded 100% loading by noon in spring under the Progressive Change and Step Change scenarios, respectively, necessitating upgrades to avoid insulation failures. Similarly, around 5.8% of both LV and MV cables surpassed their rated ampacity by 2050 under the Step Change scenario.

The impact of EVs on voltage levels was comparatively less significant than that of PVs, with only 1.07% of LV nodes experiencing undervoltage conditions during the evening peak in summer in 2050. This reduced impact is attributed to the diversified charging profiles of EVs, which moderate grid imports. However, transformer loading during this period remains a concern, with 23.14% of transformers exceeding their rated capacity. Cable overloading was minimal, with just 0.16% of LV and 0.4% of MV cables breaching ampacity limits in 2050 under maximum EV penetration.

The year 2035 was selected to evaluate the performance of various technologies on network hosting capacity, as voltage violations reached 13.36% and 5.6% under the Step Change and Progressive Change scenarios, respectively, at noon in spring. Six LV areas were chosen based on the severity of voltage violations, curtailment

levels, and network scale—areas where DNSPs are most likely to require technical interventions. Advanced technologies including STATCOMs, OLTCs, and NEx were modelled and implemented for comparative evaluation. Two STATCOM configurations were analysed: a single STATCOM rated at 50 kVA installed at the point of highest curtailment in each LV area, and a multiple-STATCOM scenario with devices distributed at the ends of LV circuits based on circuit configuration. Both OLTC and NEx implementations involved QDSL-based steady-state models developed in DIgSILENT PowerFactory, integrated at the distribution transformer level.

Among the technologies, a single STATCOM yielded the least improvement, reducing total voltage violations across the six LV areas from 62.9% to only 53.4% at noon in spring. Its performance was limited in networks with multiple circuits. In contrast, the multiple-STATCOM configuration performed better, lowering voltage violations to 23.8%. OLTC and NEx demonstrated the most effective performance, reducing violations to 7.13% and 0%, respectively. However, the OLTC's uniform phase regulation resulted in suboptimal performance in unbalanced LV networks, with some areas experiencing under-voltages. NEx overcame this limitation due to its independent per-phase voltage control, which allowed it to resolve phase-specific issues and deliver consistent performance even in complex network topologies. Because both OLTC and NEx regulate voltage at the start of LV circuits, they offered broader network-wide voltage improvements. However, in the case of NEx, careful selection of the target voltage is required to ensure downstream compliance, given its point of operation at the distribution transformer. NEx also demonstrated its ability in mitigating under-voltages during periods of high EV charging demand, particularly during the evening peak.

Considerable transformer loading reductions were observed with the integration of NEx. While the study did not include proactive transformer upgrades, which might eventually be necessary regardless of the selected technology, NEx still managed to alleviate loading stress. This reduction can be attributed to three key functions of NEx. First, its current balancing feature ensures equal current draw or injection across all phases, thereby lowering loading on any disproportionately burdened phase. Second, improvements in network voltage profiles reduce the reactive power demand from PV inverters, lowering overall current magnitude. Finally, the power factor correction function of NEx maintains unity power factor at the transformer terminals by supplying required reactive power, further reducing current flows. Together, these functionalities significantly decreased transformer loading in the studied LV areas.

A cost-benefit analysis using the CECV metric for 2035 confirmed that NEx provided the highest annual benefit, closely followed by OLTC. It is important to note, however, that the CECV captures only one dimension of economic value. Additional benefits such as avoidance of penalties, reduced customer complaints, and extended asset life were not included, but would likely enhance the economic case for these technologies, particularly for NEx.

A comprehensive suite of experimental tests was undertaken under workstream 2 to validate the performance of the NEx system under diverse operating conditions, including phase unbalance, reactive loading, voltage disturbances, and weak grid scenarios. These tests aimed to empirically evaluate the core functionalities of NEx—phase balancing, power factor correction, and voltage regulation—both independently and in combination. The phase balancing function demonstrated its capability to redistribute unbalanced single-phase, and three-phase loads effectively, resulting in balanced grid-side currents without altering load-side conditions. The power factor correction feature successfully compensated for reactive power demands, achieving unity power factor at the grid side under inductive load conditions. Voltage regulation functionality was able to maintain load-side voltages at predefined setpoints, even in the presence of significant grid-side disturbances, including voltage sags and swells.

Moreover, the NEx system maintained stable performance during regenerative loading and under conditions involving unbalanced and weak grids. When all core functionalities were simultaneously enabled in the most adverse scenarios, the system continued to operate reliably—balancing currents, correcting the power factor, and regulating load-side voltage without compromising stability. These results confirm that the NEx system offers improvements in power quality, load symmetry, and voltage stability within low-voltage distribution networks. Its robust functionality is particularly advantageous in modern grid environments characterised by high penetrations of distributed renewable generation, unbalanced loads, and reduced grid strength.

Contents

EXE	CUTIVE SUMMARY	3
LIST	OF ACRONYMS	8
1	INTRODUCTION	10
1.1	Background	11
1.2	Project Objectives and Overview	12
2	DISTRIBUTION NETWORK MODEL AND DATA	14
2.1	Zone Substation Line Drop Compensator	
2.2	Inverter Volt-Watt and Volt-Var control	16
2.3	Compliance to AS:4777.2:2020	18
2.4	Seasonal Data and Model Baselining	19
2.5	Assessment Metrics	19
3	NETWORK EXCHANGER (NEX)	23
3.1	Development of NEx Simulation Model	24
4	BASELINED NETWORK MODEL CONDITION	26
5	DEVELOPMENT OF CER PROJECTIONS	28
5.1	Future PV Characteristics	30
5.2	EV Charging Characteristics	30
6	SIMULATION RESULTS	32
6.1	Voltage and Curtailment	32
6.2	Utilization Levels of Transformers and distribution lines	40
6.3	Selection of LV areas for investigating solutions	43
6.4	STATCOM Model	44
6.5	OLTC Model	45
6.6	Comparison of Technologies	46
7	COST-BENEFIT ANALYSIS	53
8	PERFORMANCE EVALUATION OF NEX UNDER HYPOTHETICAL NETWORK SCENARIOS	55
8.1	Resolving undervoltage violations	55
8.2	Impact of line R/X ratios	55
8.3	Power distribution among phases	56
9	OPERATIONAL TESTING AND PERFORMANCE EVALUATION OF THE NEX SYSTEM IN THE O-	-30
κVA	N POWER RANGE	57
9.1	Description of test setup	57
9.2	Test scenarios and methodology	_
9.3	Phase Balancing Test (PB)	_
9.4	Power Factor Correction Test (PFC)	
9.5	Voltage Regulation Test (VR)	_
9.6	Multi-Function Tests	66

9.7	NEx Operation Tests under Weak Grid Condition	68
10	CONCLUSION	69
REF	ERENCES	71
APP	PENDIX A – NEX QDSL MODELS	72
APP	PENDIX B – Transformer current and power factor data	73

List of Acronyms

ABS - Australian Bureau of Statistics

AEMO - Australian Energy Market Operator

AER - Australian Energy Regulator

AEMC - Australian Energy Market Commission

AVC - Automatic Voltage Control

BAU - Business as Usual

BESS - Battery Energy Storage System

CECV - Customer Export Curtailment Value

CER - Consumer Energy Resource

CSIRO - Commonwealth Scientific and Industrial Research Organisation

DNSP - Distribution Network Service Provider

DOE - Dynamic Operating Envelope

dSTATCOM - Distribution Static Synchronous Compensator

EMT - Electromagnetic Transient

EV - Electric Vehicle

FMI - Functional Mock-up Interface

FMU – Functional Mock-up Unit

ICE - internal combustion engine

IEEE - Institute of electrical and electronic engineers

ISP – Integrated System Plan

LDC - Line Drop Compensator

LV - Low-voltage

LVUR - Line Voltage Unbalance Rate

NEx – Third Equation's Network Exchanger

NEMA - National Electrical Manufacturers Association

OLTC - On-Load Tap Changer

PC - Parallel Converter

PCC - Point of Common Coupling

PEARL - Power Engineering Advanced Research Laboratory

PV – Photovoltaic

PVUR – Phase Voltage Unbalance Rate

PVUF – Phase Voltage Unbalance Factor

QDSL - Quasi Dynamic Simulation Language

RMS - Root Mean Square

STATCOM - Static Synchronous compensator

SC – Series Converter

SAPN – South Australia Power Networks

SCADA - Supervisory Control and Data Acquisition

VPN/UN – Victoria Power Networks/United Energy

VUF – Voltage Unbalance Factor

1 Introduction

In recent years, the structure of low and medium-voltage distribution networks has been fundamentally reshaped by the accelerated integration of Consumer Energy Resources (CERs), particularly rooftop photovoltaic (PV) systems and battery electric vehicles (EVs). This transition has been driven by the substantial decline in the cost of CER technologies, coupled with strong national and global policy momentum aimed at achieving long-term emissions reduction and sustainability goals. In the Australian context, this transformation is especially pronounced. According to the Australian Energy Market Operator's (AEMO) 2024 Integrated System Plan (ISP), under the Step Change scenario, the installed capacity of distributed rooftop solar PV is projected to grow significantly from 21 GW in 2024 to approximately 86 GW by 2050. Simultaneously, battery electric vehicles are expected to comprise 97% of the nation's vehicle stock by mid-century, marking a profound shift in both energy consumption and grid interaction patterns.

The growing prevalence of CERs is rapidly decentralizing generation and reshaping load dynamics, introducing bi-directional power flows that diverge from traditional distribution network design assumptions. Historically, these networks operated under the principle of unidirectional energy flow—from large-scale generation through transmission to end users. However, customer-generated power now regularly flows upstream, creating new and complex operating conditions for Distribution Network Service Providers (DNSPs). These conditions are giving rise to several technical challenges, including voltage rise due to surplus PV generation during low demand periods, voltage drop associated with concentrated EV charging during evening peaks, thermal overloading of conductors and transformers, and increased phase imbalance at the low-voltage level. Indeed, DNSPs are already encountering voltage regulation issues, with frequent breaches of statutory voltage limits driven by excess rooftop PV injection—scenarios that are expected to become more severe as CER penetration continues to rise.

The simultaneous growth of rooftop PV and EVs introduces competing pressures on the network: overvoltage during the day and undervoltage during the evening peak, particularly in residential areas with high CER uptake. These trends highlight an urgent need to identify and implement effective technologies and operational strategies that will increase the hosting capacity of distribution networks—their ability to accommodate high CER penetration without violating operational limits. Enhancing hosting capacity is essential not only to prevent adverse power quality outcomes but also to ensure customers can fully utilize their CER investments. As such, this report seeks to investigate the technical implications of high CER penetration on distribution networks and evaluate emerging technologies and solutions that can mitigate these challenges under future network conditions. This will support the broader objective of enabling a reliable, flexible, and decarbonized energy system in Australia.

1.1 Background

To address the emerging challenges associated with high CER penetration and to improve hosting capacity in distribution networks, utilities are increasingly adopting a suite of advanced grid support technologies. Among these are Distribution Static Compensators (DSTATCOMs), which provide real-time voltage regulation through reactive power exchange; static export limits; Dynamic Operating Envelopes (DOEs), which offer time-varying import/export limits tailored to local network conditions; On-Load Tap Changers (OLTCs), which enable dynamic voltage adjustments at transformers; and community-scale battery energy storage systems that absorb excess solar generation and shift load to enhance system reliability and flexibility.

Regulatory measures have also evolved in response to the changing network dynamics. In Australia, compliance with AS 4777.2:2020 is now mandatory for all new rooftop PV systems. This standard requires inverters to support autonomous grid-support functions such as Volt-Var and Volt-Watt control. While these functions are effective in mitigating overvoltage conditions, they often lead to curtailment of PV generation based on the inverter's local voltage readings. This not only results in financial losses for PV owners but also raises concerns about fairness in curtailment distribution. Due to the radial nature of LV networks, PV systems located at the end of feeders are typically more exposed to higher voltages and thus experience greater levels of curtailment.

Dynamic operating envelopes have emerged as a promising solution to this fairness issue. By dynamically adjusting export and import limits based on real-time network capacity and optimizing for equity among CER participants, DOEs can help ensure a more just distribution of curtailment. Several recent trials (e.g., [1]) have demonstrated the potential of DOEs to manage CER exports more equitably, leading to regulatory changes that now require all new PV systems in Victoria to be capable of responding to dynamic export signals.

Another technology under active trial is the deployment of DSTATCOMs in voltage-constrained areas. These devices regulate the voltage at the point of common coupling by injecting or absorbing reactive power as needed. DNSPs such as Ausgrid have initiated pilot projects involving DSTATCOMs, with preliminary results showing improved voltage compliance and increased CER hosting capacity. Similarly, the use of OLTCs at distribution transformers is being explored to address both undervoltage and overvoltage scenarios. Trials conducted by United Energy suggest that deploying OLTCs at the distribution level is only economically viable in areas experiencing a combination of both voltage issues. At present, OLTCs are more commonly installed at zone substations, where the transformer's tap settings are adjusted based on broader network power flow conditions.

In this context, the present project focuses on evaluating the effectiveness of a novel technology called NEx, which is designed to enhance hosting capacity in low-voltage networks. The current iteration of the NEx device includes three core operational functions: voltage regulation at the head of the LV circuit, current balancing at the distribution transformer, and power factor correction. The aim of the project was to assess NEx's ability to mitigate network issues associated with increasing CER penetration and to experimentally validate its operational performance.

This was achieved through a twofold approach. First, a series of simulations were conducted using a high-fidelity model of a Brisbane suburb developed in DIgSILENT PowerFactory. Future network scenarios from 2025 to 2050 were constructed in alignment with CER uptake projections from AEMO's ISP, and several LV areas exhibiting voltage violations and curtailment under these scenarios were selected for targeted analysis. Second, laboratory testing was carried out at the Power Engineering Advanced Research Laboratory (PEARL) at Monash University to experimentally validate NEx's functionality under a variety of operating conditions. This combination of

11

modelling and empirical testing provides a comprehensive basis for assessing the viability of NEx as a scalable solution for enhancing CER hosting capacity in LV distribution networks.

1.2 Project Objectives and Overview

The primary objective of this study was to evaluate the effectiveness of the NEx system in increasing CER hosting capacity in low-voltage distribution networks. To achieve this, the project was structured into two main workstreams:

- Workstream o1 focused on power system modelling and hosting capacity analysis.
- Workstream 02 was dedicated to the experimental validation of NEx's operational functionality.

Workstream o1 was further divided into four key stages, as illustrated in Figure 1:

- 1. Development of a high-fidelity distribution network model.
- 2. Creation of a steady-state model of the NEx system.
- 3. Integration of CER uptake projections based on the Australian Energy Market Operator's 2024 Integrated System Plan.
- 4. Evaluation of NEx performance under future projected network conditions.

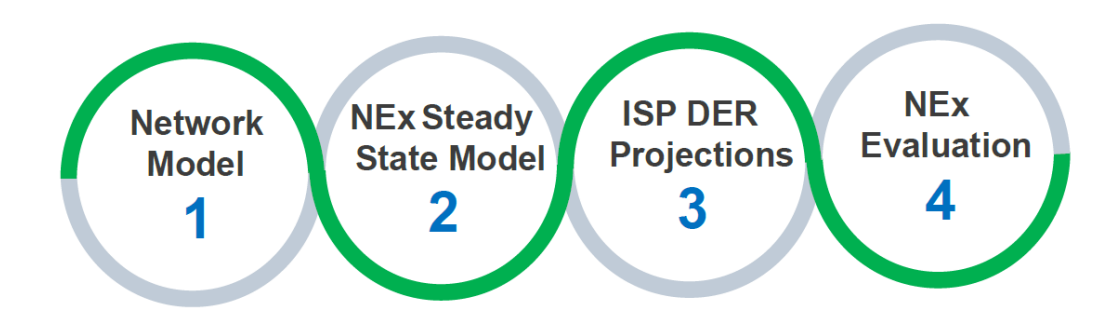


Figure 1. Project plan for workstream 01.

To facilitate a realistic and scalable analysis, a suburban distribution network located in Brisbane, Queensland, was selected as the case study. This detailed network model was developed using DIgSILENT PowerFactory as part of the *Investigation into Voltage Management Technologies for Future Australian Suburban Distribution Networks* project [2]. The model was baselined to current operating conditions using available Supervisory Control and Data Acquisition (SCADA) measurements and incorporates seasonal variations in both load demand and rooftop PV generation.

In Stage 2, a steady-state implementation of the NEx system was developed to enable its integration within the PowerFactory environment. The original NEx model, developed in MATLAB Simulink, operated dynamically based on instantaneous input signals to drive its control functions. For the purposes of this project, the control logic was restructured and implemented in PowerFactory using Quasi-Dynamic Simulation Language (QDSL), allowing the model to operate in steady-state simulations through the formulation of algebraic control equations.

Stage 3 involved the incorporation of projected CER growth into the baselined network model. These projections, based on AEMO's ISP scenarios, focused on the impact of increasing rooftop PV and EV adoption on LV network performance. Using this augmented future network model, the effectiveness of NEx was evaluated under high CER penetration scenarios.

As part of the final evaluation phase, the performance of NEx was benchmarked against existing voltage management technologies including On-Load Tap Changers and STATCOMs. A cost-benefit analysis was also conducted by calculating the Customer Export Curtailment Value (CECV) for each technology. This analysis enabled the assessment of each solution's economic viability in the context of improving hosting capacity while minimizing financial impacts to CER owners through curtailment.

In summary, the key objectives of this study were:

- To investigate the impact of projected CER growth, particularly rooftop PV and EV penetration, on a high-fidelity distribution network model of a Brisbane suburb.
- To evaluate the effectiveness of NEx in increasing CER hosting capacity, with a focus on reducing curtailment, mitigating voltage violations and phase imbalances.
- To benchmark NEx against state-of-the-art voltage management technologies, including OLTCs and STATCOMs, under future network scenarios.
- To conduct a cost-benefit analysis by comparing CECVs for NEx and alternative technologies.
- To validate the performance of NEx through controlled laboratory testing across a range of grid conditions, ensuring the system performs as intended under realistic operating scenarios.

2 Distribution Network Model and Data

The distribution network model selected for this study was sourced from [2]. This section provides a summary of the key network characteristics and data used in the development of the model. For a more detailed description of the modelling process and network parameters, readers are referred to [2], which documents the extended development and validation methodology.

To ensure confidentiality and compliance with data protection requirements, a de-identified version of the network model was used in this project. Sensitive information, such as customer connection points and geospatial locations was removed. Additionally, minor modifications were made to the original model to improve the convergence of power flow simulations. These adjustments were necessary due to several instances of non-convergence encountered during the scaling of the network model, as reported in [2].

Figure 2 shows the topological overview of the suburb which was investigated in this study. The model contains a zone substation equipped with Line Drop Compensator (LDC) algorithms, which supplies the network through ten MV feeders. The modelled network supplies a total of 13,535 residential customers spread across 229 LV areas, as well as 785 commercial and light industrial customers. The current network model consists of 5,338 PV systems, with a total capacity of approximately 27 MW.



Figure 2. Modelled distribution network.

2.1 Zone Substation Line Drop Compensator

The primary function of the Line Drop Compensator (LDC) is to regulate voltage levels at the extremities of distribution feeders, rather than merely maintaining voltage at the substation bus. This function is particularly critical in radial distribution networks, where voltage tends to decrease with increasing distance from the substation due to the cumulative effects of line impedance and varying load profiles. The LDC mitigates this issue by dynamically adjusting the tap position of the associated power transformer, thereby modulating the substation output voltage in response to fluctuations in downstream active and reactive power flows.

In the network model used for this study, the zone substation is equipped with LDC algorithms, which are implemented as piecewise linear power-voltage characteristic curves that govern the operation of the OLTCs on the three power transformers. For simplification, these LDC algorithms are represented using an aggregate power-voltage characteristic that captures the combined behaviour of all three transformers. Based on the operational characteristics of the OLTCs and their accessible tap positions, three discrete voltage levels are defined: 10.8625 kV, 11 kV, and 11.1375 kV. The midpoints between these voltage levels, 10.93125 kV and 11.06875 kV, correspond to aggregate active power flow thresholds of 14,968.2 kW and 30,643.2 kW, respectively.

Accordingly, when the total active power flow into the substation is below 14,968.2 kW, the OLTC is set to its lowest tap position, resulting in a voltage setpoint of 0.9875 per unit. If the power flow lies between 14,968.2 kW and 30,643.2 kW, the OLTCs maintain a nominal voltage setpoint of 1.0 per unit. When the active power flow exceeds 30,643.2 kW, the highest tap position is selected, setting the voltage at 1.0125 per unit. In the simulation environment, this control behaviour is implemented by directly modifying the voltage setpoint of the source element feeding the substation. This approach effectively replicates the intended function of the LDC system. Figure 3 illustrates the change in voltage at the substation as per the active power flow from the substation.

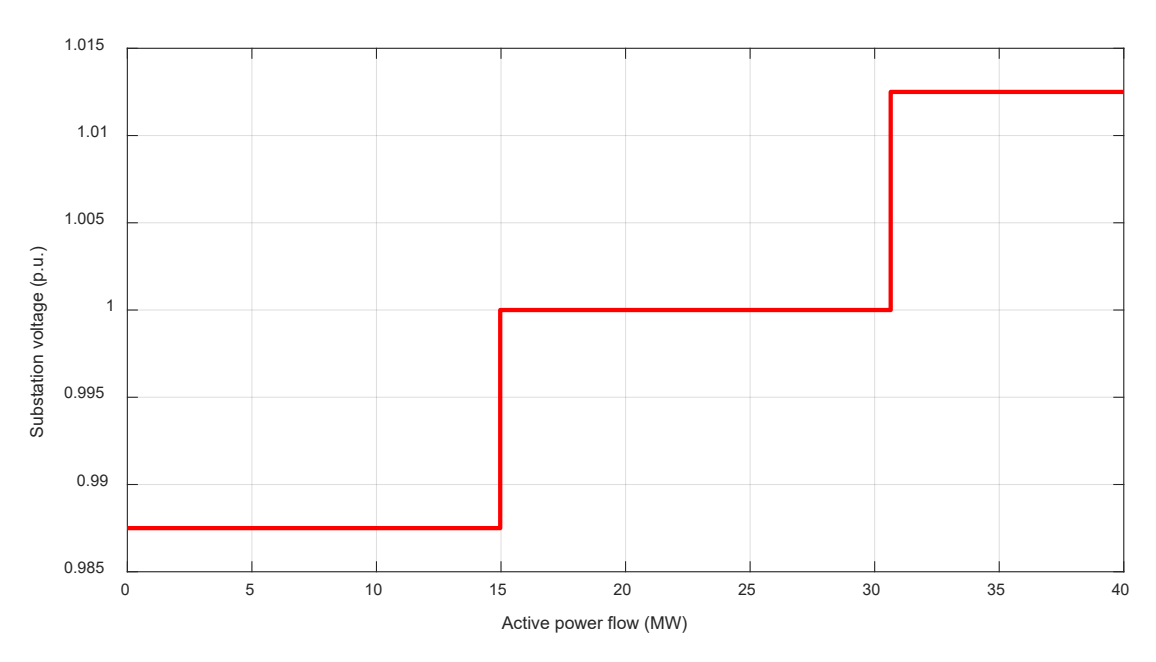


Figure 3. Modelled LDC algorithm at the zone substation in the study using three discrete voltage levels.

2.2 Inverter Volt-Watt and Volt-Var control

In accordance with AS 4777.2, all photovoltaic (PV) inverters installed in Australia are required to support and operate with both Volt-Watt and Volt-Var control functionalities. The Volt-Watt control mode specifically mandates that inverters reduce their active power output in response to rising voltage levels at their point of connection. This function is designed to mitigate overvoltage conditions in low-voltage distribution networks by dynamically curtailing inverter output as a function of the locally measured terminal voltage. The relationship between active power output and terminal voltage is defined by a piecewise characteristic curve, with specific voltage setpoints and corresponding power reduction thresholds. This control behaviour is illustrated in Figure 4, and the associated voltage and power setpoints are summarised in Table 1. Active power curtailment is commenced when the terminal voltage exceeds 253 V, reaching 20% of active power output when the voltage reaches 260 V.

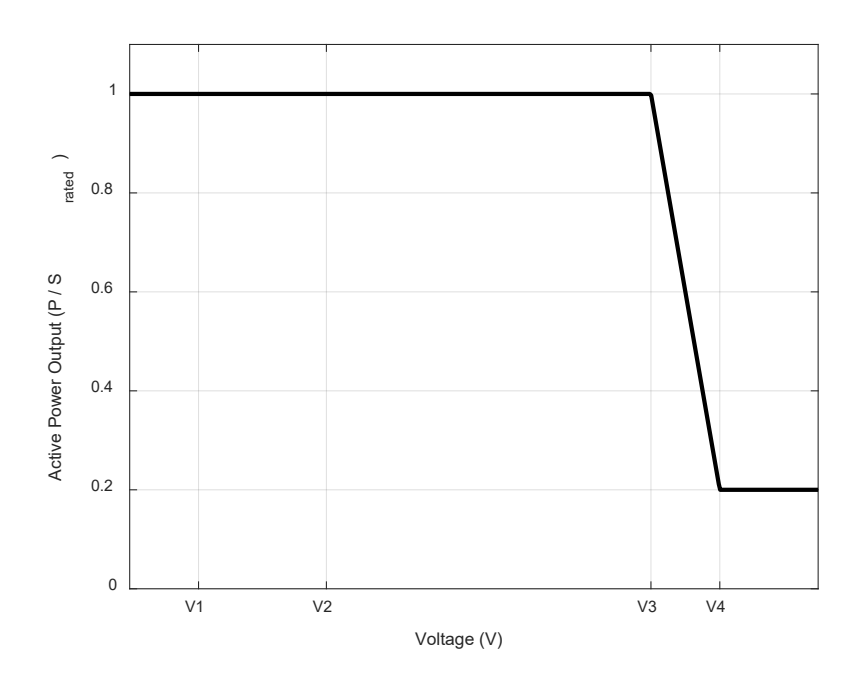


Figure 4. Required Volt-Watt response as per AS:4777.2:2020.

Table 1. Volt-Watt voltage setpoints as per AS.4777.2:2020.

V1 (V)	V2 (V)	V3 (V)	V4 (V)
207	230	253	260

Similarly, the Volt-Var control mode is implemented to support voltage regulation in distribution networks through the exchange of reactive power. This control strategy allows inverters to inject or absorb reactive power based on the locally measured terminal voltage, following a predefined piecewise-linear characteristic curve. When the voltage at the inverter's terminals falls below a lower threshold, the inverter injects reactive power (i.e., operates in capacitive mode) to raise the local voltage. Conversely, when the voltage exceeds an upper threshold, the inverter absorbs reactive power (i.e., operates in inductive mode) to reduce the local voltage. The mandated Volt-Var control settings, as specified in AS 4777.2:2020, are illustrated in Figure 5, with the corresponding voltage setpoints detailed in Table 2.

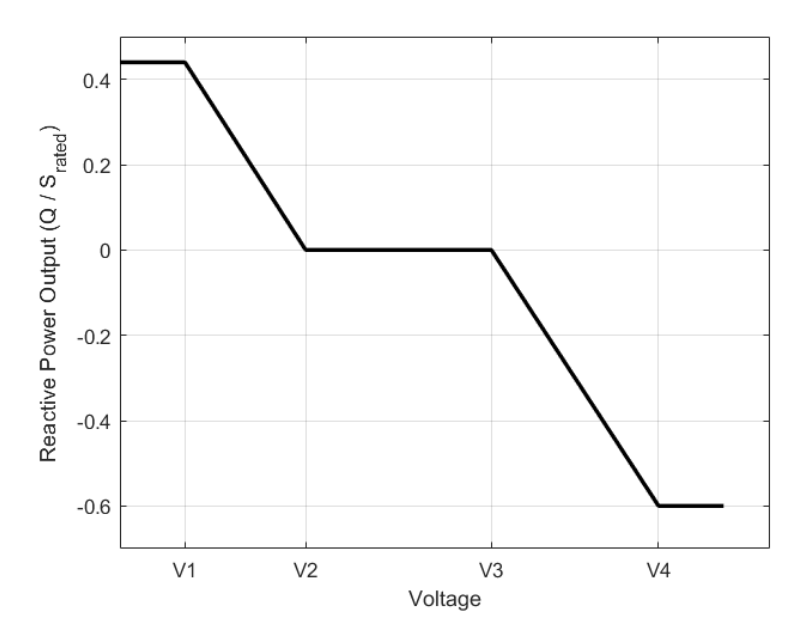


Figure 5. Required Volt-Var response as per AS:4777.2:2020.

Table 2. Volt-var voltage setpoints as per AS:4777.2:2020

V1 (V)	V2 (V)	V3 (V)	V4 (V)
207	220	240	258

It is important to note that direct implementation of Volt-Watt and Volt-Var inverter control modes for PV systems is not natively supported in DlgSILENT PowerFactory. To address this limitation, PowerFactory provides the capability to develop user-defined load flow and quasi-dynamic models, referred to throughout this report as QDSL models. These models enable the customization of steady-state behaviour for various power system components by allowing user-defined control logic to be implemented within the *load-flow control* tab. Through this approach, control schemes that are not available in the standard model library—such as voltage-dependent active and reactive power control for inverters—can be effectively emulated. Specifically, QDSL scripting allows for the modification of power output from PV units by iteratively adjusting their active and reactive power setpoints in response to local voltage measurements, until load flow convergence is achieved.

In this study, QDSL models were developed for PV systems equipped with Volt-Watt and Volt-Var functionality, enabling realistic representation of inverter behaviour under varying voltage conditions within steady-state simulations. Furthermore, the apparent power capacity of the inverter is explicitly considered in the QDSL models, ensuring that the combined active and reactive power output does not exceed the inverter's rated capacity during the implementation of Volt-Watt and Volt-Var control strategies. It is also important to note that Volt-Var has priority over Volt-Watt in the developed framework.

2.3 Compliance to AS:4777.2:2020

Although compliance with AS 4777.2:2020 is mandatory for all new PV installations in Australia, instances of non-compliant inverters remain common. The AEMO report titled "Compliance of Distributed Energy Resources with Technical Settings: Update" provides a detailed analysis based on recent compliance surveys. While compliance rates have improved in recent years, this progress has been largely driven by targeted actions from both Original Equipment Manufacturers (OEMs) and DNSPs.

OEMs have taken several steps to improve adherence to the standard, including the removal of legacy grid codes, deployment of remote firmware updates, and the provision of training programs for installers. These initiatives have contributed to increased alignment with AS 4777.2:2020 settings across newly deployed inverters.

Figure 6 presents a comparison between reported compliance rates from various OEMs and the actual compliance levels observed through smart meter data analysis conducted by Victoria Power Networks/United Energy (VPN/UE) and South Australia Power Networks (SAPN) for Volt-Var support functionality. The figure clearly highlights a discrepancy between reported and observed compliance, with several OEMs indicating higher self-reported compliance than what is reflected in field data.

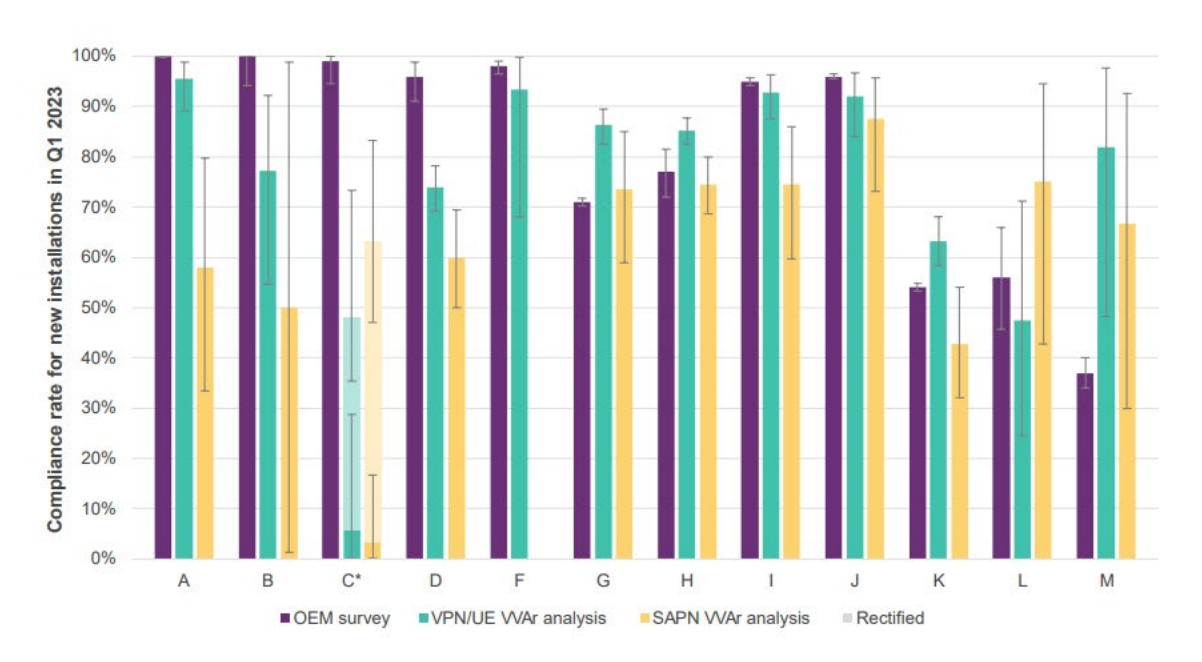


Figure 6. Comparison of compliance rates as per OEM data against Volt-Var assessment from smart meter data [3].

AEMO continues to recommend a compliance target of at least 90% for new inverters with respect to the AS 4777.2:2020 standard, recognising its importance in increasing CER hosting capacity and reducing system security risks [3].

In this study, the impact of non-compliant inverters has also been taken into account. The initial network model reflects a range of inverter behaviours based on the commissioning year of PV systems and the relevant standards at the time:

- PV systems commissioned after 2021 are assumed to include both Volt-Watt and Volt-Var functionalities, in line with AS 4777.2:2020.
- PV systems commissioned between 2017 and 2020 are equipped with Volt-Watt functionality only.
- PV systems commissioned before 2016 are modelled without either Volt-Watt or Volt-Var control features.

• Export limits are applied only to PV installations for which an export limit value is explicitly recorded.

To account for non-compliance, it is assumed that 20% of existing PV systems in the baselined model—despite being equipped with inverter control—are non-compliant, meaning they do not provide Volt-Watt or Volt-Var support in the future versions of the model. Furthermore, 10% of all new PV installations are assumed to be non-compliant under both the Progressive Change and Step Change scenarios. This modelling approach allows the study to assess how partial compliance may influence network performance, particularly in terms of hosting capacity and voltage regulation.

2.4 Seasonal Data and Model Baselining

To capture seasonal variations in load and generation, four separate versions of the network model have been developed—one for each season—based on representative daily load and generation profiles. Each seasonal model was baselined using transformer monitor data and SCADA measurements provided by Energy Queensland, ensuring a high degree of accuracy. Of the 259 distribution transformers in the modelled network, 159 were instrumented with monitors that recorded phase-to-ground voltages, phase currents, total harmonic distortion (THD), and power factor. Additionally, SCADA data from the 11 kV feeders—including line-to-line voltages and phase currents—were used to derive transformer-level load and generation profiles. This ensured alignment between the aggregated transformer power flows and the measured feeder-level power flows. For each season, two sets of load profiles were developed: one representing high solar generation conditions and the other reflecting low-solar periods. Figure 7 illustrates the active power flow of a representative 11 kV feeder under high solar conditions in summer after the baselining process.

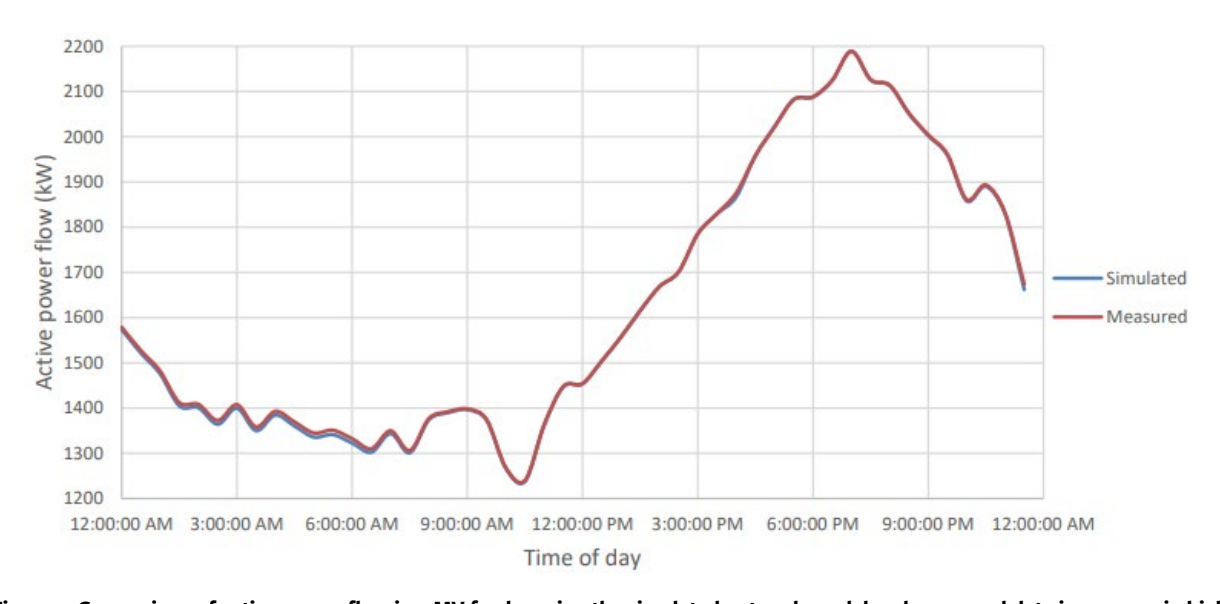


Figure 7. Comparison of active power flow in a MV feeder using the simulated network model and measured data in summer in high solar conditions [2]

2.5 Assessment Metrics

The term CER hosting capacity is widely used in distribution network studies to describe the maximum amount of CER that can be integrated into the network without violating operational or physical limits. With the increasing penetration of CERs over recent years, DNSPs are increasingly encountering breaches of these limits, prompting a range of responses. One of the initial measures involved imposing fixed export constraints for new PV systems in areas approaching their hosting capacity limits. For instance, DNSPs such as SAPN in South

Australia and CitiPower, Jemena, AusNet, United Energy in Victoria have implemented export limits of ranging from 1.5-5 kW for new PV installations. These limits, however, are often overly conservative and can discourage customers from investing in PV systems due to prolonged payback periods. In response, DNSPs such as SAPN and AusNet have begun offering customers a choice between fixed export limits and flexible export (aka DOE), which adapt export capacities based on network conditions such as demand and network loading. Furthermore, DNSPs are trialling additional technologies, including STATCOMs and community batteries, to alleviate network constraints and enhance hosting capacity.

The primary constraints that define hosting capacity include voltage limits, transformer and line loading, and increasingly, voltage unbalance—exacerbated by phase asymmetries in both load and generation.

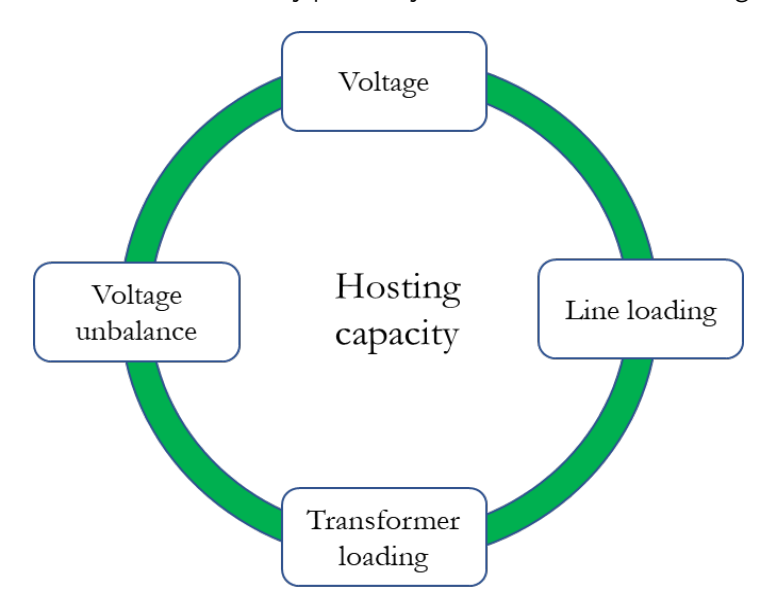


Figure 8. Metrics for determining hosting capacity in a distribution network.

To evaluate the impact of CERs on the network and to evaluate hosting capacity improving technologies 4 key metrics are considered, which are:

- Voltage compliance (magnitude)
- Asset overload
- Voltage unbalance
- PV Curtailment

Voltage Compliance

There are two standards for steady-state voltage magnitudes at customer connection points that are relevant to electricity supply networks in Australia: AS 60038 and AS 61000.3.100. The current version of AS 60038 defines an allowable voltage range of $\pm 10\%$ from the nominal voltage of 230 V at the point of supply. In contrast, the current version of AS 61000.3.100, which has yet to be updated to align with AS 60038, specifies a fixed upper voltage limit of 253 V and a lower voltage limit of 216 V.

For this study, the acceptable line-neutral voltage range is defined as 216 V to 253 V. Voltage compliance is assessed at each node within the LV areas, enabling a detailed evaluation of the network's performance in response to any new customer connections or upgrades from single-phase to three-phase supply during the evaluation period.

Asset Overload

Transformers and cables within the distribution network are also required to operate within their rated loading capacities. In this study, the loading levels of these assets are assessed in DIgSILENT PowerFactory using the following methodology:

• Loading level of transformers: The nominal current (I_{nom}) for each phase on both the primary and secondary sides of the transformer is calculated using:

$$I_{nom} = \left(\frac{S_{rated}}{\sqrt{3} \times V_{nom}}\right)$$

where S_{rated} is the rated transformer capacity in kVA, and V_{nom} is the nominal voltage at the respective side of the transformer in kV. The transformer loading level is then determined as the ratio of the maximum measured phase current to the calculated nominal current.

Loading (%) =
$$\left(\frac{\max(I_a, I_b, I_c)}{I_{nom}}\right)$$

• Loading level of conductors: The conductor loading level is calculated as the ratio of the actual current flowing through the conductor to its rated ampacity. This provides a direct measure of how close the conductor operates to its thermal limit.

Voltage Unbalance

Voltage unbalance in a power system typically arises from unequal loading across phases, unbalanced integration of CERs or asymmetrical network configurations. It can result in increased system losses, overheating of three-phase equipment such as motors and transformers, and a general decline in operational efficiency. Several definitions exist in the literature for quantifying voltage unbalance. These include the Line Voltage Unbalance Rate (LVUR), defined by the National Electrical Manufacturers Association (NEMA), the Phase Voltage Unbalance Rate (PVUR) or Phase Voltage Unbalance Factor (PVUF), defined by IEEE, and the Voltage Unbalance Factor (VUF), which is widely regarded as the most accurate or "true" definition [4].

While LVUR and PVUR rely solely on voltage magnitude measurements and therefore neglect phase angle information, VUF captures both magnitude and phase angle effects. VUF is defined as the ratio of the negative-sequence voltage to the positive-sequence voltage, expressed as a percentage.

$$VUF\ (\%) = \frac{Negative\ sequence\ voltage(V^-)}{Positive\ sequence\ voltage(V^+)} \times 100$$

Due to its comprehensive nature, VUF is commonly used in academic and industry analyses for evaluating voltage unbalance. PVUF considers line-neutral voltage magnitudes only and is calculated at each bus using the below equation.

$$PVUF (\%) = \frac{\max(|V_{an} - V_{\mu}|, |V_{bn} - V_{\mu}|, |V_{cn} - V_{\mu}|)}{V_{\mu}} \times 100$$

where V_{an} , V_{bn} , V_{cn} are the line-neutral voltages of phase A, phase B and phase C respectively, while V_{μ} represent the mean voltage of the bus. This study evaluates voltage unbalance using both VUF and PVUF.

PV Curtailment

PV curtailment can occur as a result of the response of PV inverters operating in accordance with AS 4777.2:2020, which mandates that active and reactive power output must vary based on the voltage measured at the inverter terminals. Under this standard, inverters are required to reduce active power output (Volt-Watt response) and adjust reactive power injection or absorption (Volt-Var response) when local voltages deviate from nominal limits. While these responses are intended to support voltage regulation, they can also lead to reduced energy export during high-voltage conditions, particularly in areas with high PV penetration. Curtailment is expressed in kWh and is also used in the cost benefit analysis when calculating CECVs for each technology.

3 Network Exchanger (NEx)

The NEx system, developed by Third Equation Ltd, is a grid-support technology designed to enhance the hosting capacity of LV distribution networks. Its core functionalities include voltage regulation, current balancing, and power factor correction, all implemented at the LV terminals of distribution transformers. This section of the report outlines the implementation of NEx within the DIgSILENT PowerFactory environment and provides an overview of its operational principles.

NEx is intended to be installed on the LV side of the distribution transformer and comprises two main power electronic subsystems: a series converter (SC) and a parallel converter (PC), both connected via a common DC link. The series converter interfaces with each phase through individual series transformers and is responsible for regulating voltage at the point of connection. This is achieved by injecting or absorbing real power in accordance with a predefined voltage setpoint, which it maintains by modifying the voltage at its terminals as dictated by the control logic.

The parallel converter supports three key functions:

- 1. Current balancing across phases to mitigate unbalanced loads,
- 2. Power factor correction by compensating for reactive power, and
- 3. DC link voltage regulation by exchanging real power with the grid to maintain the energy balance of the system.

Real-time measurements of voltage and current are obtained through voltage sensors and current transformers (CTs). These signals are processed by the NEx controller, which determines the appropriate converter outputs required to meet the operational targets. Figure 9 provides a schematic overview of the NEx system integrated into the distribution network.

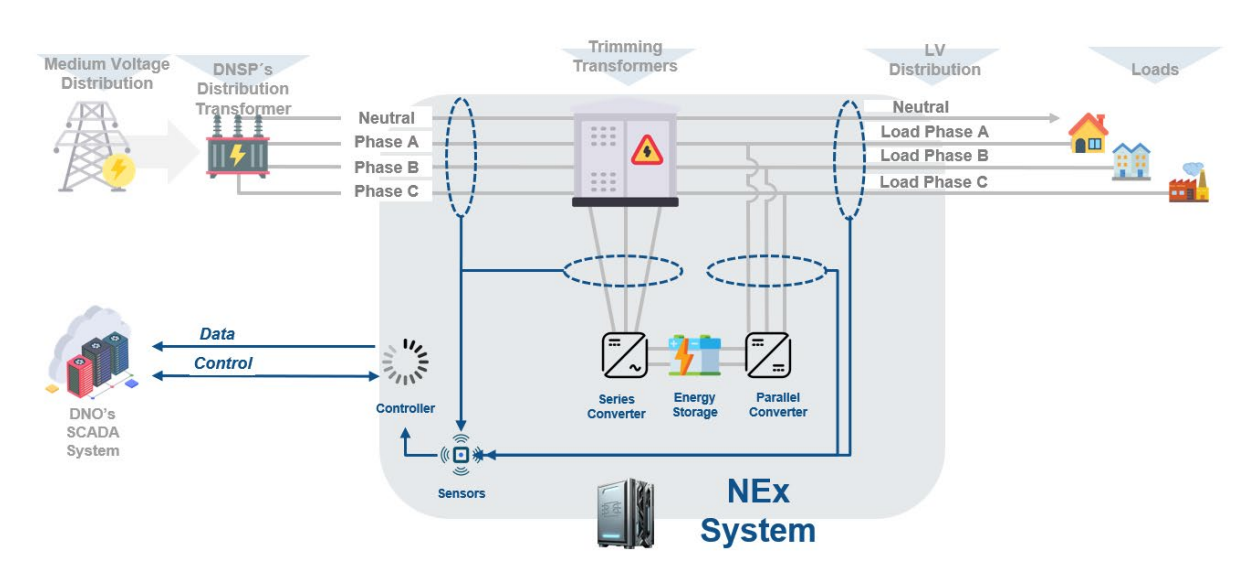


Figure 9. Overview of the Network Exchanger (NEx).

3.1 Development of NEx Simulation Model

The initial simulation model of NEx was developed by Third Equation Ltd. using the MATLAB Simulink environment. This model was a dynamic system operating with a time step of 267 µs, wherein the controller required instantaneous measurements of current and voltage to generate control signals for the series and parallel converters of the NEx system. The controller was encapsulated as a Functional Mock-up Unit (FMU), which adheres to the Functional Mock-up Interface (FMI)—an open standard that enables the exchange of dynamic simulation models across a wide range of simulation tools. Given that DIgSILENT PowerFactory supports the FMI standard, the initial approach involved importing the FMU into PowerFactory and developing each component of NEx as a composite model to conduct simulations within this platform. Due to the controller's dynamic nature and its reliance on instantaneous system values, simulations had to be performed using the Electromagnetic Transient (EMT) simulation mode in PowerFactory. Although this approach yielded accurate results, the computational burden was substantial. Considering that hosting capacity assessments necessitate a large number of simulations across a wide range of scenarios—combined with the complexity of the high-fidelity Brisbane distribution network model—this method was ultimately deemed impractical for largescale analysis. The most effective solution was to develop a steady-state load flow model of the NEx system that accurately captures its core functionalities. To facilitate this, the QDSL feature in DIgSILENT PowerFactory was employed. QDSL models are typically used to conduct a sequence of load flow analyses at specified time intervals, allowing the assessment of network behaviour over a defined simulation period. However, an important capability of QDSL is its support for user-defined load flow control algorithms, which was leveraged in this case to replicate the operational logic of NEx within a steady-state framework. Using this functionality, a QDSL-based load flow model for NEx was developed. The control algorithms governing voltage regulation, power factor correction, and phase balancing were implemented as mathematical expressions within the QDSL environment. These expressions and NEx control logic aren't revealed in this report. Separate QDSL models were created for the series and parallel converters of the NEx system. Figure 10 shows an overview of the required data and output signals of the developed steady state models of NEx.

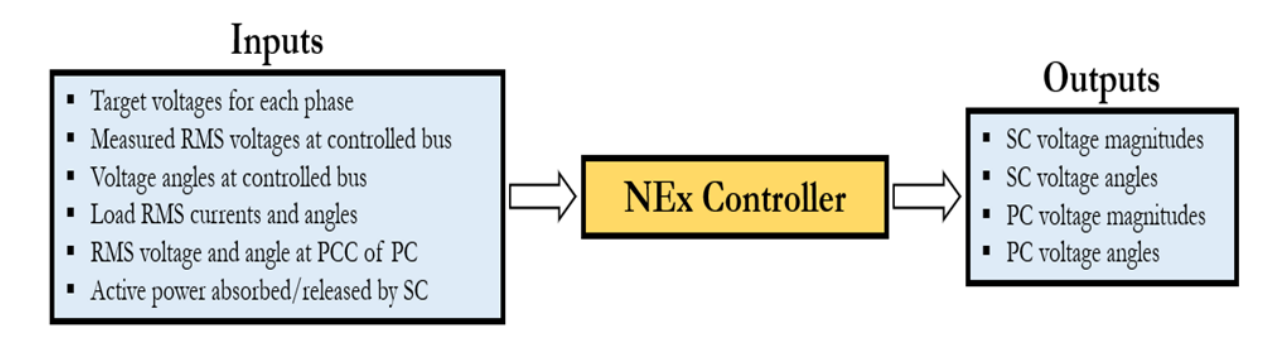


Figure 10. Control signals exchanged by the developed NEx QDSL model.

It is also important to note that the SC and PC of NEx have been implemented in the model as single-phase AC voltage sources in DIgSILENT PowerFactory. In the case of the SC, which is responsible for voltage regulation, a QDSL model has been developed where the user inputs the target voltage for each phase. At each iteration, the measured voltages at the point of regulation are fed back into the model. Based on these inputs and the internal NEx control logic, the model calculates the required output voltage magnitude and angle for each phase, which are then applied to the respective voltage sources. Constraints such as the maximum allowable voltage generation of the SC are also embedded within the model.

The target voltage is a parameter that must be set by the DNSP during operation of NEx. This may be defined using historical voltage data, results from load flow studies with expected generation and demand forecasts, or real-time measurements from critical nodes within the LV area. To enable automation during time-series simulations, the SC model receives continuous voltage measurements from the LV area. Initially, the target voltage for each phase is set at 230 V, the nominal value. If a voltage violation is detected during this set voltage, the model adjusts the target voltage of the affected phase in 2 V increments (either upward or downward) until the violation is resolved or the operational constraints of NEx are reached. This approach allows exploration of the full operational capability of NEx.

The PC is responsible for executing current balancing, power factor correction, and maintaining the DC link voltage. The model replicates the control capabilities available in the physical NEx device, allowing users to selectively enable or disable the current balancing and power factor correction functionalities. The PC receives input signals including load current measurements, voltage magnitude and angle at the point of connection, and the real power exchanged by the SC. Based on these inputs and the embedded control logic, the PC computes the appropriate voltage magnitude and phase angle, which are then applied to each voltage source in the model.

4 Baselined Network Model Condition

The current state of the network was assessed under high solar generation conditions during two key time periods: midday (12:00 p.m.) and evening peak (7:30 p.m.), across all four seasons of the year. The evening scenario was selected to capture network behaviour under peak demand conditions. Table 3 presents the distribution of line-to-neutral voltages observed across all phases at LV buses, as well as the corresponding voltage unbalance factors recorded throughout the network for each season. Note that the network consists of 8382 LV buses.

Table 3. Voltage and VUF percentiles for all LV buses in the present-day network model at midday and evening time periods across all seasons.

Season	Condition	LV voltages average (V)	LV voltages 1 st percentile (V)	LV voltages 99 th percentile (V)	VUF average (%)	VUF 99 th percentile (%)
Spring	Noon	240.78	230.346	250.059	0.138	0.611
Spring	Evening	239.906	229.984	247.336	0.193	0.674
Summer	Noon	239.443	230.230	247.497	0.127	0.543
Summer	Evening	239.016	229.449	248.196	0.236	0.867
Autumn	Noon	239.798	229.874	249.364	0.111	0.515
Autumm	Evening	239.288	229.986	248.215	0.207	0.758
Winter	Noon	241.179	231.471	250.380	0.187	0.765
vviitei	Evening	239.792	229.897	247.345	0.186	0.726

The present-day condition of the network model shows no over-voltage violations at any node during midday in summer and autumn. In contrast, during spring and winter, 0.024% and 0.167% of nodes, respectively, exceed the upper voltage limit at midday. This slight increase is primarily due to lower load demand during these seasons, which, when combined with high solar generation, results in elevated voltage levels at certain nodes. Nevertheless, these violation rates are minimal when viewed across the entire network and do not suggest any significant overloading from PV systems. Furthermore, the energy curtailed during the high solar conditions at each season is negligible.

With respect to the lower statutory voltage limit during the evening peak (7:30 p.m.), no violations were recorded in spring, autumn, or winter. In summer, only 0.0199% of nodes fell below the 216 V threshold.

These results are consistent with expectations, given that the average residential PV system capacity in the present-day network model is relatively low and no EVs are included in the model.

Figure 11 presents the distribution of transformer loading under present-day conditions during the midday period across all seasons. The LV network is supplied through 229 distribution transformers. None of these transformers exceed the 100% loading threshold during peak PV generation, indicating the absence of overloading at midday. During the evening peak, a single 100 kVA-rated transformer exceeds the threshold in all seasons, with the highest recorded loading being 120% in winter. Overall, transformer loading remains within acceptable levels under current network conditions.

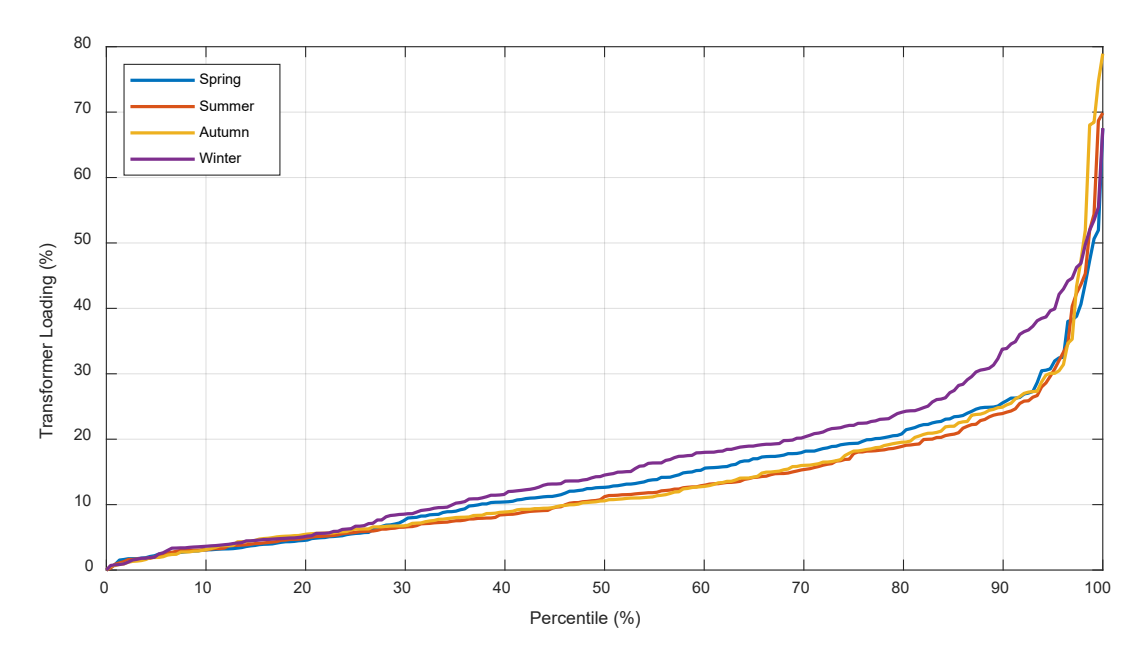


Figure 11. Percentiles of loading levels of transformers in the present-day network model at midday during each season under high solar conditions.

Table 4 presents the loading levels of conductors within the network model. The model comprises a total of 746 medium-voltage (MV) cables and 32,737 low-voltage (LV) cables, including associated neutral conductors. These figures account for both overhead and underground line segments, providing a comprehensive representation of all conductor routes in the system.

Table 4. Line loading data of MV and LV cables in the present-day network model across all seasons in high solar conditions.

Season	Condition	MV cables loading 99 th percentile (%)	LV cables loading 99.9 th percentile (%)	MV cables maximum loading (%)	LV cables maximum loading (%)
Spring	Noon	16.662	53.509	23.691	86.114
Spring	Evening 34	34.649	67.645	38.260	169.078
Summer	Noon	18.663	52.995	23.984	129.515
Summer	Evening	43.081	64.360	49.208	150.156
Autumn	Noon	18.510	54.296	24.042	87.604
Autumn	Evening	40.107	60.610	46.731	139.157
Winter	Noon	16.625	36.120	26.762	69.394
vviiller	Evening	35.082	56.041	42.454	142.220

It is noted that all MV cables operate within their rated capacities across all time periods and seasons. In contrast, a very small proportion of LV conductors exceed their rated capacities during the evening peak across all seasons. The percentage of overloaded LV conductors is 0.0672% in spring, and 0.0061% in summer, autumn, and winter. These exceedances are minimal relative to the total number of LV conductors in the network and do not indicate any widespread overloading under present-day conditions.

5 Development of CER projections

This section of the report outlines the methodology used to develop future projections for CER uptake within the network, with a primary focus on rooftop PV systems and EVs. Battery Energy Storage Systems (BESS) at the residential level were not included in the scope of this study. Energy programs such as 'Cheaper Home Batteries Program' have been recently introduced to increase residential BESS penetration by providing customers with considerable discounts in purchase costs. This program would likely to lead to a significant increase in residential batteries in the coming years. This research commenced prior to the rebate and therefore excludes it, presenting a worst-case scenario. While it is acknowledged that BESS can support distribution network operation during periods of high CER penetration, their impact under typical deployment scenarios remains limited.

Specifically, BESS units installed as part of standard PV packages and operated with off-the-shelf controllers have shown limited effectiveness in mitigating voltage rise and export curtailment during peak solar generation periods. As demonstrated in [5], where commercially available BESS solutions were assessed for their potential to improve hosting capacity in PV-rich low voltage networks, these systems exhibited no significant improvement compared to the business-as-usual (BAU) scenario. This outcome was primarily attributed to operational constraints, such as the inability of BESS units to fully discharge overnight due to reduced household consumption, and the tendency of batteries to reach full state-of-charge early in the day. Consequently, during peak PV production hours, the BESS are unable to absorb excess generation, resulting in persistent voltage and curtailment issues within the network.

While these systems offered limited network-wide benefits, they were found to be advantageous from the perspective of individual PV owners, as they reduced energy imports from the grid which would result in lower energy bills. The need for more effective coordination has led to increasing research interest in the intelligent control of BESS. To enable their use as a tool for addressing network-level challenges, future deployment models would require that DNSPs be granted a degree of control or coordination capability over these distributed assets or development of intelligent controls for BESS as proposed by [5].

Projections for PV and EV uptake under the Progressive Change and Step Change scenarios were calculated on a per-household basis using data provided in [6] [7]. As the distribution network is located in Queensland, rooftop PV projections relevant to the state for each scenario were obtained from the Integrated System Plan (ISP) for each financial year. Given that the network model encompasses both residential and commercial/industrial areas, PV projections were computed separately for each sector.

Using data from [8], the ratio of residential small-scale rooftop PV capacity to business small-scale rooftop PV capacity was derived for each scenario across the study period beginning in 2025. The average ratio was determined to be 0.83 and applied to calculate the respective residential and commercial rooftop PV capacities for both scenarios in Queensland.

The number of residential dwellings in Queensland as of the 2025 financial year was obtained from ABS data [9]. Future dwelling numbers were extrapolated using population growth rates for each scenario—1.1% for Progressive Change and 1.3% for Step Change—as per [7]. To determine the number of dwellings suitable for rooftop PV installation, the proportion of separate dwellings was applied for each scenario based on future housing composition forecasts from [8]. The total number of dwellings was multiplied by the corresponding percentage of separate dwellings to estimate the number of rooftops likely to host PV systems annually. The average residential rooftop PV capacity per household was then calculated by dividing the total residential

rooftop PV capacity by the number of separate dwellings in each year. Figure 12 shows the calculated average PV capacity per household in each of the two scenarios.

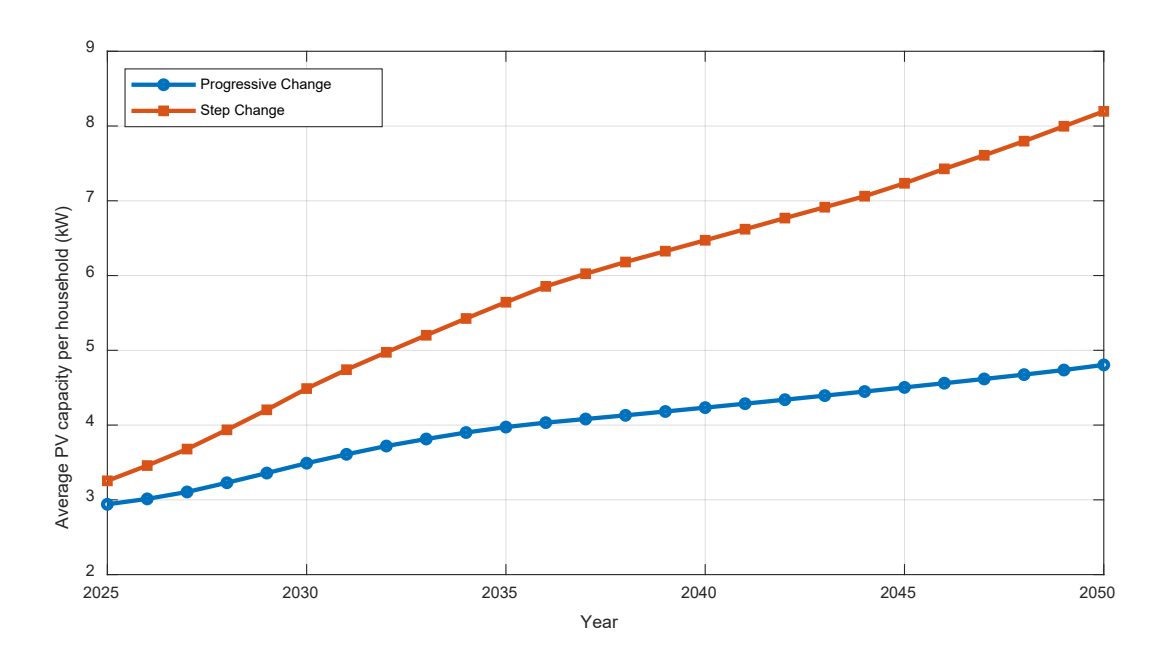


Figure 12. Projections for average PV capacity per household across Queensland for progressive and step change scenarios.

For small-scale business PV capacity, the original installed capacity in the model was scaled according to the annual growth in total rooftop PV capacity in Queensland under each scenario. To decouple the impact of population growth from these projections, the resulting values were normalised by dividing by the respective scenario-specific population growth rates.

Similarly, the average number of EVs per household was estimated for both scenarios. Based on recent census data for the transport sector, the current average number of motor vehicles per household is 1.8 [10]. This figure, combined with projected EV fleet share data under each scenario, was used to calculate the expected average number of EVs per household. The fleet share represents the proportion of electric vehicles in the overall vehicle market and reflects the anticipated replacement of internal combustion engine (ICE) vehicles by EVs over time. It is important to note that only fleet share data related to light vehicles (i.e., passenger cars) were considered, as these represent the most common vehicle type in residential households. Figure 13 shows the calculated average number of EVs per household.

Using the calculated PV and EV projections, future versions of the network model were developed for the years 2025 to 2050 in 5-year intervals under both the Progressive Change and Step Change scenarios. For each time step, expected CER penetration levels were integrated into the model to reflect the projected uptake of rooftop PV systems and EVs. This integration was performed by randomly selecting customers to adopt new PV systems and EVs, using uniform distribution sampling. The process was iteratively continued until the average PV capacity per customer and EV ownership level in the model matched the scenario-specific projections for the corresponding year.

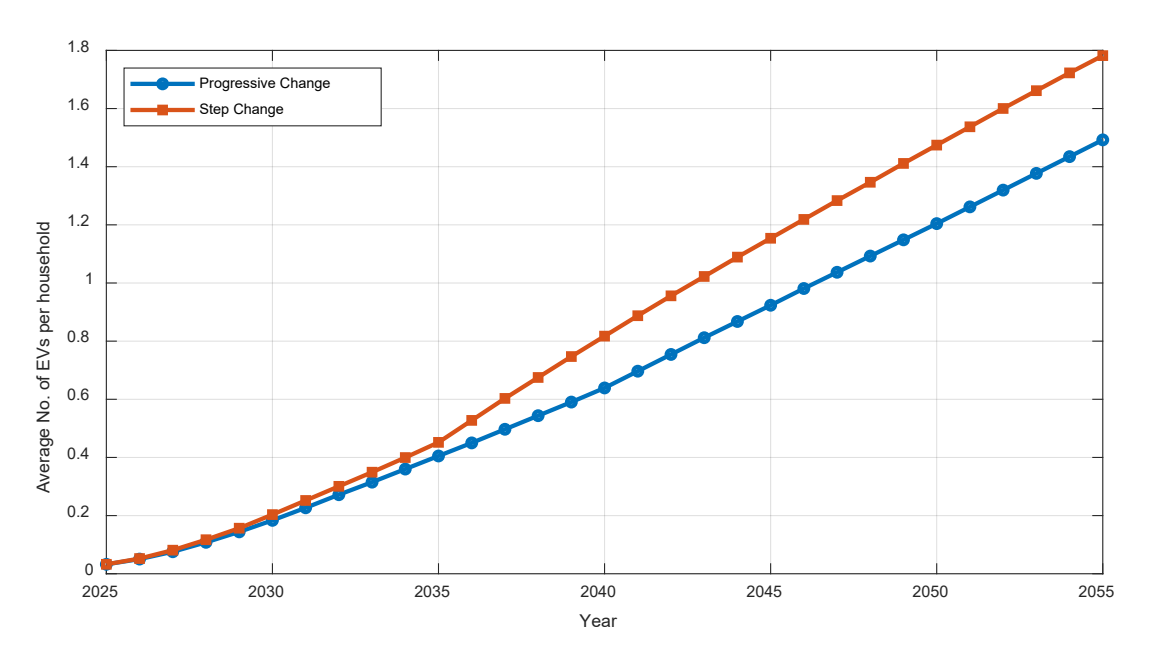


Figure 13. Projections of average number of EVs per household under progressive and step change scenarios.

5.1 Future PV Characteristics

The average capacity of newly installed residential PV systems today is approximately 8.6 kW [8]. For modelling purposes, a capacity of 8 kW is assumed, as this corresponds to a commonly installed inverter size in the market. Although the overall installed PV capacity is expected to grow in the coming years, the impact on the model remains negligible since the PV growth in the network is considered on a per-household basis. Seasonal generation characteristics of PV systems added at new locations in the network were modelled using peak PV utilization factors of 100% for spring and summer, 97.63% for autumn, and 82.89% for winter. These factors were derived from simulations of the study area using a commercial PV design tool, under the assumption of negligible cloud cover [2]. It was also observed in the baselined network model that some existing PV systems exhibited low peak output values. As a result, when additional PV capacity was introduced at these locations in future scenarios, the net injection remained relatively small compared to the newly added capacity. To better reflect the impact of the increased capacity at these existing PVs—while still accounting for locational and operational factors—a scaling factor of 0.8 was applied to the newly added capacity. This scaled value was then further adjusted by the seasonal peak utilization factor to capture realistic PV output variations across the year.

5.2 EV Charging Characteristics

In this study, EV owners are assumed to be equipped with either 3.68 kW or 7.36 kW AC chargers, representing common residential charging configurations. The assignment of charger size is based on the customer's phase connection type: customers with single-phase or two-phase connections are allocated the 3.68 kW charger, while customers with three-phase connections are assigned the 7.36 kW charger. To model realistic EV charging demand, diversified charging curves were adopted from [11], which are based on empirical data collected from an EV trial in the UK and have been validated for use in Australian distribution networks. These curves represent the probabilistic nature of EV charging behaviour. Only weekday charging profiles were used in this analysis, as they exhibit more pronounced evening peaks compared to weekend profiles, thereby representing a more conservative case with higher potential network impact. Incorporating diversified charging profiles is critical for accurately capturing the impact of EVs on the distribution network. Unlike static load modelling or simultaneous charging assumptions, these curves prevent overestimation of aggregate demand by recognizing that not all EVs

charge concurrently. This approach provides a more nuanced and representative estimation of demand peaks, voltage variations, and loading patterns across feeders. The maximum number of EVs allocated per customer is 2, and the selection of customers to be equipped with EVs have been performed using sampling from uniform distributions.

The activation of EV charging in the network model was carried out using a repetitive random sampling process. For each charger size (3.68 kW and 7.36 kW), customers were probabilistically selected for activation or deactivation to ensure that the aggregate charging demand aligned with the corresponding diversified EV charging profile. At each simulation time step, the required proportion of active EVs was calculated based on the existing EV population and the target value from the charging diversity curve for each charger size. Customers equipped with each charger type were then randomly sampled and activated until the total number of active chargers matched the target demand for that interval.

6 Simulation Results

6.1 Voltage and Curtailment

As outlined in chapter 5, future versions of the network model were assessed under both Progressive Change and Step Change CER uptake scenarios. According to simulation outputs from a commercial PV analysis tool, peak PV generation from new customer installations in the modelled area occurs during the spring and summer months. However, spring was selected as the primary season for investigation due to typically lower midday electrical demand, largely attributed to reduced air conditioning use compared to summer. This lower demand exacerbates voltage rise issues by increasing the net power exported from distributed PV systems to the grid.

The simulations focused on the midday period, which coincides with maximum PV output, making it the most critical time for overvoltage risk. In each future year modelled, all newly installed PV inverters were assumed to be 90% compliant with AS 4777.2:2020, incorporating Volt-Var and Volt-Watt control. To quantify the extent of overvoltage, the maximum voltage at each LV bus was extracted and compared against the standard upper limit of 253 V.

Figure 14 presents the percentage of LV buses exceeding the upper voltage threshold for both scenarios from 2025 to 2050. The results demonstrate a clear upward trend in voltage violations, driven by increasing PV penetration and consistently low midday loading. Under the progressive change scenario, the percentage of affected LV buses increases modestly from approximately 3% in 2025 to just under 9% in 2050. In contrast, the step change scenario exhibits a much steeper increase, reaching 23.4% by 2050, highlighting the greater strain placed on the network under aggressive DER growth assumptions.

Despite existing voltage mitigation mechanisms such as OLTCs at the zone substation—configured to operate at their lowest tap settings—and the integrated inverter-based control functionalities, these measures were found to be insufficient in mitigating the voltage rise issues, particularly under the step change scenario.

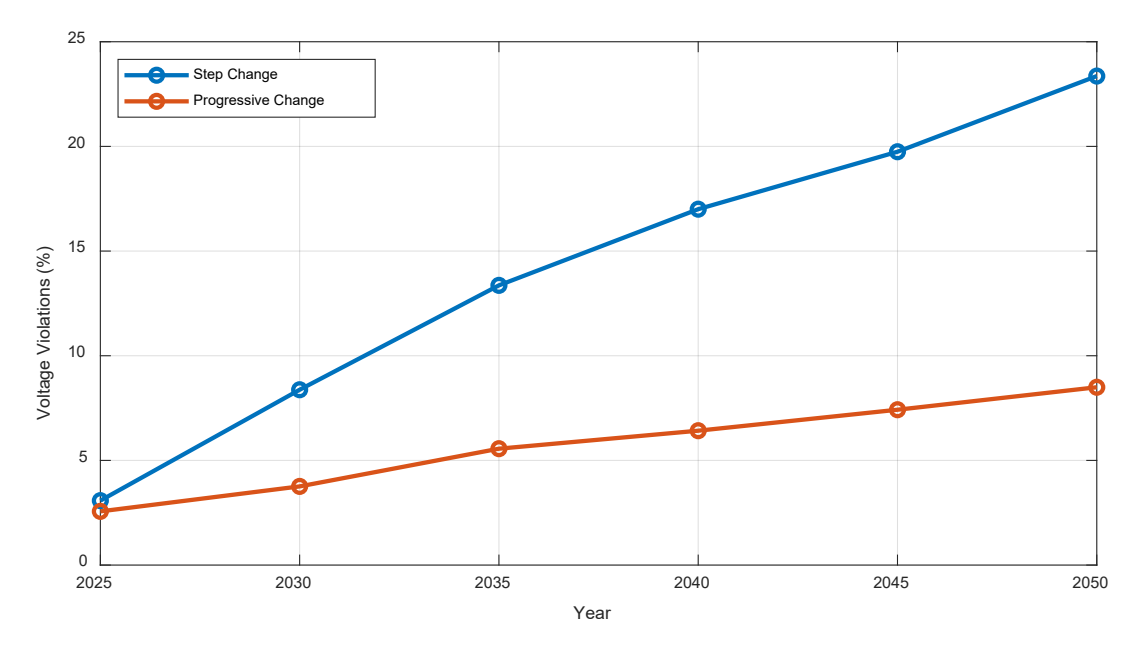


Figure 14. Proportion of LV buses with maximum phase voltage exceeding the upper voltage limit during spring at midday under high solar conditions.

In addition to analysing the percentage of buses exceeding voltage limits, the voltage distribution across all LV buses (maximum) was examined using key statistical percentiles (50th, 75th, 90th, 95th, and 99th) for each investigated year.

Figure 15 and Figure 16 illustrate the evolution of voltage levels under the progressive change and step change scenarios, respectively. Under the progressive change scenario, voltage levels rise gradually across all percentiles over time. By 2050, the median (50th percentile) voltage remains within a manageable range at approximately 246 V, and even the 90th percentile voltage remains below regulatory upper limit of 253 V. The 99th percentile exceeds the statutory limit even in the year 2025, although the 95th percentile only exceeds the 253 V-voltage limit in 2040. This indicates that while some buses experience elevated voltages, most remain within acceptable thresholds, reflecting the slower and more distributed nature of CER adoption in this scenario.

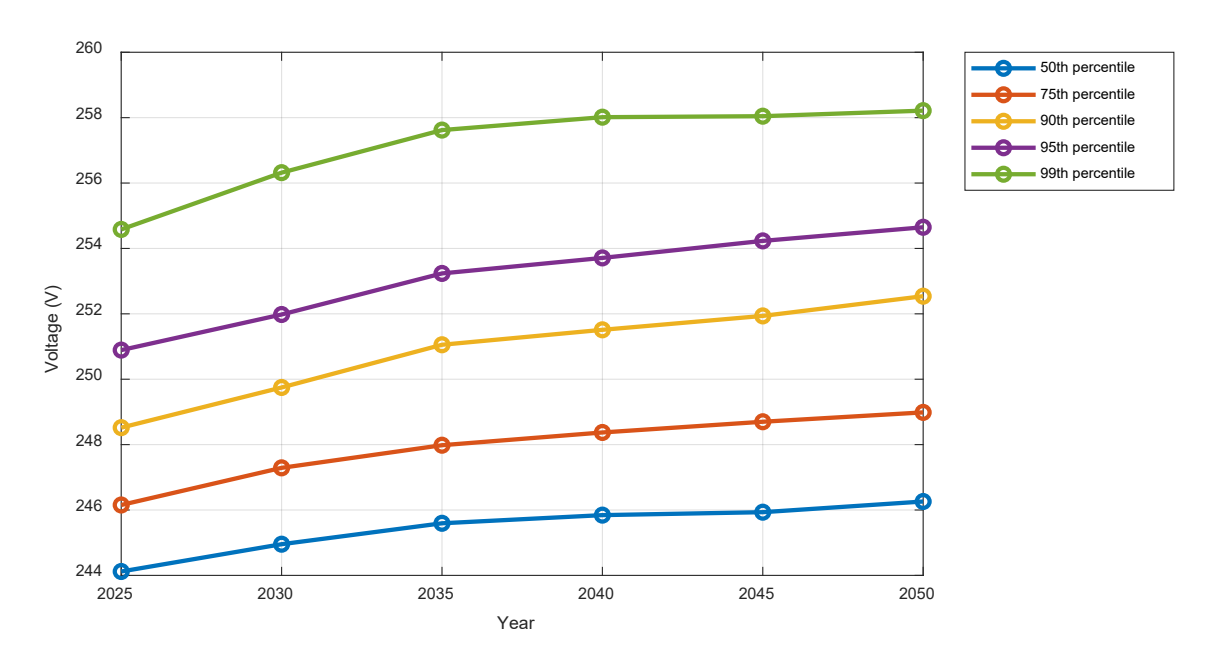


Figure 15. Percentiles of voltage distribution across all LV buses, based on the maximum line-to-neutral voltage observed at each bus in spring at noon under high solar conditions in the Progressive Change scenario.

In contrast, the step change scenario reveals a significantly more aggressive increase in voltage levels across the entire distribution. The 99th percentile reaches 268 V by 2050, far exceeding the statutory limit. Additionally, the 95th and 90th percentiles surpass the limits in 2030 and 2035 respectively, indicating that a large portion of the network will be operated under unsatisfactory voltage conditions. The median voltage also rises to approximately 249 V, which, while still below the limit, shows a clear upward trend that could pose challenges if CER growth continues unabated.

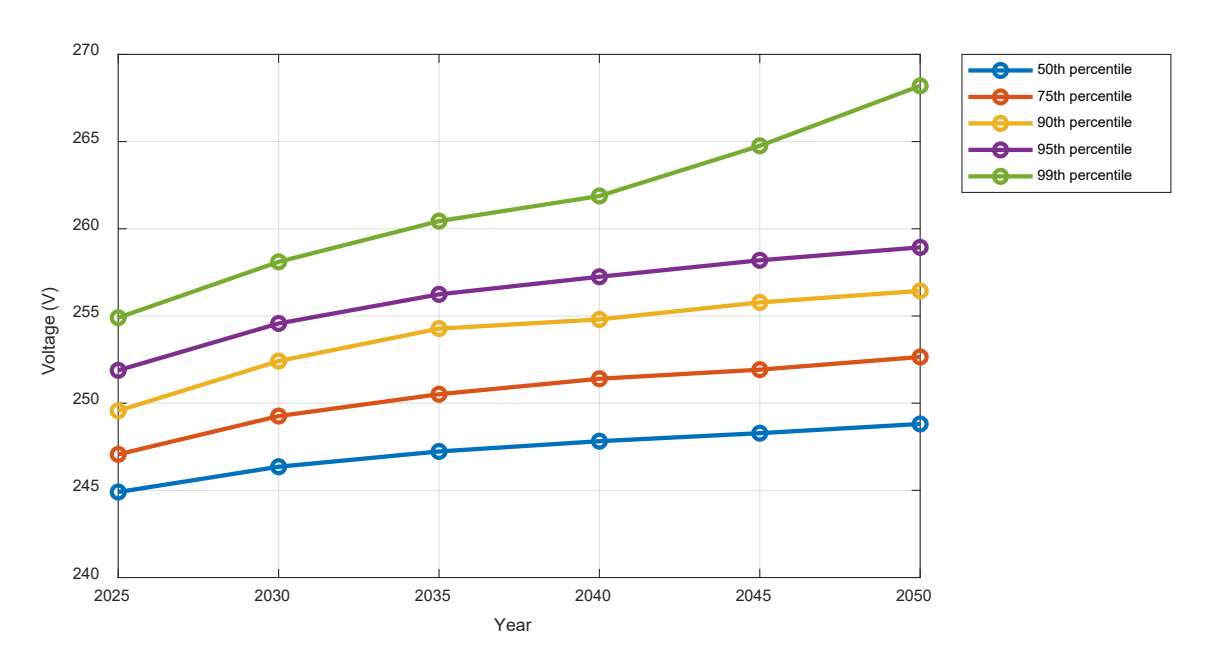


Figure 16. Percentiles of voltage distribution across all LV buses, based on the maximum line-to-neutral voltage observed at each bus in spring at noon under high solar conditions in the Step Change scenario.

Figure 17 shows key percentiles of the mean line-to-neutral voltages observed at LV buses under the step change scenario at noon during high solar generation conditions. Although the mean voltages exhibit an increasing trend over time, the upper statutory limit is exceeded only in the 99th percentile from 2035 onwards. This outcome also highlights the presence of voltage imbalance across the network, as evidenced by the discrepancy between the mean voltage percentiles and those of the maximum voltage distribution. Given that new customer connections can occur on any phase at any bus, and upgrades to three-phase connections are possible, it is essential to analyse the maximum voltage levels at each bus to assess potential effects on the network.

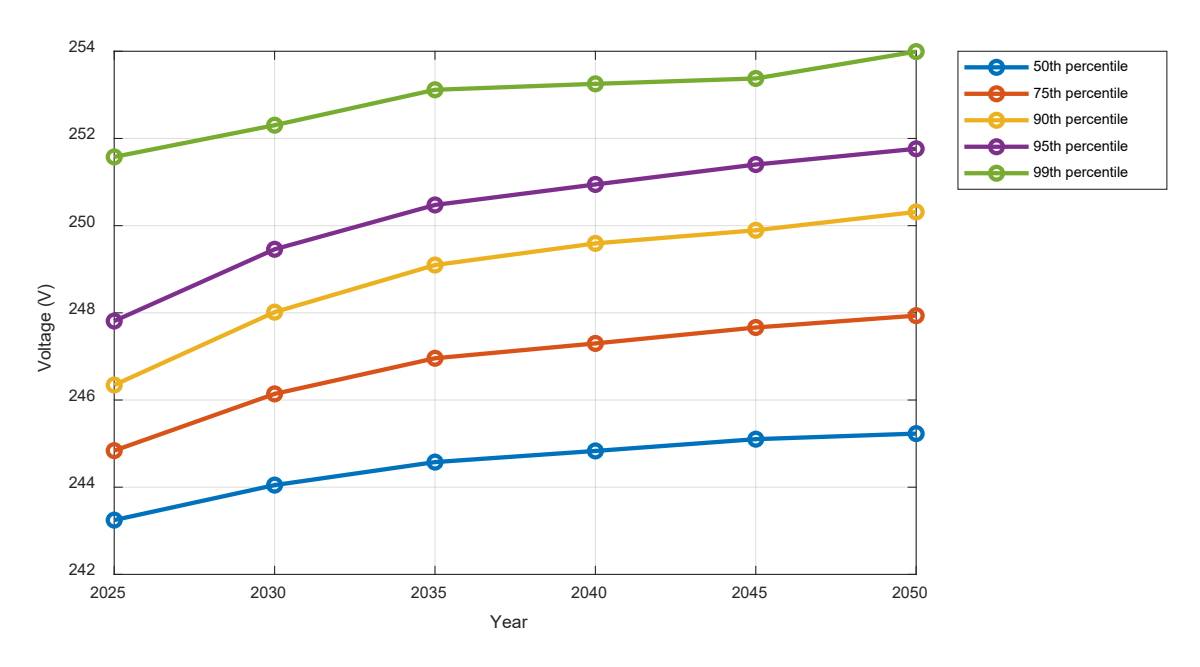


Figure 17. Percentiles of voltage distribution across all LV buses, based on the average line-to-neutral voltage observed at each bus in spring at noon under high solar conditions in the Step Change scenario.

The voltage imbalance due to unbalanced generation and loads were evaluated using both VUF and PVUF and evaluated for selected 2025,2035 and 2050. Table 5 shows the voltage imbalance for both progressive change and step change scenarios.

Table 5. Percentiles of voltage unbalance at LV buses under the Progressive Change and Step Change scenarios during midday in spring under high solar conditions.

Parameter-percentile	Pro	gressive Chang	ge	9	Step Change	
Parameter-percentile	2025	2035	2050	2025	2035	2050
VUF - 50 (%)	0.400	0.631	0.749	0.624	0.975	1.375
VUF - 75(%)	0.646	1.011	1.324	0.912	1.517	2.108
VUF - 90 (%)	0.943	1.519	1.962	1.221	2.202	3.102
VUF - 95 (%)	1.182	1.960	2.406	1.433	2.794	3.679
VUF - 99 (%)	1.759	3.022	3.519	2.067	4.002	5.731
PVUF - 50 (%)	0.615	0.849	0.991	0.786	1.142	1.484
PVUF - 75(%)	1.152	1.517	1.729	1.316	1.874	2.424
PVUF - 90 (%)	1.828	2.350	2.786	2.012	2.947	3.828
PVUF - 95 (%)	2.492	3.096	3.620	2.575	3.840	4.912
PVUF - 99 (%)	4.000	5.0201	5.601	3.937	5.797	7.444

It is evident from the results that voltage imbalance would also increase over the years with increase in PV penetration and would require corrective actions to be taken by DNSPs. Increase in voltage unbalance would have negative impacts on the assets in the network, such as overheating of distribution transformers and inductive motors, and reduced torque in motors [12], [13].

The rise in voltage levels also leads to the activation of Volt-Watt and Volt-Var control in PV inverters. This control mechanism dynamically limits the inverter's output power based on the voltage measured at its terminals, thereby curtailing PV generation when voltage thresholds are exceeded. Figure 18 illustrates the comparison between the maximum potential energy output (assuming no curtailment) and the actual energy generated, accounting for Volt-Watt curtailment, across the years. The analysis focuses on a half-hour window at midday during spring under high solar irradiance conditions and considers both progressive and step change CER growth scenarios. In the progressive change scenario, the impact of curtailment remains minimal, as evidenced by the close alignment of the two curves. By 2050, the total curtailed energy is limited to 0.551 MWh, indicating that Volt-Watt activation does not significantly restrict PV generation across the whole network in this scenario.

The step change scenario exhibits a noticeably higher curtailment rate compared to the progressive change scenario, with a total of 1.96 MWh curtailed by 2050. This represents only 4.39% of the maximum possible energy generation in the absence of Volt-Watt curtailment. However, the impact of Volt-Watt control is not evenly distributed across all customers; its effect is highly location-dependent. In radial LV networks, voltage tends to rise toward the end of the feeder, meaning customers located at the extremities of the network are more likely to experience greater curtailment.

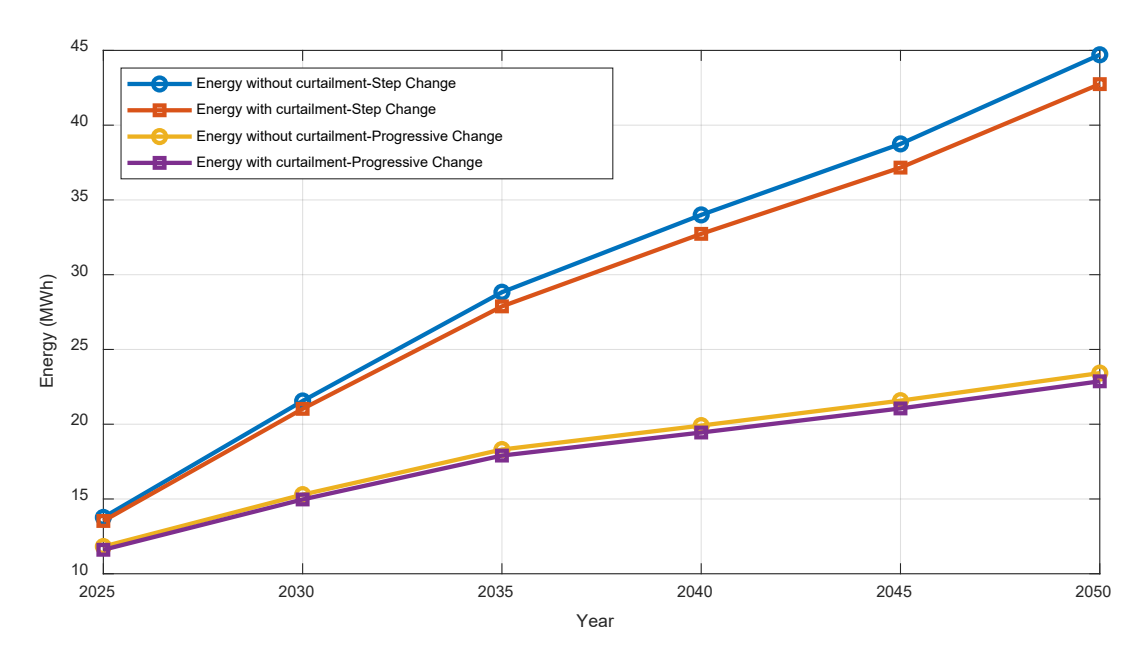


Figure 18. Energy supplied from rooftop PVs across the half-hour period at noon in spring under high solar conditions.

To better illustrate this disparity, key percentiles of the curtailment distribution have been plotted. Figure 19 and Figure 20 show the evolution of curtailment across the years for both progressive and step change scenarios, respectively. The 50th percentile, representing the median customer, consistently shows 0% curtailment in all years for both scenarios. Even the 75th percentile in the step change scenario reflects minimal curtailment, indicating that the majority of customers remain largely unaffected.

However, the upper percentiles—particularly the 95th and 99th—show a marked increase in curtailed energy over time. This indicates that a small proportion of customers are disproportionately impacted, facing significant energy and financial losses. This highlights an emerging equity concern associated with the widespread implementation of Volt-Watt control: while it benefits the overall network, it imposes uneven burdens on certain users.

It is also important to note that Volt-Watt control does not eliminate voltage violations entirely. Under current standards (i.e. AS 4777.2:2020), PV inverters begin curtailing only once voltage exceeds 253 V, meaning that voltage excursions can still occur despite curtailment

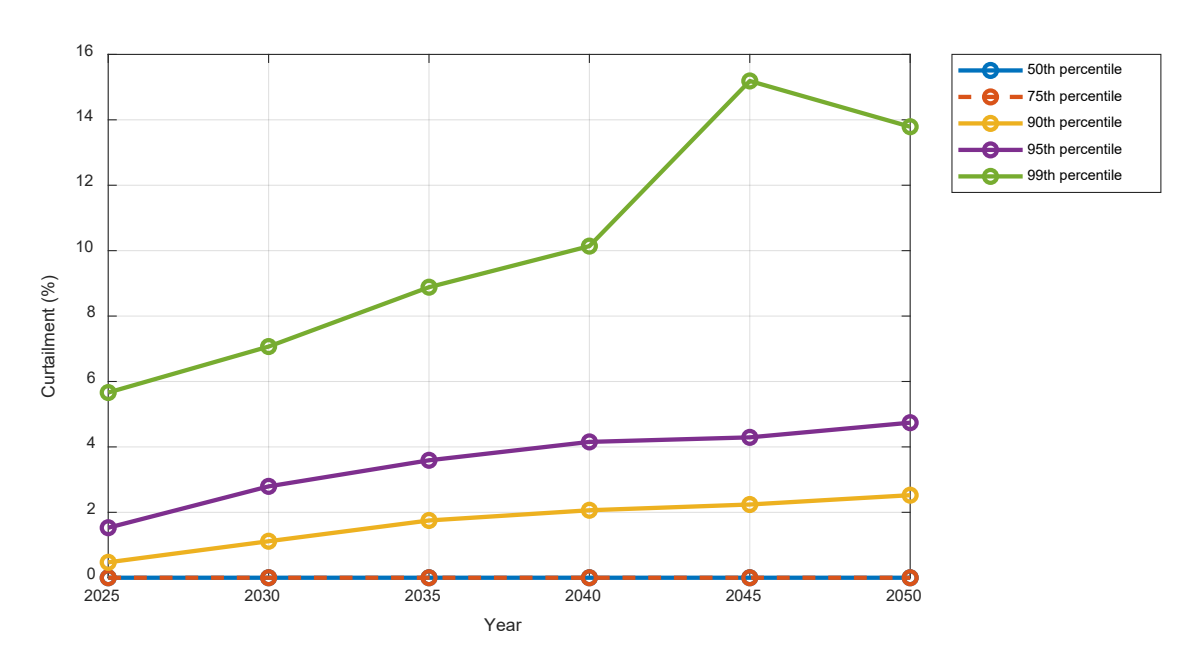


Figure 19. Percentiles of curtailment distribution across PVs in Progressive Change scenario at noon in spring under high solar conditions.

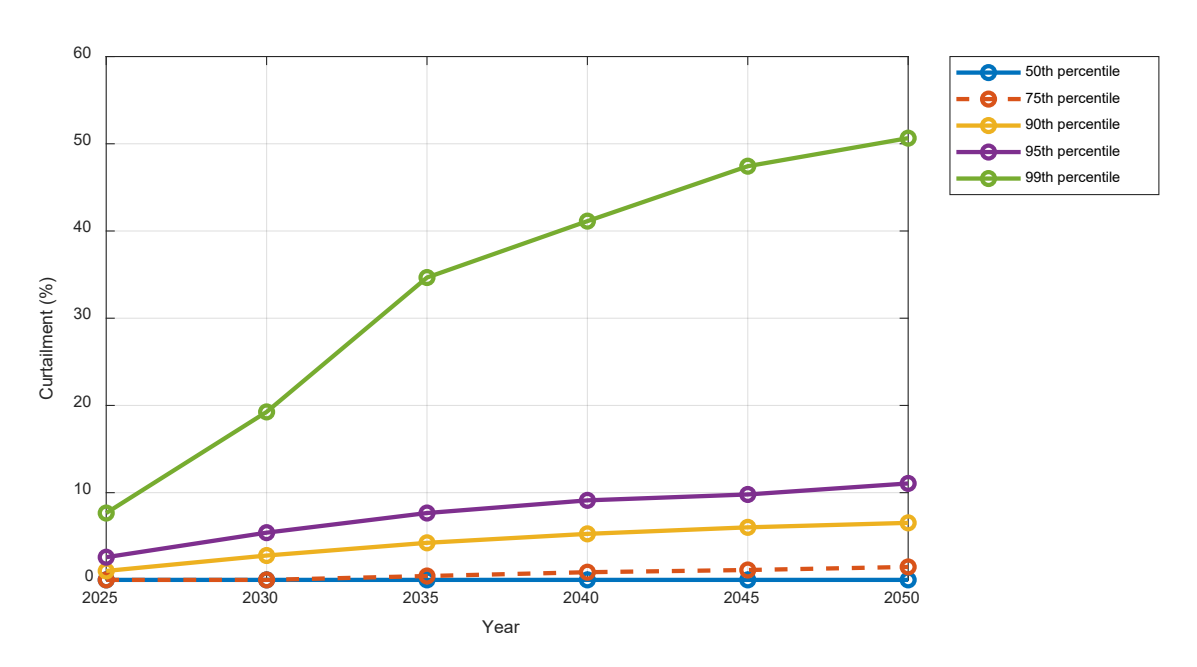


Figure 20. Percentiles of curtailment distribution across PVs in Step Change scenario at noon in spring under high solar conditions.

Figure 21 illustrates the variation in percentage curtailment observed at noon during high solar conditions for three PV systems located at different positions within the same LV network, under the step change scenario. As the rated sizes of the PV inverters increase over the years, curtailment is presented as a percentage of the maximum possible output to enable fair comparison across years.

The figure highlights the emerging fairness issue associated with Volt-Watt control in distribution networks. PV 3, located closest to the LV transformer, operates without any curtailment throughout the entire period, consistently exporting its full output. In contrast, PV 2, situated further from the transformer, begins to experience curtailment from 2040, with curtailment levels steadily increasing until 2050. The most affected system, PV 1, located furthest from the transformer, is curtailed in every year of the analysis, with curtailment worsening over time. These results demonstrate the spatial inequity introduced by voltage-based control

schemes, where customers located farther from the transformer face greater energy losses, despite having comparable system sizes and solar conditions.

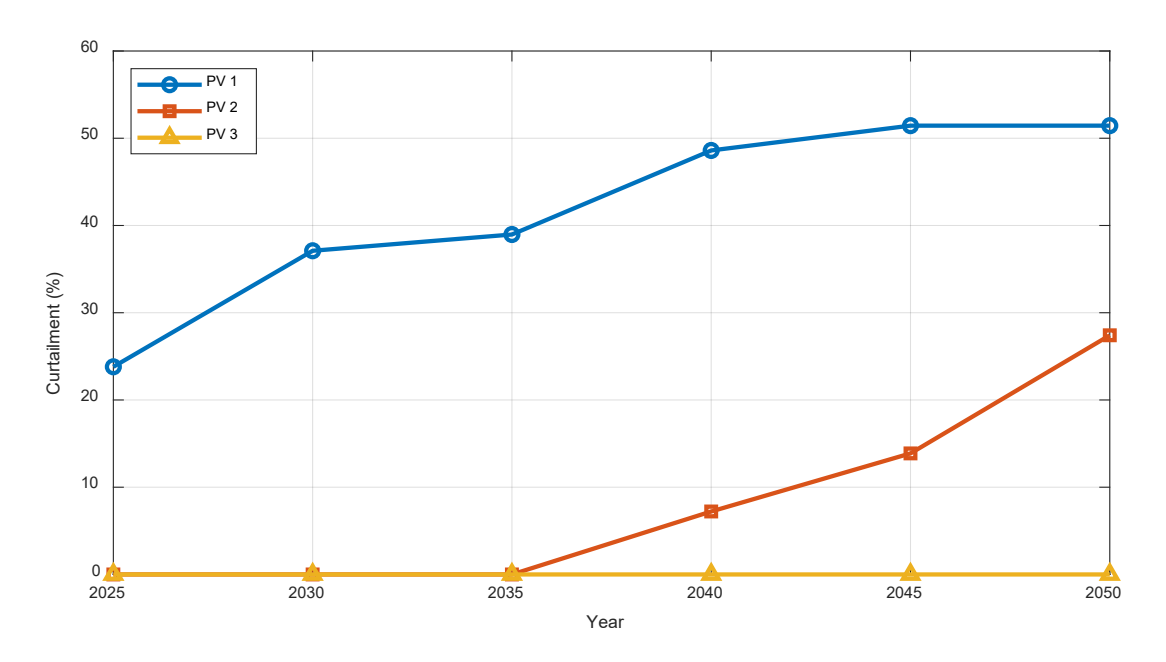


Figure 21. Variation of curtailment across three PV inverters located in the same LV area during spring at noon under Step Change scenario in high solar conditions.

Figure 22 presents the lower voltage violations observed during the evening peak in both spring and summer. Summer was included in the analysis because the baselined exhibited the highest loading levels during this season under high solar conditions, primarily due to the widespread use of air conditioning.

For this analysis, the minimum voltage at each LV bus was considered to identify the worst-case conditions across the network. The time of 7:30 p.m. was selected as the representative evening peak period, as this corresponded to the time when baselined load curve was at its highest, and coincided with the peak of the diversified EV charging curve.

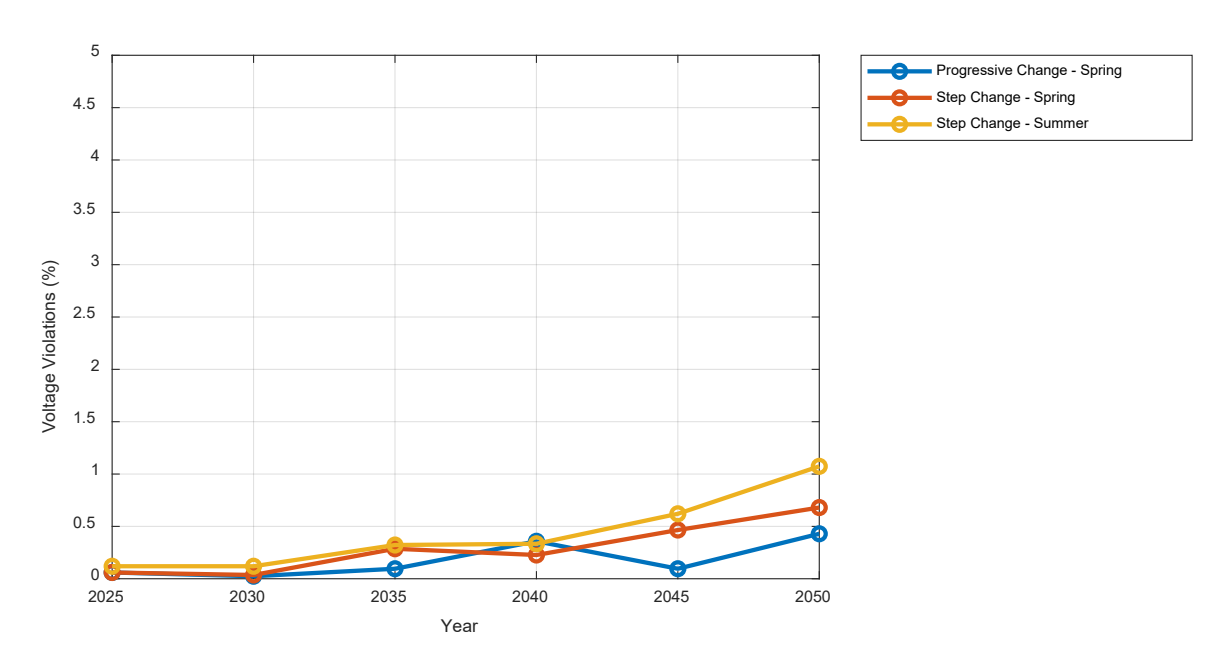


Figure 22. Proportion of LV buses with minimum phase voltage exceeding the lower voltage limit during spring and summer at 7.30 p.m. under high solar conditions.

Voltage limit violations associated with EV penetration are found to be insignificant in the distribution network under both the progressive and step change scenarios. In summer, during high solar conditions, only 1.07% of LV buses fall below the lower voltage limit of 216 V in the progressive change scenario, which is substantially lower than the overvoltage violations observed during the midday period due to PV penetration.

This outcome is primarily attributed to the diversified charging behaviour of EVs. Although approximately 19,900 EVs are added to the network by 2050 under the step change scenario, not all vehicles charge simultaneously. The average EV charging load, based on the diversified demand curve, is approximately 1.1 kW for 3.68 kW chargers and 2.1 kW for 7.36 kW chargers. As a result, the total EV-induced load is lower than the maximum installed capacity, reducing its impact on network voltage levels.

Figure 23 presents key percentiles of the minimum voltage distribution across LV buses at 7:30 p.m. in summer, under the step change scenario in high solar conditions. In 2050, only the 1st percentile of buses falls below the 216 V threshold, indicating that the vast majority of the network remains within acceptable limits. While there is a gradual downward trend in all percentiles over the years, the decline is not significant.

An important observation is the increase in voltage levels from 2030 to 2035, which is caused by the activation of the LDC algorithm. Up to 2030, the voltage setpoint at the zone substation is maintained at 1.0 p.u.; however, as active power flow increases due to higher EV demand, the LDC algorithm adjusts the voltage setpoint to 1.0125 p.u. This results in a corresponding rise in downstream voltages, partially offsetting the voltage drop caused by increased loading.

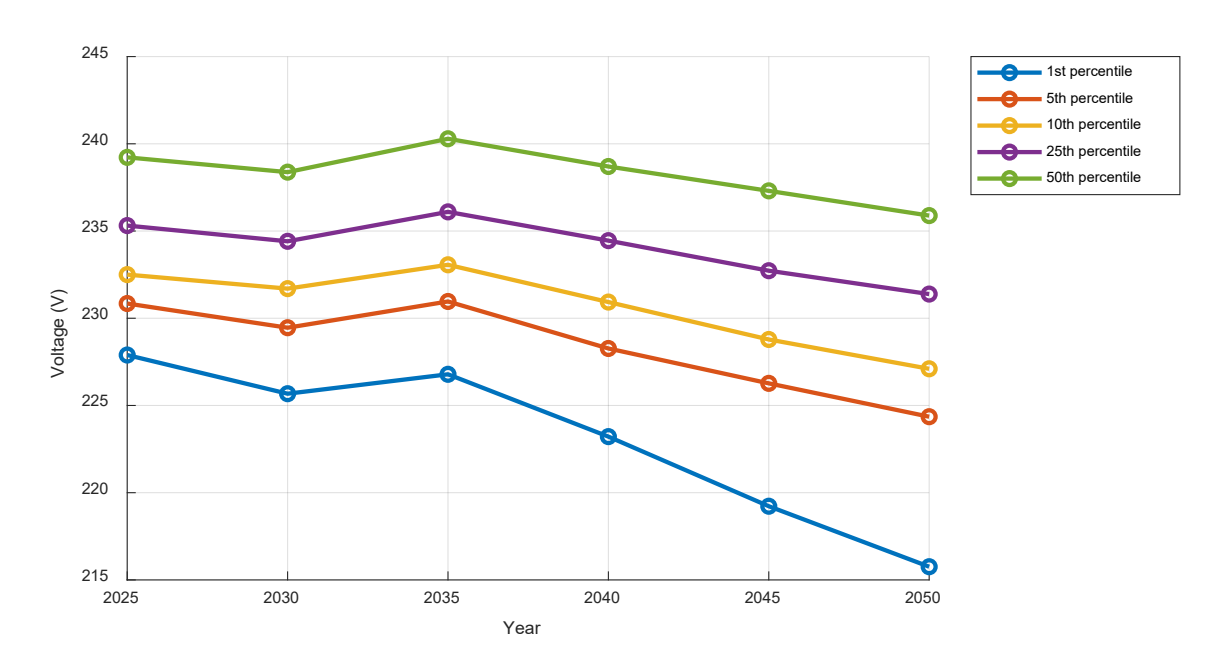


Figure 23. Percentiles of voltage distribution across all LV buses, based on the minimum line-to-neutral voltage observed at each bus in summer at 7.30 p.m. under high solar conditions in the Step Change scenario.

6.2 Utilization Levels of Transformers and distribution lines

The impact of high CER penetration extends beyond voltage regulation and generation curtailment—it also affects the thermal loading and operational lifespan of critical network assets such as distribution transformers and cables. These assets are designed to operate within their rated capacity, and prolonged operation above these limits can lead to excessive heating, insulation degradation, and ultimately catastrophic failure.

To manage these risks, DNSPs typically define maximum allowable loading thresholds for network assets, which vary depending on the duration of exposure. While temporary overloading above 100% of rated capacity may be permitted, it must remain within specified thermal limits to avoid long-term degradation. If the magnitude and duration of the overloading exceed safe thresholds, DNSPs may be required to undertake asset replacements or upgrades.

However, such interventions are often costly, particularly in the case of underground cable replacement, which involves complex excavation, specialised labour, and significant restoration work. These replacements also tend to have long lead times and may require extended network outages, making them challenging from both a financial and operational standpoint.

Figure 24 and Figure 25 illustrate the distribution of transformer loading levels at midday during spring under the progressive change and step change scenarios, respectively. The graph represents the number of transformers (in the x-axis) exhibiting a loading level higher than the value represented by the y-axis. In the 2050 progressive change scenario, approximately 29% of transformers exceed 100% of their rated loading, while only around 6% exceed 150% loading. In contrast, the step change scenario shows a significantly higher level of loading across transformers in the network, with around 68% of transformers exceeding 100% loading, and 47% exceeding 150% of their rated capacity in 2050.

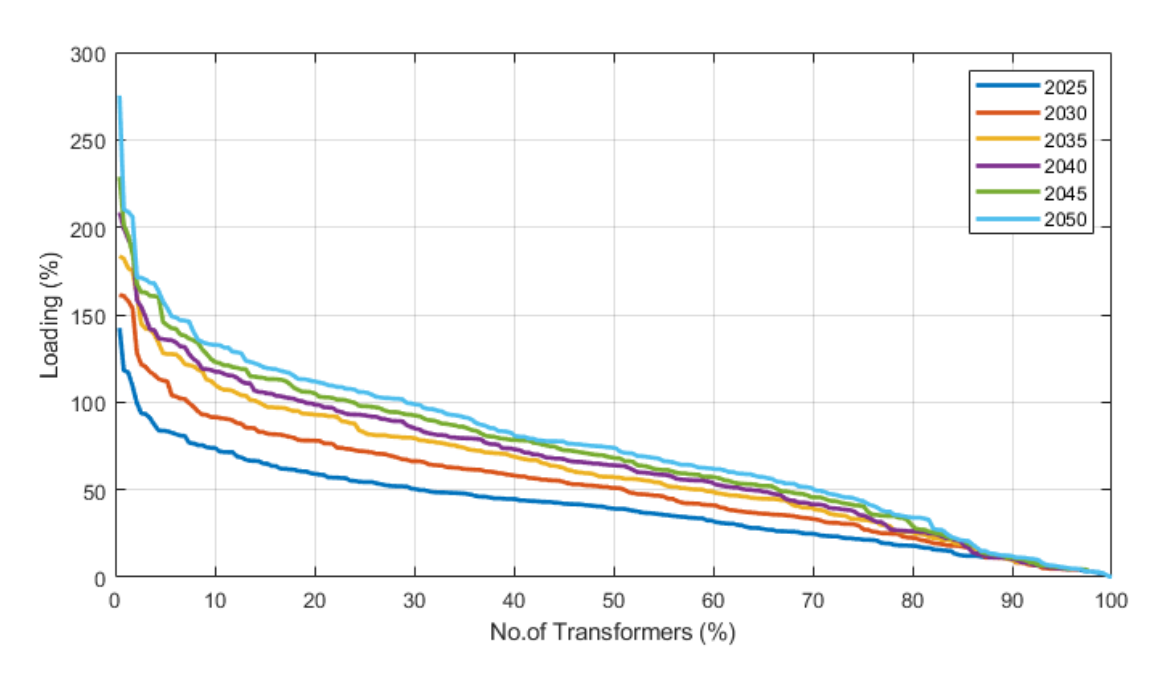


Figure 24. Distribution of loading levels of transformers in spring at noon under high solar conditions in the Progressive Change scenario.

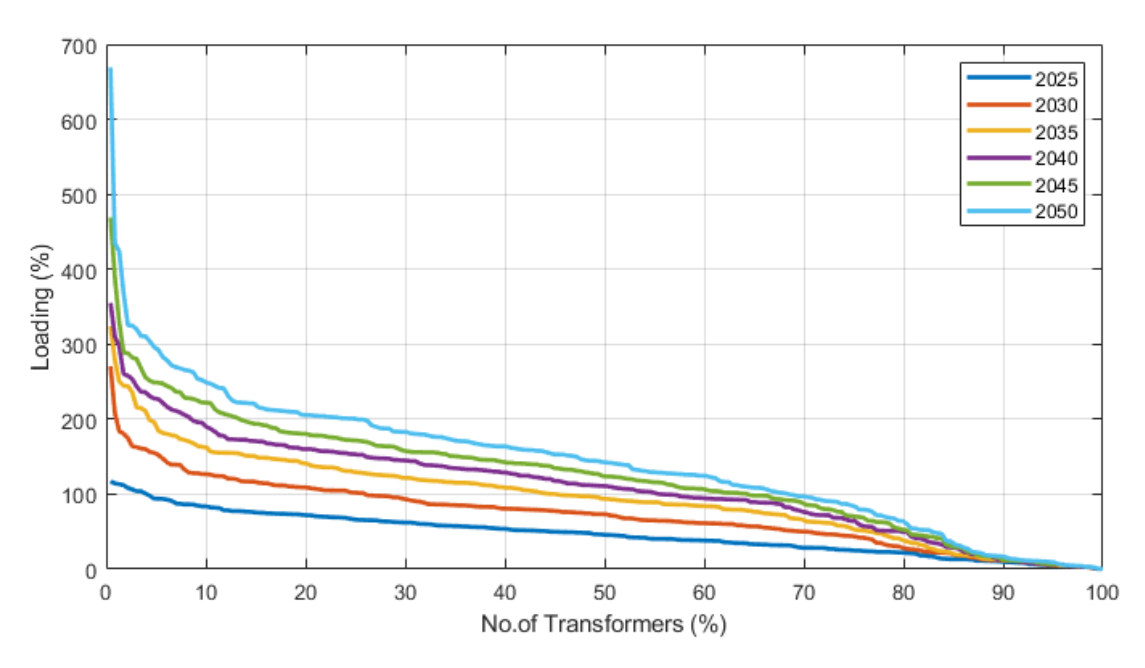


Figure 25. Distribution of loading levels of transformers in spring at noon under high solar conditions in the Step Change scenario.

These results highlight that DNSPs will need to initiate transformer upgrades in the near future to facilitate the anticipated increase in PV penetration, particularly under the step change ISP scenario where transformer overloading is significantly more pronounced.

Figure 26 illustrates the percentage of distribution cables, including both overhead and underground types, that exceed 100% of their rated ampacity at midday during spring across the investigated years. Under the step change ISP scenario, the proportion of LV and MV cables exceeding their thermal limits reaches approximately 5.8% by 2050. While the incidence of thermal overloading in cables is significantly lower than that observed in transformers, the implications can still be critical, particularly for MV cables. Cables operating beyond their thermal capacity may experience accelerated insulation degradation, and failures in MV cables can impact a large number of customers due to their upstream position and broader service coverage. As such, MV cables that reach unacceptable loading levels would likely require replacement sooner, despite the high costs and complexity associated with cable upgrades.

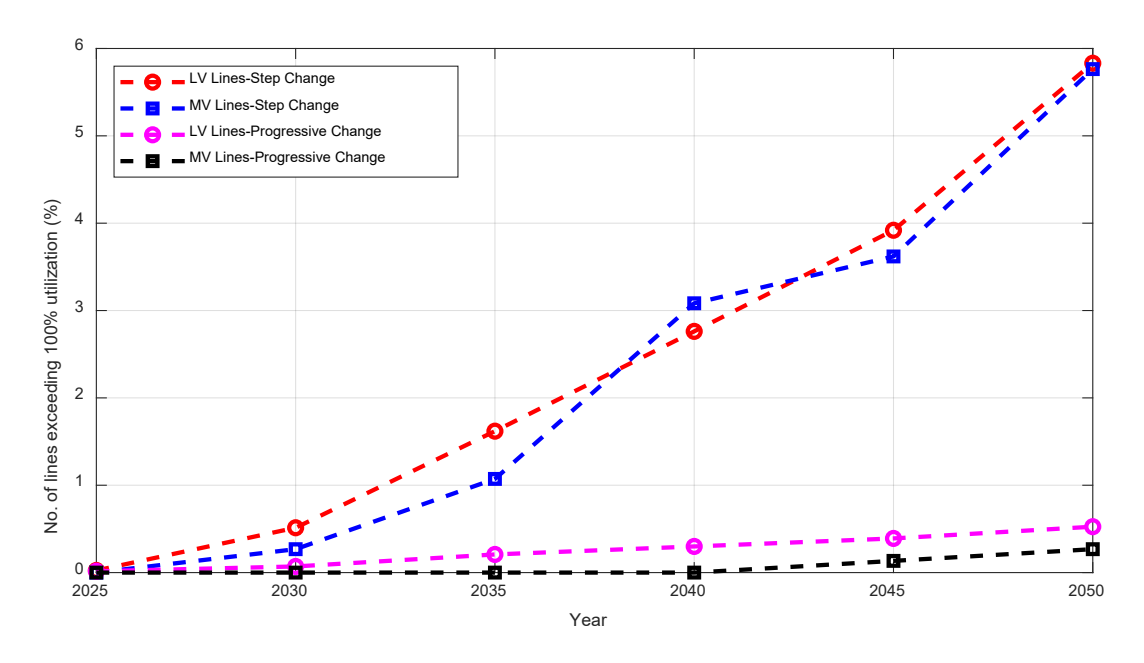


Figure 26.Number of MV and LV cables exceeding their ampacity at noon in spring under high solar conditions.

The impact of EVs on asset utilisation levels is relatively modest compared to the influence of PVs during the midday period. Table 6 summarises the effect of increasing EV penetration across the years during summer under the step change scenario at the evening peak. By 2050, approximately 23% of transformers in the network exceed 100% of their rated capacity, while only 2.62% surpass the 150% loading threshold. Similarly, both MV and LV cables exhibit fewer instances of thermal overload compared to those observed at midday due to high PV output. This outcome is primarily attributed to the diversified charging patterns of EVs, which distribute the load more evenly over time and reduce the simultaneous demand on network assets. As a result, the coincidence factor for EV charging remains low, alleviating excessive stress on transformers and cables during peak loading periods.

Table 6. Statistics on loading levels of cables and transformers at 7.30 p.m. in summer high solar conditions under the Step Change scenario.

Parameter	Year									
r di dilletei	2025	2030	2035	2040	2045	2050				
Transformers exceeding 100% loading (%)	0.4367	0.8734	1.3100	6.1134	13.9738	23.1441				
Transformers exceeding 150% loading (%)	0	0.4367	0.4367	0.4367	1.3100	2.6200				
LV cables exceeding 80% loading (%)	0.0672	0.0733	0.0825	0.1466	0.3085	0.6445				
LV cables exceeding 100% loading (%)	0.0061	0.0061	0.0061	0.0183	0.0305	0.1558				
MV cables exceeding 80% loading (%)	0	0	0	0.1340	0.4021	1.7426				
MV cables exceeding 100% loading (%)	0	0	0	0	0	0.4021				

6.3 Selection of LV areas for investigating solutions

As demonstrated by the preceding results, continuing to operate the network under BAU conditions is no longer feasible and would necessitate proactive intervention by DNSPs to accommodate the anticipated growth of CERs. This study explores the application of several existing solutions currently available in the market, alongside an in-depth evaluation of NEx, which serves as the primary focus of the investigation.

It is important to note that the purpose of this study is not to prescribe a single optimal solution for DNSPs, as the most appropriate approach will depend on a range of factors—including the specific characteristics of the distribution network, the financial implications of implementation, and the strategic objectives of individual DNSPs. Furthermore, voltage and curtailment issues were used as the key criteria to identify specific LV areas that would require the implementation of hosting capacity enhancement technologies to ensure safe and reliable network operation. The year 2035 was selected for this analysis, as it marks a point where overall voltage violations reached 13.36% under the step change scenario, and 5.6% under the progressive change scenario, indicating a growing need for intervention to maintain compliance with operational standards. Replacement of transformers, overhead lines, and underground cables exhibiting high loading levels has not been considered in the BAU scenario, as it is difficult to define the exact criteria DNSPs would apply to determine when such replacements should occur. Moreover, as indicated in [2], the application of transformer and conductor upgrades alone had minimal impact on improving the hosting capacity of the network, as voltage violations persisted even after such upgrades.

It is important to note that the replacement of distribution transformers and cables will still be required over time if thermal limits are exceeded by a significant margin, regardless of whether other hosting capacity enhancement technologies are implemented. These replacements are necessary not only for network performance but also to prevent asset failure and maintain safety standards.

All LV areas in the modelled network under the step change scenario were analysed for voltage violations and PV-related curtailment. Based on this analysis, six LV areas (which are identified by A-F in this study) were selected for further investigation, as they exhibited a higher incidence of voltage violations and curtailment compared to the others.

In addition to these performance metrics, several network characteristics were considered during the selection process, including the method of cable installation (i.e., overhead vs underground), the physical size of the LV area, and the number of LV circuits. These factors were included to ensure the selection captured a diverse and representative range of operating conditions typically found in distribution networks. This diversity allows for a more comprehensive evaluation of the performance of each hosting capacity enhancement technology across different network topologies.

Each LV area was investigated using three different technologies: STATCOMs, OLTCs for distribution transformers, and NEx. The performance of the network with the integration of each technology was analysed individually. For the STATCOM scenario, two cases were considered. The first involved placing a single STATCOM at the location with the highest PV curtailment—typically at the end of the LV circuit. In the second case, multiple STATCOMs were deployed, particularly in larger LV areas or those with several circuits. STATCOM placement also accounted for the upstream cable size. If the immediate upstream cable had a limited current carrying capacity, the STATCOM was instead placed at the nearest upstream bus connected to a larger cable. This approach aimed to avoid additional thermal stress on cables, as STATCOMs draw current from the grid, potentially increasing cable loading if not properly sited. Both OLTCs and NEx control were integrated to each

transformer in the LV area with the transformer size equivalent to the BAU condition. Note that NEx can also be installed further along the feeders if required.

6.4 STATCOM Model

In this study, STATCOMs are modelled with a total reactive power capacity of 50 kVAr, with each phase independently capable of exchanging up to 16.67 kVAr. This sizing aligns with the configurations used in recent pole-mounted STATCOM trials conducted across Australia. Figure 27 illustrates the V–Q characteristic of the modelled STATCOM. Each phase operates independently and follows a linear voltage–reactive power (V–Q) droop control strategy within the voltage range of 225 V (V_1) to 235 V (V_3), with 230 V (V_2) representing the nominal voltage in the LV network. In this control logic, negative reactive power values correspond to absorption, while positive values indicate injection. The operational point of each phase of the STATCOM is determined based on line-to-neutral voltage measurements. When the terminal voltage of a phase exceeds the defined droop limits, the STATCOM transitions to operate at its rated reactive power capacity.

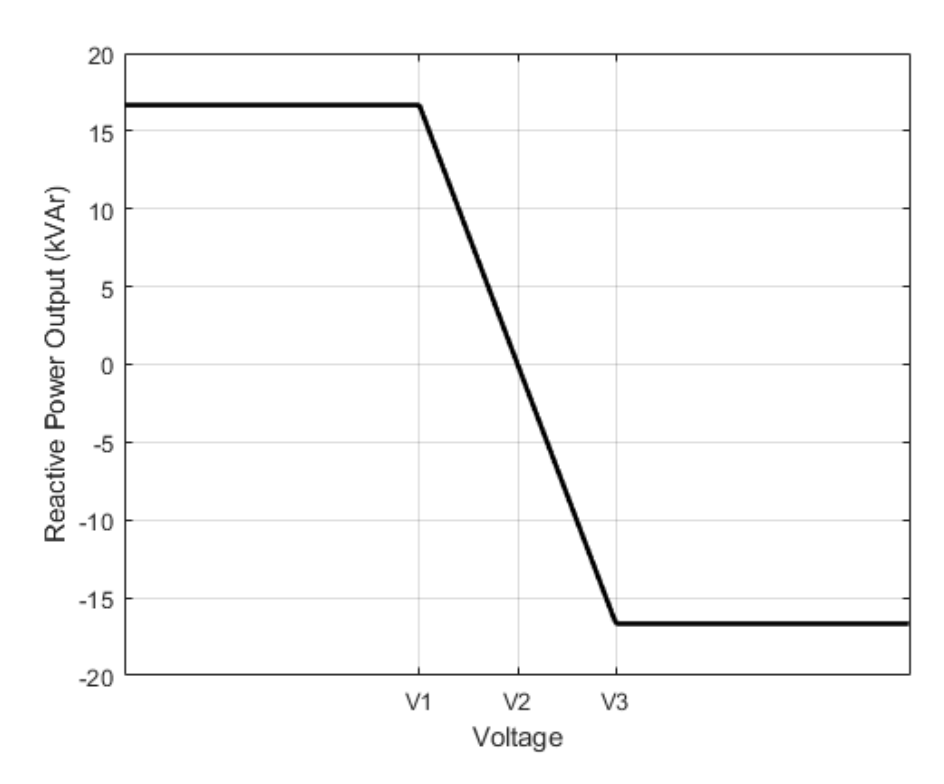


Figure 27. Voltage-reactive power characteristic for each phase of the modelled STATCOM.

It is important to note that STATCOMs may exhibit different V–Q characteristics depending on the manufacturer and the specific network conditions. However, in this study, the STATCOMs have been strategically placed at the end of LV circuits, where over-voltage conditions are most likely to occur. During peak solar generation periods, the upper voltage threshold of $235\,V\,(V_3)$ is regularly exceeded at these locations, causing the STATCOMs to operate at their maximum reactive power capacity. As a result, the specific shape of the V–Q droop curve becomes less influential, since the STATCOMs consistently operate at their rated limits under these conditions.

6.5 OLTC Model

OLTCs are used to control the tap position of transformers and are typically installed on the primary side. They serve to raise or lower the voltage at the start of a feeder to compensate for voltage rise or drop along its length. The secondary-side voltage is measured using a VT and fed to the Automatic Voltage Control (AVC) relay, where it is compared against predefined target values and allowable bandwidths. If the voltage exceeds these limits, a tap change is triggered. To prevent unnecessary tap changes caused by short-term voltage fluctuations, a time delay is applied before executing the control action [5].

In this study, OLTCs are considered as a solution to address voltage and curtailment issues in LV areas. To maximise OLTC effectiveness, it is assumed that the DNSP has access to smart meter data within the relevant LV area. Importantly, full visibility is not required—voltage measurements from critical nodes are sufficient. A similar trial was conducted in [14], where substation voltage setpoints were adjusted based on readings from a limited number of smart meters and state estimation. This approach significantly reduced voltage violations and showed strong potential for improving CER hosting capacity compared to the typical OLTC operation. As smart meter penetration increases across Australia—and with an accelerated rollout aiming for universal uptake by 2030 as per AEMC—DNSPs will increasingly have access to the data needed to implement such control strategies.

A QDSL model was developed in DIgSILENT PowerFactory for each OLTC in the investigated LV areas using a closed-loop approach. Line-neutral voltage measurements are provided to the model at each control cycle to determine the appropriate tap change. If a voltage violation is detected, a tap position adjustment is initiated (increase or decrease) within the transformer's tap limits to alleviate the issue. For the time-series simulations in this study, the initial tap position at the start of the simulation was set to the current tap position of the transformer.

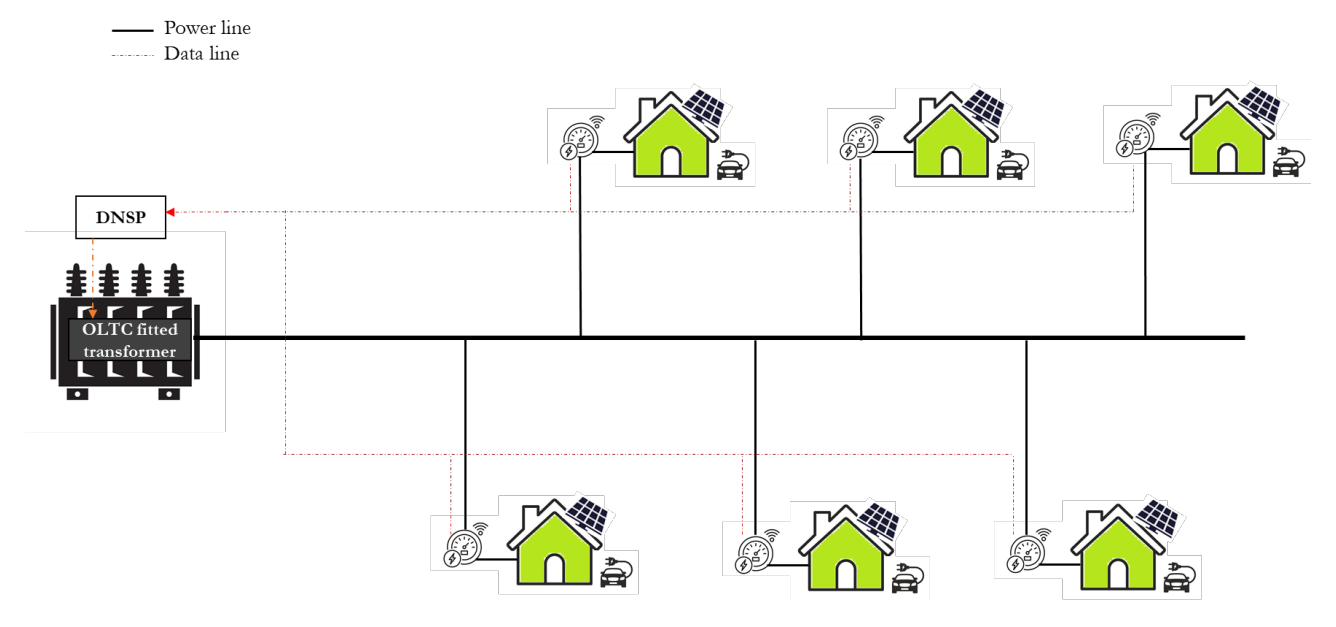


Figure 28. Overview of the architecture of the modelled OLTC controller in each LV area.

6.6 Comparison of Technologies

Each technology was assessed for its effectiveness in mitigating or alleviating grid constraints such as voltage violations, thermal loading, and total PV curtailment within the LV areas. Regarding cable installation methods, LV areas A, B, and D consisted of underground cables, LV area C included a mix of underground and overhead conductors, while LV areas E and F used overhead conductors. In terms of distribution system configuration, LV areas A to E, followed a typical radial arrangement with multiple circuits extending from the LV transformer, while LV area F was structured as a ring-type distribution system.

Table 7 presents the voltage violations observed at noon during spring under each technology scenario. A voltage violation was defined as any instance where a phase voltage at an LV bus exceeded the upper or lower statutory limits. The lower voltage threshold was included due to the high level of voltage unbalance observed in the modelled network.

Table 7. Voltage violations of each investigated LV area at noon in spring with the integration of different technologies.

	Voltage violations (%)										
LV Area	BAU	Single STATCOM	Multiple STATCOMs	OLTC	NEx						
Α	83.2	68.4	10.5	0.0	0.0						
В	88.0	84.0	54.0	8.0	0.0						
С	72.2	52.8	16.7	47.2	0.0						
D	27.8	19.55	4.5	0.0	0.0						
Е	51.6	41.9	19.4	0.0	0.0						
F	73.1	69.2	69.2	19.2	0.0						
Total	62.9	53.4	23.8	7.13	0.0						

Under the BAU condition, all six LV areas exhibited severe voltage violations, primarily due to high PV penetration. Figure 29 shows the variation of line-neutral voltage magnitudes and asset utilization levels of LV area E under the BAU condition. Note that the maximum voltage observed at each bus has been used for the analysis. Red indicates voltages exceeding 253 V and loading levels (in lines and transformers) exceeding 100%. Orange highlights voltages above 250 V, yellow represents voltages above 240 V—where Volt-Var control begins in inverter operation—and green corresponds to voltages below 240 V and loading levels below 100%. If inverters are non-compliant to AS: 4777:2:2020, the voltage levels reach much to higher levels. Figure 30 shows the impact of disabling Volt-Watt and Volt-Var control in the investigated LV areas under the BAU condition on LV area E, as all buses have now exceeded the upper statutory limit. Hence it is vital that inverters comply to the required grid code to reduce the impact of high PV penetration on the distribution network.

In the single STATCOM scenario, where a single STATCOM was placed at the location of highest PV curtailment, only modest reductions in voltage violations were achieved. The maximum improvement observed was a 19.4% reduction in LV area C. This limited effectiveness is attributed to the presence of multiple LV circuits within each area; while the STATCOM improved voltages locally within its own circuit, it had negligible impact on other circuits in the same LV area experiencing overvoltage conditions.

In the multiple STATCOM scenario, the number of STATCOMs installed in each LV area was based on the number of circuits and the distribution of voltage violations. As a result, two LV areas received two STATCOMs, one area received five, another received four, one received three, and one area received only one. The LV area with only one STATCOM was the ring-type network (LV area F), which showed no significant benefit from additional STATCOMs. Therefore, to maintain cost-effectiveness, this area was operated under the same configuration as the single STATCOM scenario. Considerable improvement in reduction of voltage violations can be observed in

the multiple STATCOM scenario compared to the BAU and single STATCOM scenario, with a maximum reduction of 72.7 % in LV area A. Figure 31 shows the variation of voltage and loading levels of LV area E under the multiple STATCOM scenario.

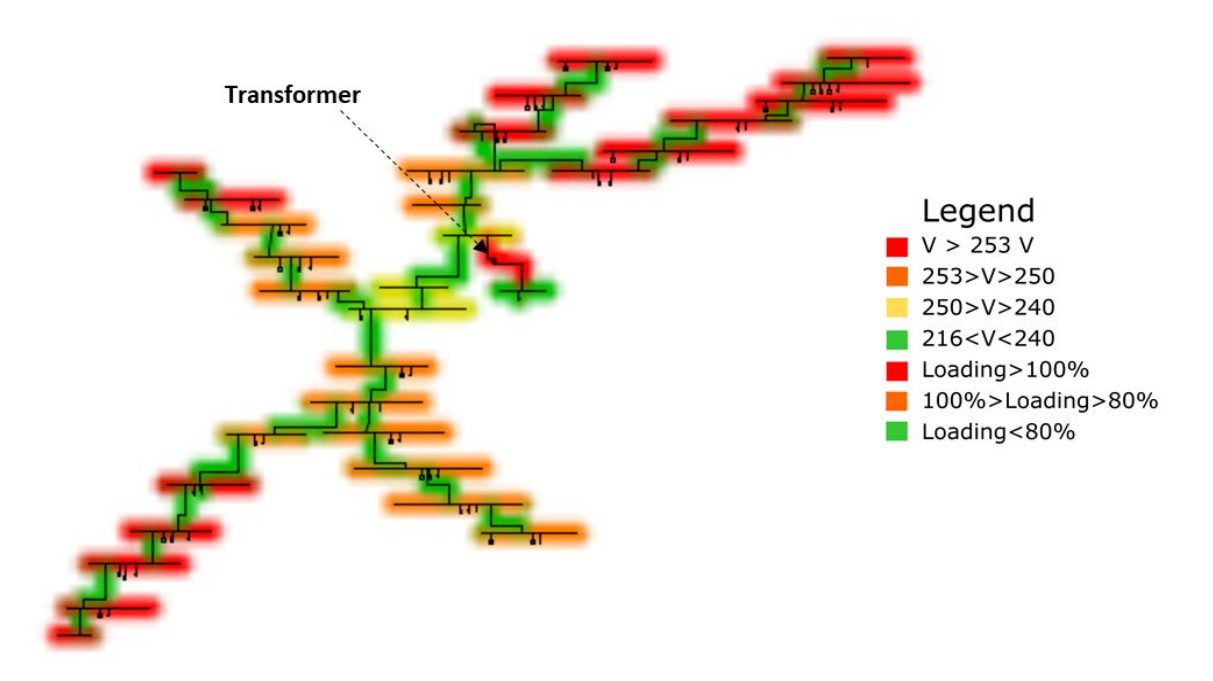


Figure 29. Heatmap illustrating the variation of line-neutral voltages and loading levels of lines and transformer in an investigated LV area in BAU condition.

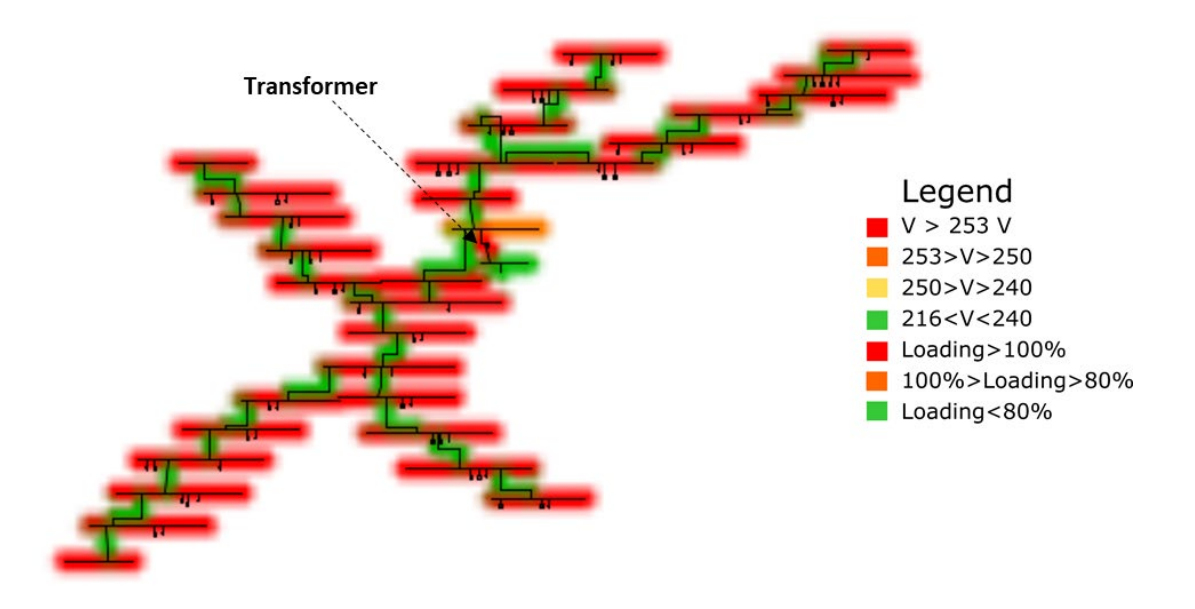


Figure 30. Heatmap illustrating the variation of line-neutral voltages and load levels of lines in an investigated LV area with Volt-Watt and Volt-Var disabled under BAU condition.

OLTCs and NEx demonstrated the most substantial improvements in voltage management, with total voltage violations across all six LV areas reduced to 7.13% and 0%, respectively. Under OLTC integration, all six distribution transformers operated at the minimum tap position (tap position 1) at midday, aiming to suppress elevated voltages at the ends of the LV circuits. Figure 32 illustrates the variation in transformer tap position for LV area C throughout the day during spring. The transformer tap position begins with the default BAU setting at the start of the simulation.

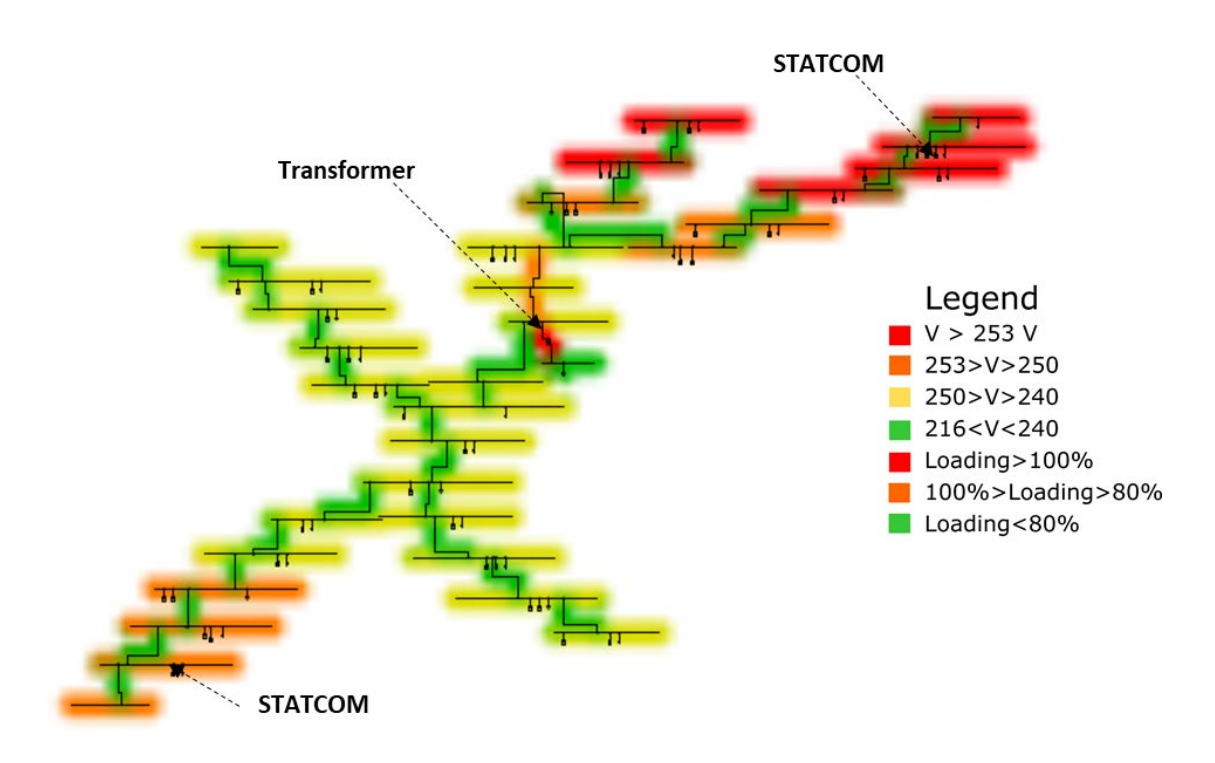


Figure 31. Heatmap illustrating the variation of line-neutral voltages and loading levels of lines and transformer in an investigated LV area with multiple STATCOM integration.

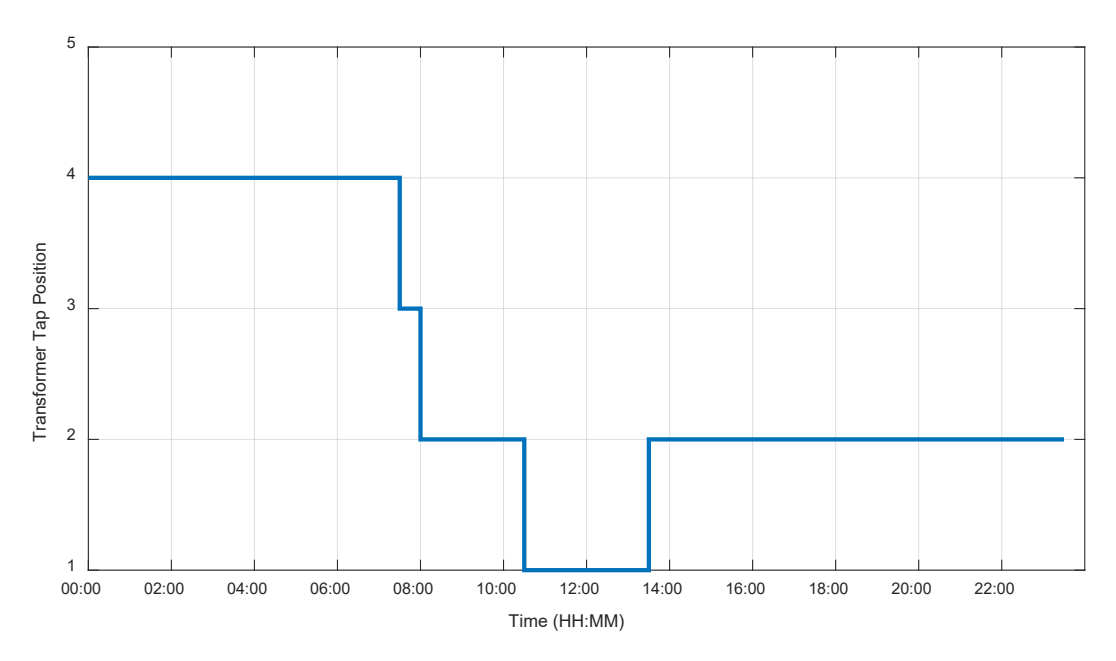


Figure 32. Variation of transformer tap position of LV area C across the day in spring under high solar conditions.

An interesting observation arises in LV area C, where voltage violations persist even with OLTC integration—not due to over voltages, but due to under voltages in phase C, which fall below the lower statutory limit of 216 V. This issue is attributed to a high degree of voltage unbalance in the network, where phase C consistently operates at a lower voltage compared to phases A and B. When the OLTC reduces the tap position to mitigate overvoltage in phases A and B, it simultaneously lowers the already reduced voltage in phase C, resulting in new undervoltage violations. This highlights a key limitation of OLTCs: they adjust the tap position uniformly across all three phases, lacking the capability to independently regulate each phase. In highly unbalanced networks, this uniform control strategy can inadvertently worsen conditions for one or more phases.

This is where NEx demonstrates a clear advantage over OLTCs, as it has the capability to regulate each phase independently. The application of the developed NEx model resulted in the complete elimination of voltage violations (0%) across all LV areas. Since NEx is installed at the secondary terminals of the LV transformer, it can influence the voltage of all downstream LV circuits, similar to the function of an OLTC. In the model, the initial target voltage for each phase was set to the nominal value of 230 V and was adjusted as needed to address voltage limit breaches. These adjustments were made while considering the operational constraints of the NEx device, specifically the ±10% buck-boost capability of the series converter. It is important to note that the current version of NEx can increase or decrease voltage by up to 10% at the point of connection on the transformer's secondary side. This enables it to effectively correct any overvoltage or undervoltage conditions as long as the required correction falls within the ±10% operating range. As such, NEx is able to fully mitigate voltage violations in the scenarios examined in this study. Figure 33 shows the variation of line -neutral voltage magnitudes and asset loading levels of LV area E with the integration of NEx. When compared with Figure 29, all voltages are within statutory limits.

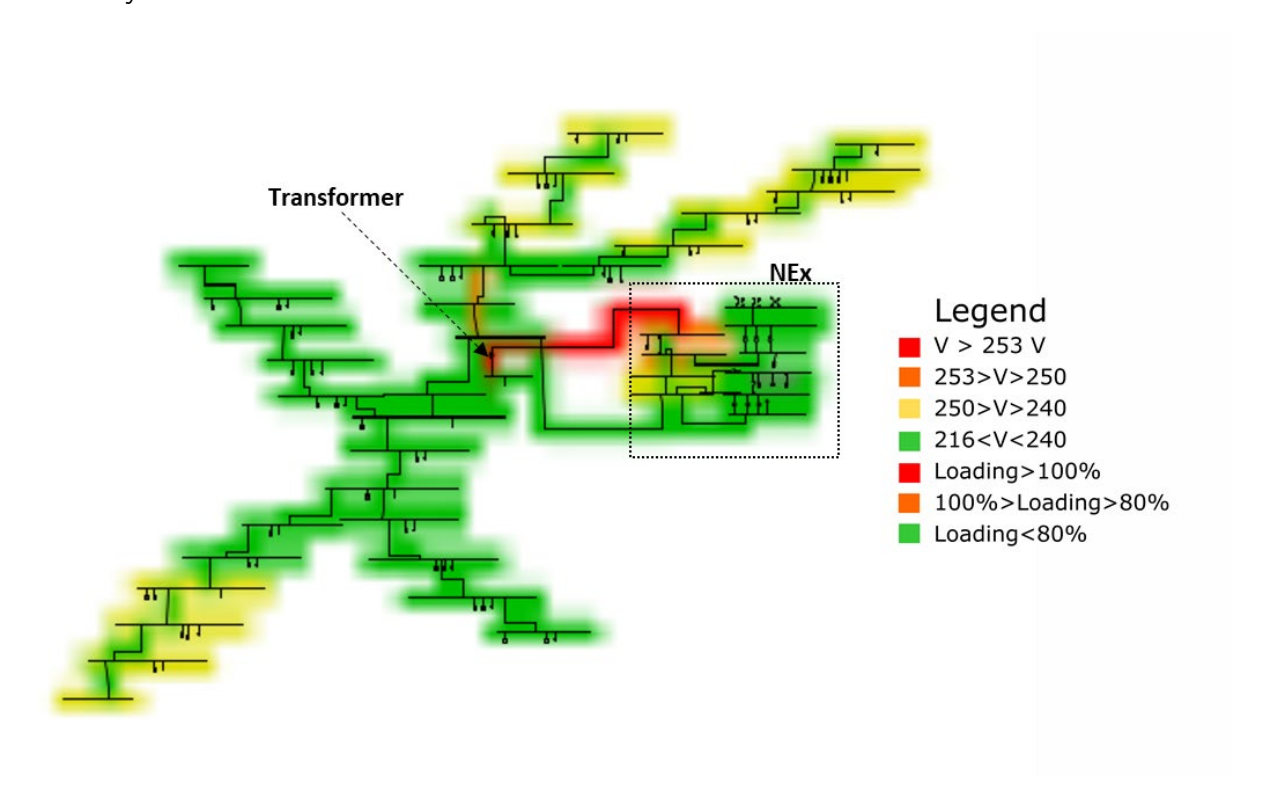


Figure 33. Heatmap illustrating the variation of line-neutral voltages and loading levels of lines and transformer in an investigated LV area with NEx integration.

Table 8 presents key percentiles of voltage unbalance at noon, calculated using VUF and PVUF for all LV buses in the six selected LV areas. VUF, which accounts for both voltage magnitudes and phase angles, shows an improvement with NEx integration relative to other technologies and scenarios, while PVUF, which considers only line-to-neutral voltage magnitudes, increases with both NEx and OLTC integration. This divergence arises because NEx regulates voltage only at the transformer secondary terminals—i.e., at the start of LV circuits—while the remainder of the network continues to operate in an unbalanced manner. Furthermore, since voltage violation mitigation is prioritized by altering the target voltage at the beginning of the LV circuits, each phase may have a different target voltage, thereby affecting PVUF. In addition, the reduction in voltage levels leads to decreased curtailment, resulting in greater PV injection that, when unevenly distributed among phases, amplifies the deviation between individual phase voltages and their mean, further increasing PVUF.

Table 8. Percentiles of voltage unbalance at noon in spring across the 6 LV areas with the integration of different technologies.

Daramatar nargantila		Voltage unbalance									
Parameter- percentile	BAU	Single STATCOM	Multiple STATCOMs	OLTC	NEx						
VUF - 50 (%)	1.9139	1.8085	1.6778	1.3431	0.7665						
VUF - 75(%)	2.3962	2.3277	2.0234	1.8362	1.1720						
VUF - 90 (%)	3.3106	3.1701	3.0699	2.7792	2.1964						
VUF - 95 (%)	3.9071	3.6958	3.8275	3.5223	3.0722						
VUF - 99 (%)	4.2609	4.1070	4.4724	3.9360	3.4455						
PVUF - 50 (%)	2.0220	2.0313	1.9817	2.2396	2.2866						
PVUF - 75(%)	2.8658	2.9007	3.0666	4.0308	4.0226						
PVUF - 90 (%)	4.1152	4.5991	4.4341	6.2542	5.9493						
PVUF - 95 (%)	5.0274	5.2087	5.2394	7.7436	6.9302						
PVUF - 99 (%)	6.1533	6.3758	6.3122	8.5236	8.2783						

Table 9 presents the curtailment observed during the half-hour period at noon in spring under each of the investigated technologies. A trend similar to that observed in the voltage distribution analysis is evident, with OLTCs and NEx delivering the best overall performance in terms of curtailment reduction.

Table 9. Curtailment during the half-period at noon in spring across the 6 LV areas with the integration of different technologies.

LV Area	BAU	Single STATCOM	OLTC	NEx	
Α	23.5	18.9	5.0	0.2	0.5
В	24.5	19.1	8.5	1.8	0.0
С	16.9	11.2	6.9	1.7	2.5
D	14.0	10.5	6.0	0.6	1.1
Е	15.0	7.5	5.2	0.0	0.4
F	14.2	8.8	8.8	0.7	0.6
Total	108.1	76.0	40.4	5.0	5.1

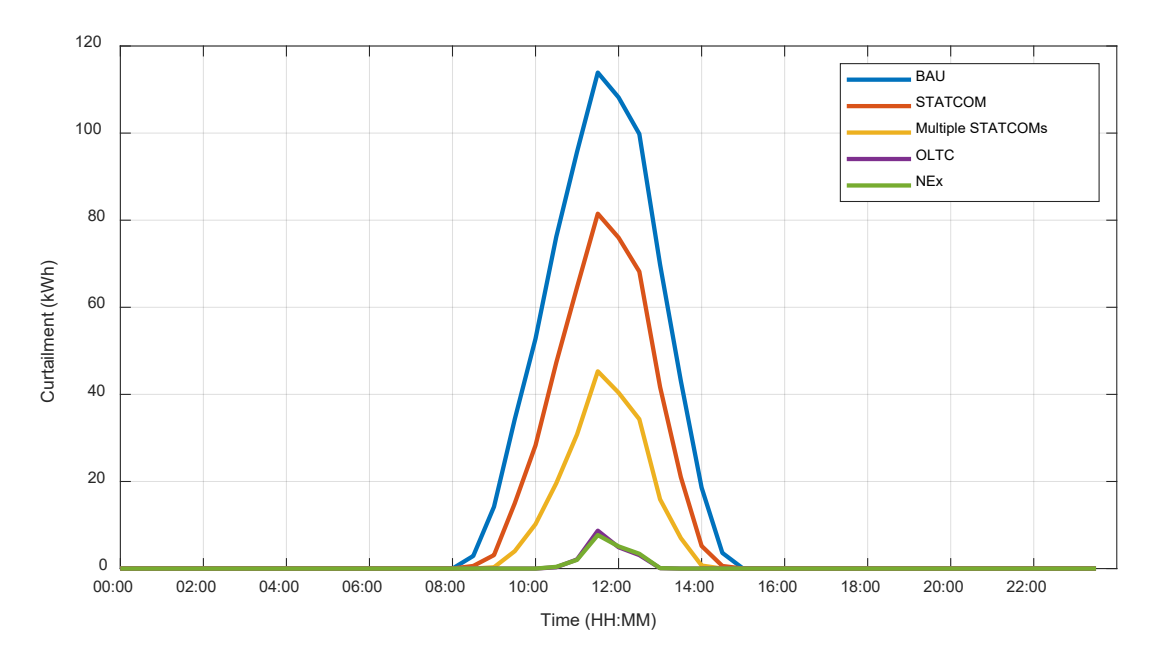


Figure 34. Variation of total curtailment of the investigated areas under high solar conditions in spring.

Interestingly, some curtailment still occurs in both the OLTC and NEx scenarios, despite the absence of voltage violations. This is primarily due to the implementation of Volt-Var priority in the inverter control logic. According

to this scheme, the inverter must prioritise reactive power support (Volt-Var response) when operating near its rated capacity. As a result, active power output is curtailed in certain instances to ensure the inverter does not exceed its apparent power rating. This behaviour is consistent with current inverter standards and reflects the inherent trade-off in prioritising network stability and voltage regulation over maximising active power export under constrained operating conditions.

Table 10 presents the transformer loading levels at each LV area during noon in spring. A significant improvement is observed under the NEx scenario when compared to the BAU condition, and this enhancement can be attributed to several key factors. First, the reduction in voltage levels across the LV areas achieved by NEx results in lower reactive power demand from inverters operating under Volt-Var control, thereby reducing the phase current magnitudes at the transformer terminals. Additionally, NEx actively performs power factor correction, supplying the necessary reactive power locally, which further alleviates the reactive power burden on the transformer. Another important contribution comes from NEx's ability to balance the phase currents drawn by the transformer. This means that each phase is adjusted to draw approximately equal current, effectively corresponding to the average of the three phase currents. In cases where one phase is heavily loaded, this current balancing function reduces the current drawn by the overloaded phase and redistributes it more evenly. As a result, the overall transformer loading (which is influenced by the most heavily loaded phase) is significantly reduced. Furthermore, slight increase in loading levels are observed in the STATCOM scenarios, as more reactive power is drawn from the grid to correct the voltages at the STATCOM integrated locations. Figure 35 shows the variation of loading levels of a transformer during the day in spring, in an investigated LV area with the integration of different solutions. Detailed data on transformer currents and power factor data are provided in appendix B.

Table 10. Transformer loading levels at noon in spring with the integration of different technologies.

		Transformer loading (%)										
LV Area	Transformer size (kVA)	BAU	Single STATCOM	Multiple STATCOMs	OLTC	NEx						
А	750	112.0	115.5	128.0	116.8	79.7						
В	500	150.0	154.6	167.9	150.3	121.9						
С	315	147.5	152.7	156.6	154.0	87.8						
D	500	216.7	219.2	224.4	220.8	163.2						
Е	315	126.4	139.9	148.9	150.7	101.8						
F	315	182.3	185.2	185.2	189.7	124.2						

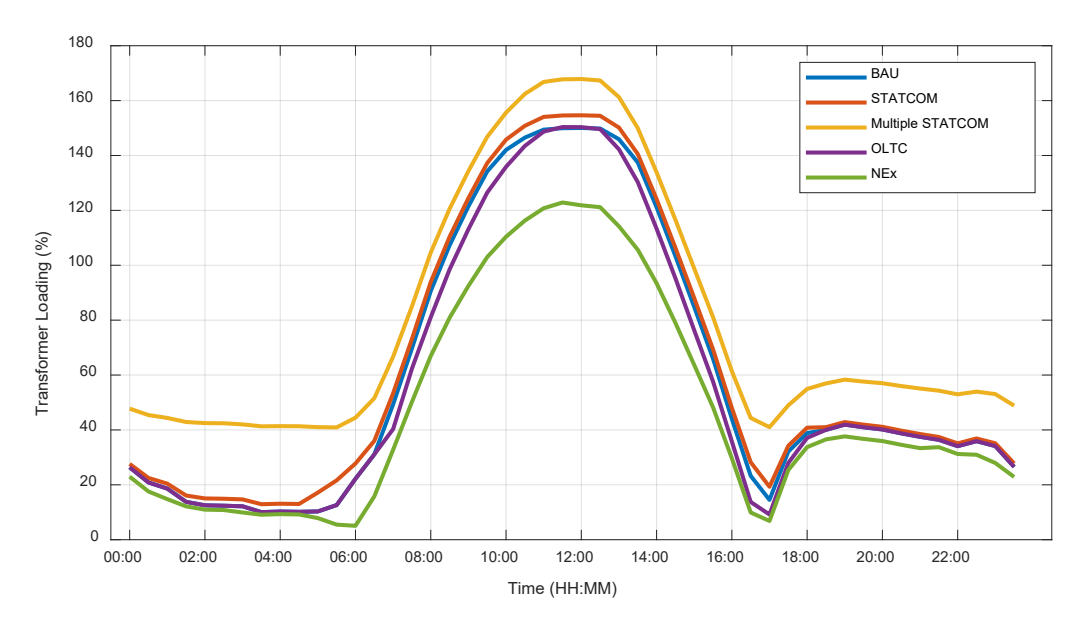


Figure 35. Comparison of loading levels of a transformer in an investigated LV area in spring under high solar conditions.

Table 11 presents the distribution of loading in LV cables of all 6 LV areas under the implementation of each investigated technology using key percentiles. A modest increase in loading levels at higher percentiles is observed across all technologies when compared to the BAU scenario. In the case of STATCOMs, particularly under the multiple STATCOM scenario, the increased absorption of reactive power contributes to higher cable loading. It is important to note that all technologies result in reduced PV curtailment relative to BAU, leading to greater active power injection into the grid and, consequently, increased loading on LV cables. This effect is notable in both the OLTC and NEx scenarios, where significant reductions in curtailment result in increased cable utilization. However, despite greater curtailment reduction, the loading levels at higher percentiles in OLTC and NEx cases remain lower than those observed in the multiple STATCOM scenario, highlighting the influence of reactive power flow on cable loading. Ultimately, any cables that are inadequately sized and exceed acceptable loading thresholds would require replacement, irrespective of the technology deployed.

Table 11. Percentiles of loading levels of all LV cables in the investigated LV areas at noon in spring under high solar conditions with the integration of different technologies.

Metric		LV line loading (%)											
Metric	BAU	Single STATCOM	Multiple STATCOMs	OLTC	NEx								
50 th percentile	19.455	20.317	25.422	21.245	21.306								
75 th percentile	43.279	44.958	46.918	42.848	43.288								
90 th percentile	75.493	77.894	83.941	79.988	79.003								
95 th percentile	95.528	100.42	110.66	102.43	101.14								
99 th percentile	136.13	147.17	154.12	147.1	144.99								

7 Cost-Benefit Analysis

To evaluate the financial benefits of each technology, a cost-benefit analysis (CBA) was conducted using the Customer Export Curtailment Value (CECV) metric introduced by the Australian Energy Regulator (AER). The CECV reflects the value of curtailed energy that could have been exported to the grid, serving as a proxy for lost revenue or benefit. It is important to note that CECV does not represent the full spectrum of financial impacts faced by DNSPs. Other factors such as customer complaints, penalties for regulatory non-compliance, and damage to consumer appliances or network assets can impose significant additional costs. However, for the purposes of this CBA, only the financial benefit derived from avoided curtailment (as represented by the CECV) has been considered.

To calculate the CECV for the investigated year, half-hourly CECV values were obtained for the calendar year 2035 using the CECV workbooks specific to Queensland. It is important to note that the CECV framework was first introduced in 2022 and is updated annually. A noticeable shift in average CECV values during spring—particularly during peak PV generation periods—was observed in the 2035 data in the 2023 and 2024 versions of the CECV workbooks, indicating a reduction in the financial benefit of curtailed energy. Figure 36 illustrates the variation in average CECV values at each half-hour interval (referred to as time steps) for spring in the year 2035, as sourced from both the 2023 and 2024 workbooks.

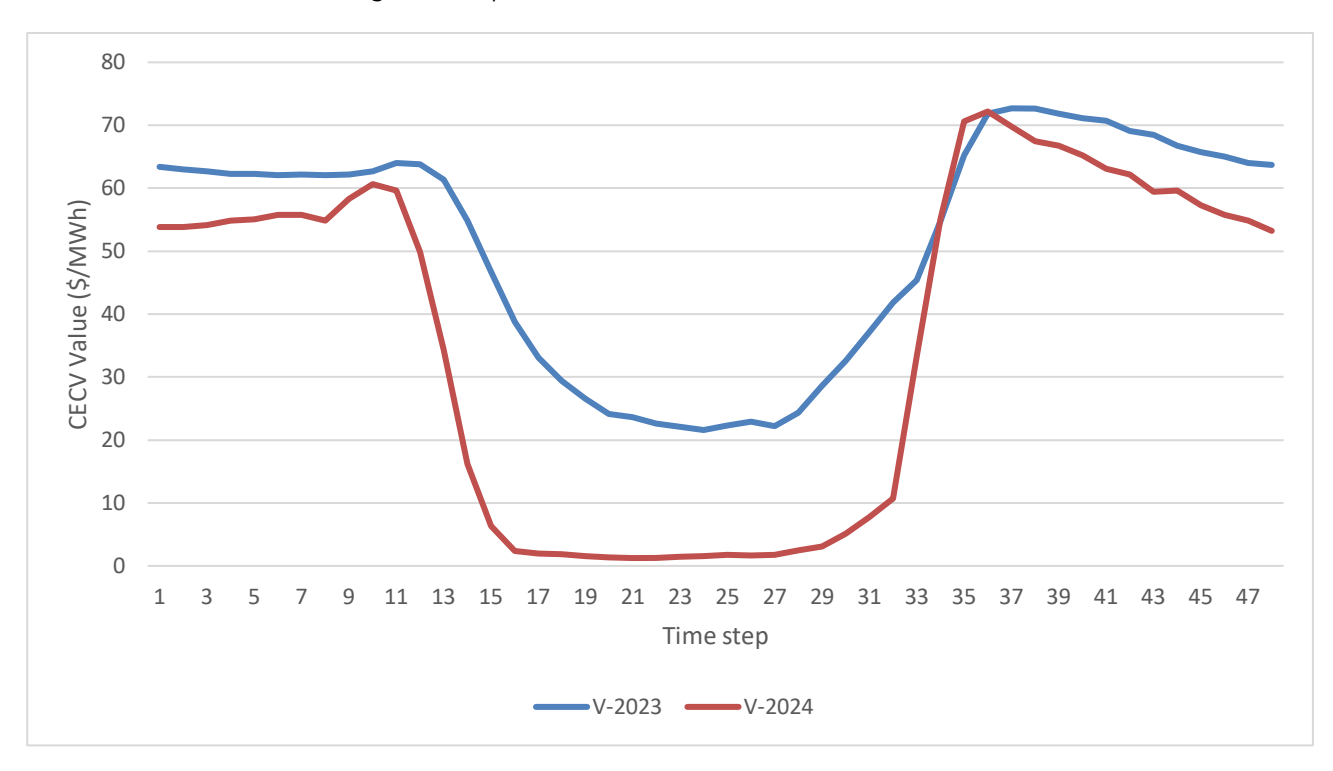


Figure 36. Average CECVs for each half-hour period in spring for Queensland region in the year 2035.

This suggests that the financial benefit from solar PVs, as quantified by CECV, may not be substantial in the coming decade. For the analysis, the CECV values were separated by season, and average half-hourly CECV values were calculated for each season of 2035. This allowed for the construction of average daily CECV profiles for each season. Similarly, daily curtailment profiles were developed for high irradiance conditions across the investigated areas (as shown in Figure 34). Using historical irradiance data for the modelled location, the number of high solar irradiance days per season was determined and assumed to remain consistent in 2035. The seasonal curtailment curves were then multiplied by the corresponding daily seasonal CECV profiles and the number of high irradiance days to estimate the seasonal CECV value. Finally, these seasonal values were summed up to determine the annual average CECV value for each technology.

Table 12 presents the final CECV results for each technology considering the investigated six LV areas. The cost values reflect the implementation of each technology across all six LV areas and are indicative only, as actual costs may vary based on manufacturer pricing, technology advancements, and installation-specific factors. For instance, the current estimated target price of a 1 MVA-rated NEx unit (in significant production volumes) is approximately \$20,000 (AUD), according to Third Equation Ltd. Additional installation costs would apply, particularly due to required network downtime for connecting the NEx at the LV transformer secondary terminals.

Among the technologies assessed, NEx offers the highest annual CECV benefit at AUD 3,855 (2023 CECVs), followed closely by OLTC. Under the BAU condition the CECV was calculated to be \$3,895 (2023 CECVs). The multiple STATCOM configuration provides a moderate benefit, while a single STATCOM per LV area yields the lowest CECV benefit. However, it is critical to acknowledge that the payback period cannot be evaluated based solely on the CECV metric. Ensuring compliance with voltage standards and grid codes remains a fundamental obligation for DNSPs, with non-compliance potentially leading to significant technical and financial risks.

Table 12. Cost benefit analysis results for each technology considering all six LV areas.

Technology	Approximate total cost (\$)*	Annual CECV benefit (\$) - 2023 version	Annual CECV benefit (\$) - 2024 version
Single STATCOM per LV area	150,000 - 240,000	1807.13	476.92
Multiple STATCOMs per LV area	425,000 - 680,000	3058.94	762.94
OLTC	510,000	3841.35	900.21
NEx	120,000 + installation costs	3854.57	902.01

^{*} Note that approximate costs have been used for each technology and actual costs may vary depending on installation costs and different manufacturers for each technology.

It is important to emphasise that the economic analysis has been presented using the lens of CECV metric. This would only measure the revenue lost through constrained exports. However, the financial impact due to voltage breaches and asset overloading (compliance costs, degraded life of assets, etc) for DNSPs needs to be considered in the full cost benefit analysis. Furthermore, maintaining customer voltages within statuary levels is an obligation for DNSPs, hence investments on grid support technologies would be required in the coming years to integrate the expected CER penetration, to meet these obligations. The lower product cost associated with the NEx together with its performance in mitigating voltage issues, reducing overloading, while increasing prosumer exports presents the NEx as a viable solution for DNSPs to manage networks with high CER penetration.

8 Performance Evaluation of NEx Under Hypothetical Network Scenarios

8.1 Resolving undervoltage violations

To evaluate the performance of NEx under higher loading conditions and in grids with undervoltage violations caused by increased demand, a modified EV charging scenario was developed. The peak of the diversified charging curve was adjusted to 2.0 kW for 3.68 kW chargers and 4.5 kW for 7.68 kW chargers, thereby increasing evening peak demand due to greater EV charging activity. The summer season in the year 2050 was selected for this analysis, as it corresponds to the highest projected EV penetration and peak loading conditions. As shown in Figure 37, which presents the line-to-neutral voltage distribution (in percentiles) for an affected LV area, the BAU scenario reveals undervoltage issues predominantly on phases B and C, while phase A remains above the lower statutory voltage limit. With NEx integration, these undervoltage violations on phases B and C are mitigated, resulting in voltage values within acceptable limits. Meanwhile, phase A voltage remains largely unchanged compared to BAU, highlighting the ability of NEx to control each phase separately. It is important to note that determining the ideal target input voltage would be the key in alleviating the voltage issues using NEx, and in this study it is calculated from the developed NEx QDSL model.

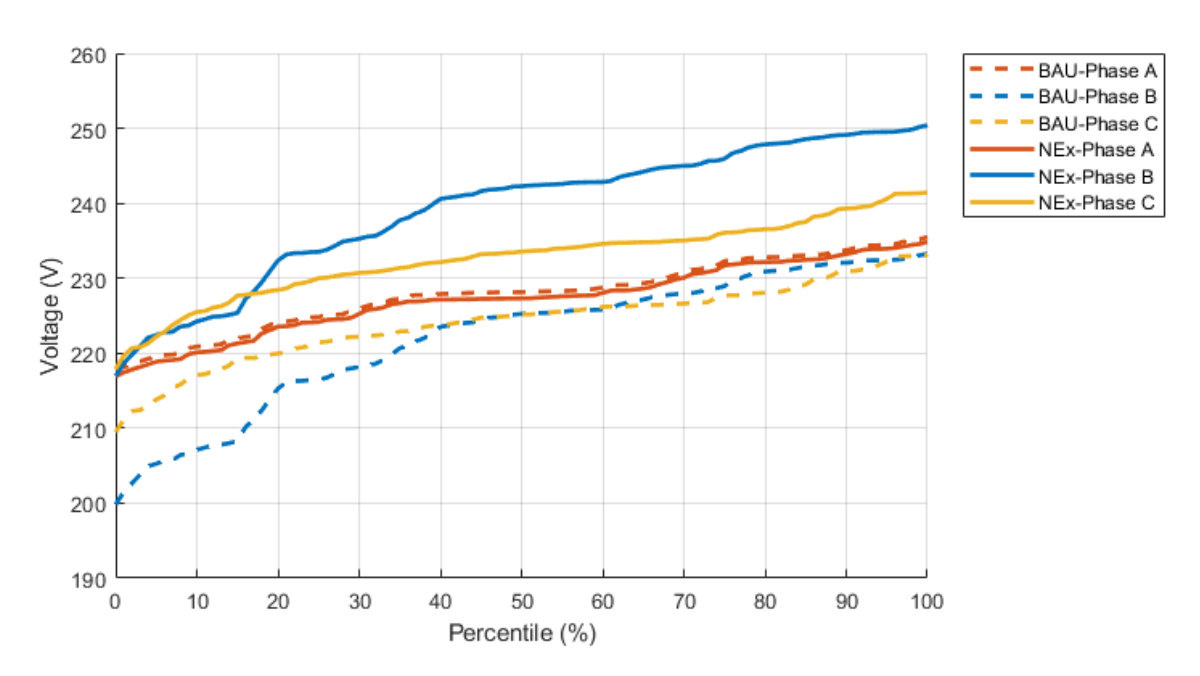


Figure 37. Comparison of voltage distribution percentiles across all nodes at 7:30 p.m. in summer under BAU and NEx scenarios.

8.2 Impact of line R/X ratios

The impact of NEx in higher resistive LV grids was evaluated by modifying line parameters in a selected LV area. For this analysis, the LV area was isolated from the rest of the network and supplied by a source connected to the MV bus, operating at 0.95 p.u. CER penetration and operating conditions reflected those expected in 2035 during spring midday under high solar conditions. The resistance of the cables was increased using a scaling factor (1,1.5 and 2.5).

Figure 38 shows the line-neutral voltage distribution across all nodes in the LV area for different resistance scaling factors. The x-axis represents the number of nodes exhibiting a higher voltage than the value denoted by

the y-axis. As expected, increased resistance led to greater voltage rise, resulting in more upper voltage limit violations. With NEx integrated, voltages remained within acceptable limits.

Compared to STATCOMs, NEx performance would not be affected by changes in R/X ratio. This is because voltage regulation is handled at the start of the LV area by the series converter, with no reactive power exchange. In simple terms, if a ±10% voltage change per phase (relative to nominal) at the feeder head is sufficient to resolve voltage issues downstream, NEx will be effective. Therefore, selecting the correct target voltage at the feeder head is critical and must be based on the behaviour of the downstream network. The dynamic response of NEx under a weak grid scenario is presented in chapter 9.

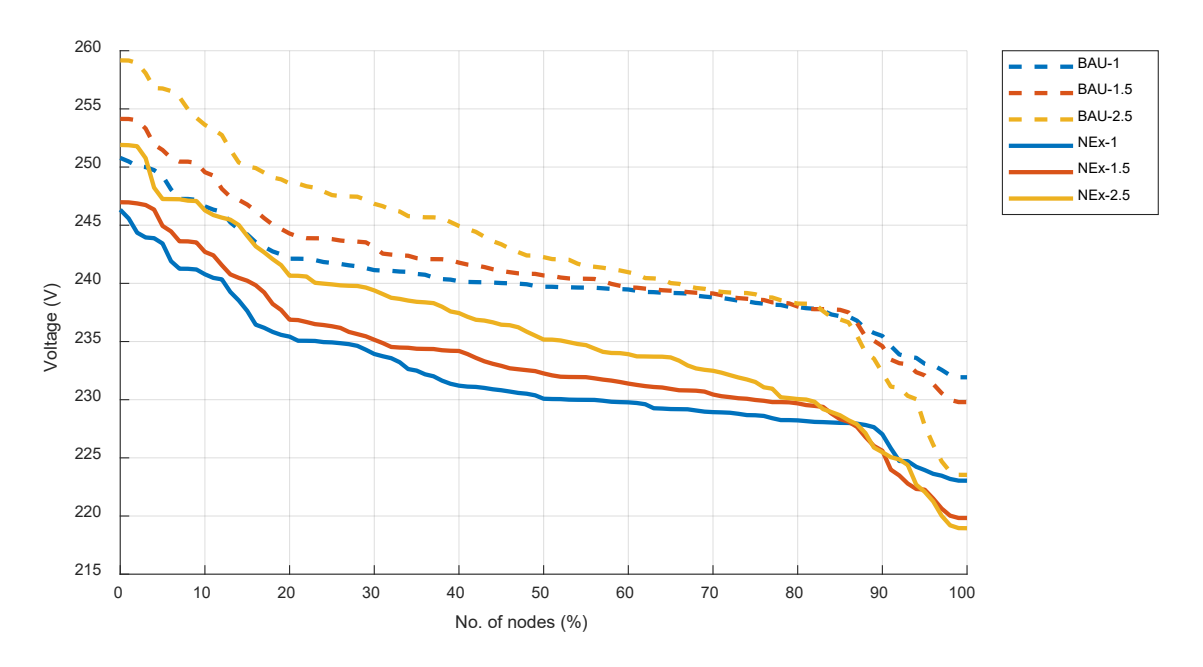


Figure 38. Voltage distribution of all nodes under BAU and NEx scenarios with different scaling factors.

8.3 Power distribution among phases

Another key capability of NEx is its ability to dynamically redistribute power among phases under unbalanced loading or generation conditions. In scenarios where one phase experiences excessive solar generation—resulting in reverse power flow—while the other phases continue to draw power from the grid, NEx can internally balance the system by shifting the excess energy to the phases which draw power from the grid, thereby reducing the loading level of the transformer.

9 Operational Testing and Performance Evaluation of the NEx System in the o-30 kVA Power Range

9.1 Description of test setup

The test setup consists of a 30 kVA grid simulator (TopCon TC.ACS Regatron), capable of applying controlled disturbances in voltage magnitude, phase angle, and frequency. A variable resistive load bank is employed to emulate different load conditions on the system.

For data acquisition, an Imperix B-Box 3.0 is used to record the input and output voltages and currents of the NEx trimming transformer unit at a sampling rate of 1 kHz. All voltage and current measurements are reported in RMS values.

This setup enables the emulation of various grid-side and load-side scenarios, including dynamic load changes and grid disturbances. Additionally, an inductive load bank is incorporated to generate different reactive load components, allowing for comprehensive testing under mixed load conditions.

A solar inverter emulator is also integrated into the setup to provide simulated generation conditions, enabling the assessment of the NEx performance under regenerative (back-feeding) load scenarios.

Measurement Convention:

- Grid-side measurements are denoted by "1" (e.g., V1_ABC, I1_ABC, P1, PF1).
- Load-side measurements are denoted by "2" (e.g., V2_ABC, I2_ABC, P2, PF2).

The test system schematic is presented in Figure 39, and the photograph of the NEx system and laboratory setup is shown in Figure 40.

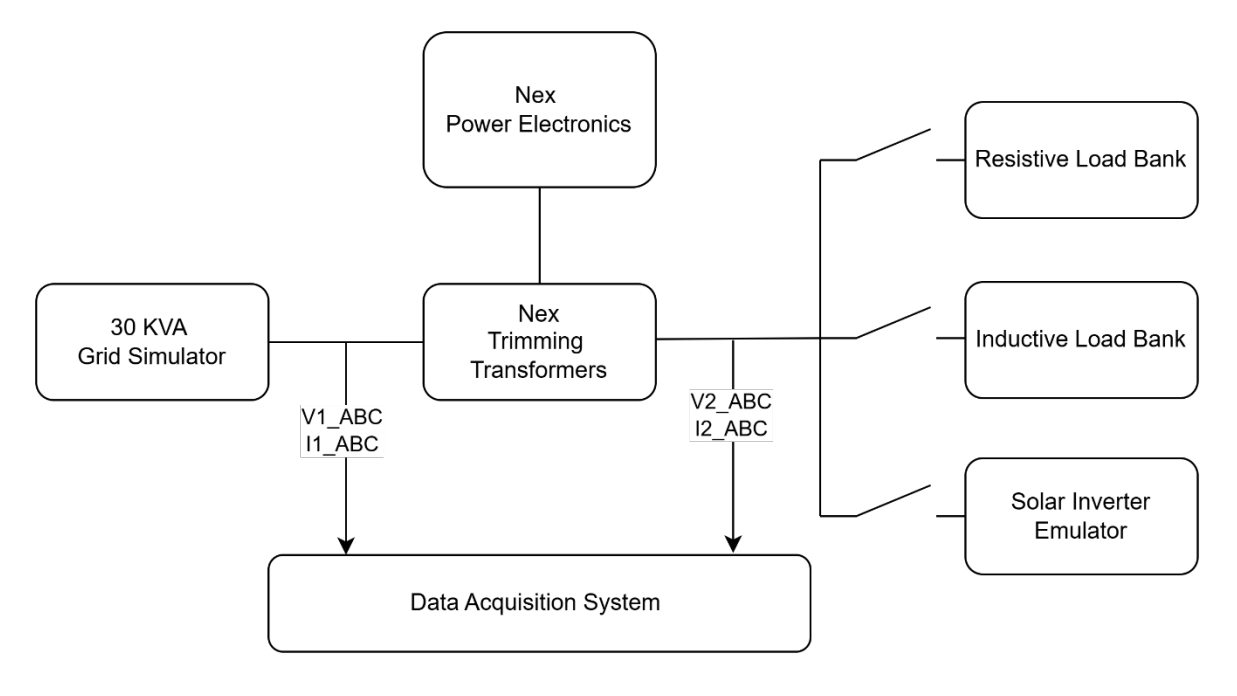


Figure 39. Test system schematic.

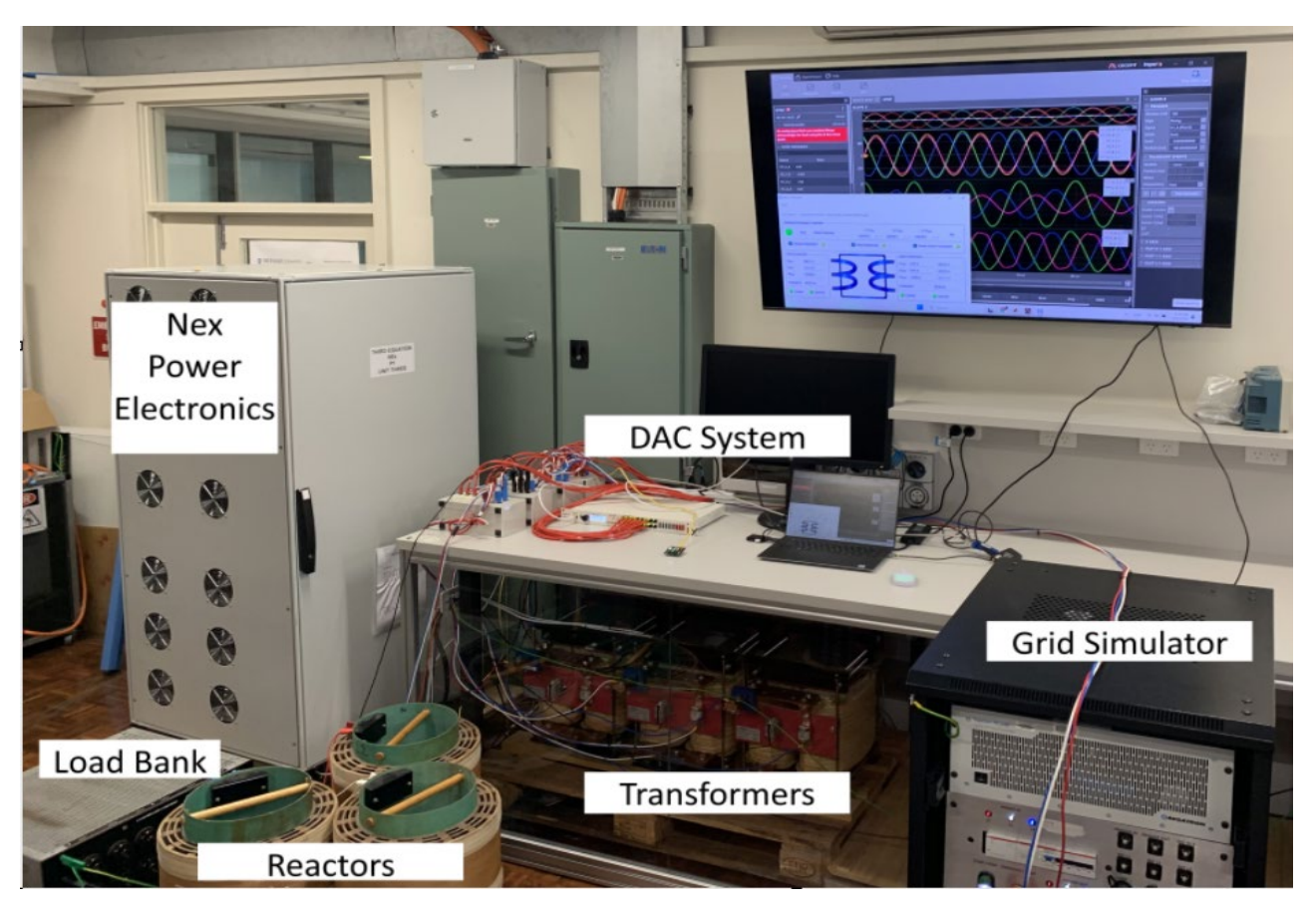


Figure 40. NEx system and laboratory setup.

9.2 Test scenarios and methodology

Initially, each function of the NEx system — Phase Balancing (PB), Power Factor Correction (PFC), and Voltage Regulation (VR) — was tested individually to ensure proper operation. Subsequently, different combinations of these functions were activated to evaluate the NEx system's performance under various grid conditions and load scenarios.

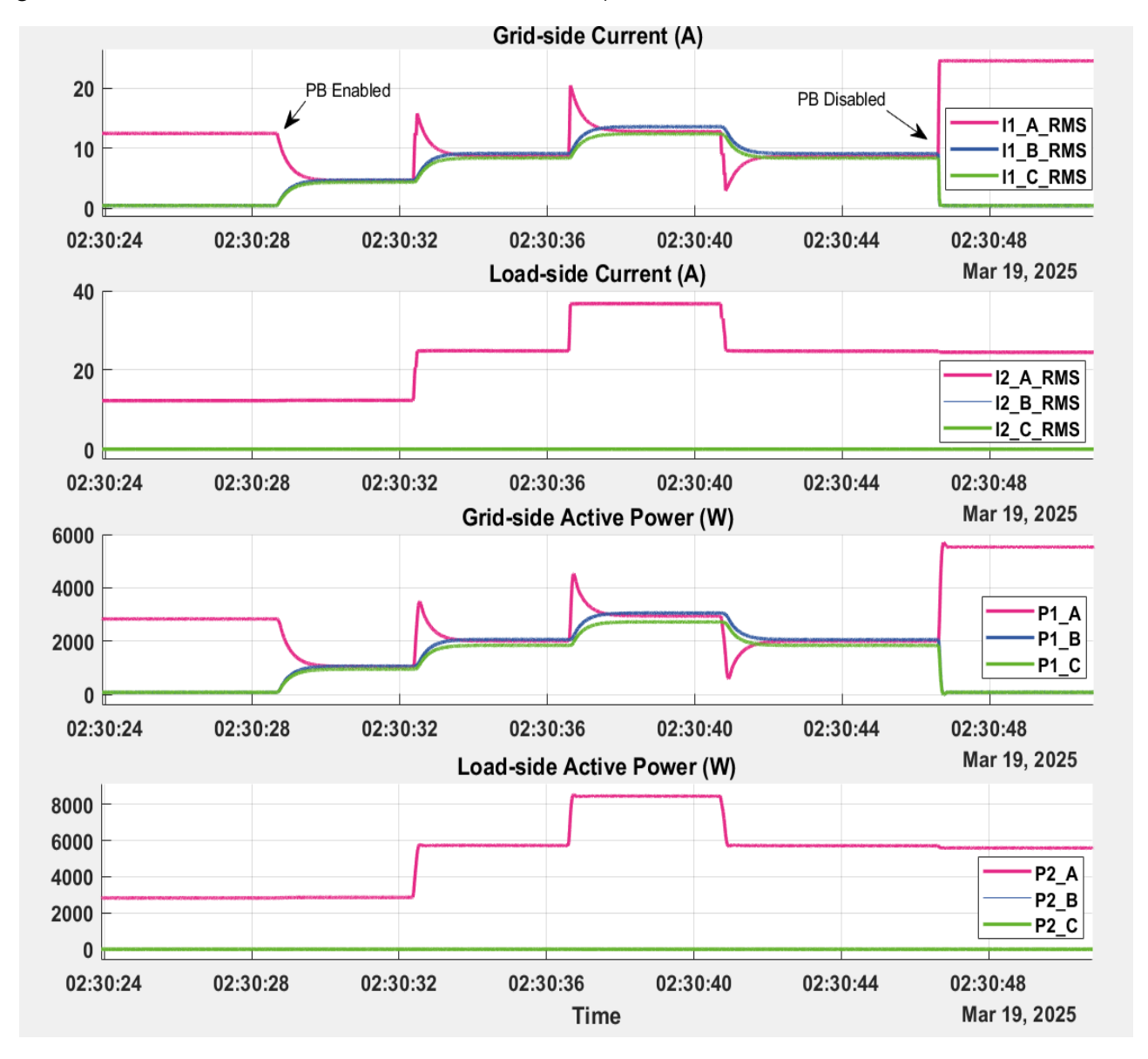
The tests were designed to capture both steady-state and transient performance, assessing the NEx system's response to disturbances originating from either the load side or the grid side.

In addition, the NEx performance under weak grid conditions was also evaluated. This involved testing the system's stability and control behaviour when operating under reduced grid strength, which was emulated by configuring the grid simulator parameters and introducing additional virtual line impedances.

9.3 Phase Balancing Test (PB)

1. Single-Phase Resistive Load

This test evaluated the NEx system's phase balancing (PB) function. A 2.8 kW unbalanced load was first applied to Phase A, resulting in 12.2 A in Phase A, while Phases B and C remained at o A, as confirmed by both load-side and grid-side measurements. After enabling the current balancing function, the load-side current stayed unbalanced, but the grid-side current became balanced at 4 A per phase. The load on Phase A was then increased to 8.4 kW in 2.8 kW steps. The load-side current reached 36 A, while the grid-side current remained balanced at 12 A per phase. Reducing the load to 5.6 kW lowered the grid-side current to 8 A per phase. The test results are shown in Figure 41. When the current balancing function was disabled, the system reverted to an unbalanced grid-side current of 24.3 A in Phase A and o A in the other phases.



Figure~41.~Phase~A~resistive~load~stepped~from~2.8~to~8.4~kW, then~reduced~to~5.6~kW; PB~function~toggled~on~and~off.

2. Three-Phase Unbalanced Resistive Load Test

In this test, an unbalanced resistive load was applied across the three phases: 1.9 kW on Phase A, 3.8 kW on Phase B, and 5.7 kW on Phase C. The load-side and grid-side measurements confirmed the expected unbalanced currents, with Phase A reaching 8 A, Phase B 16 A, and Phase C 24 A. After enabling the current balancing function, the load-side currents remained unbalanced, but the grid-side currents became balanced, with each phase carrying approximately 16 A. The load on Phase C was then increased to 8.4 kW, resulting in load-side currents of 8 A, 16 A, and 36 A for Phases A, B, and C respectively. Meanwhile, the grid-side currents remained balanced at around 20 A per phase. Disabling the current balancing function restored the unbalanced condition on the grid side, matching the load-side currents. These results are shown in Figure 42.

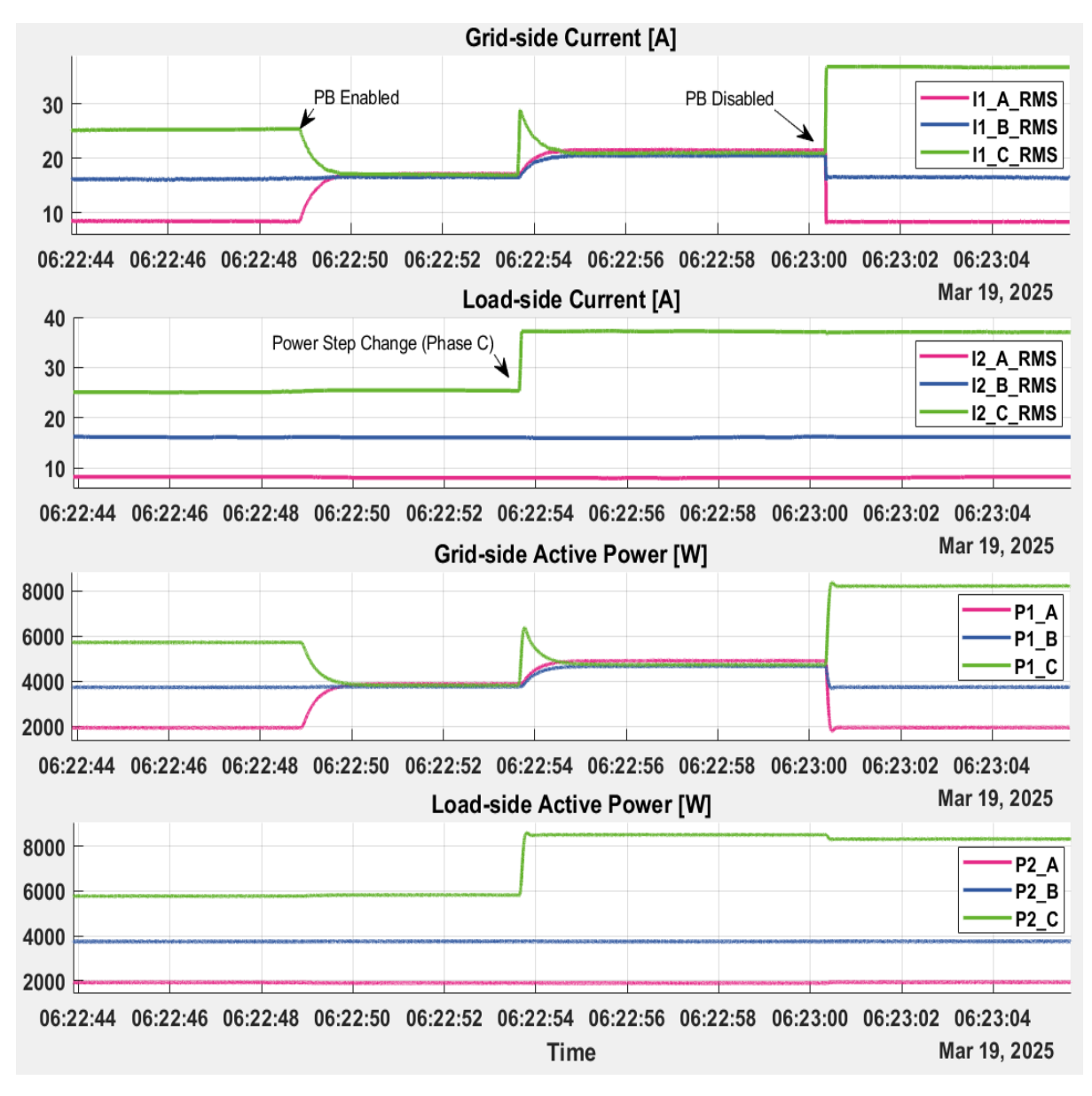


Figure 42. Resistive unbalanced three-phase load (1.9, 3.8, and 5.7 kW) with Phase C increased to 8.4 kW. Phase balancing (PB) enabled and disabled during the test.

3. Phase Balancing Function under Regenerative Load

The system was started, and a PV inverter began generating 4 kW on Phase A. Unbalanced loads of 1.8 kW and 2.8 kW were applied to Phases B and C, respectively. Initial measurements showed Phase A current at 17.4 A (regenerating), Phase B at 8 A, and Phase C at 12.2 A, as recorded on both load-side and grid-side sensors. After enabling the current balancing function, the grid-side currents balanced to approximately 2 to 4 A per phase, while the load-side currents remained unbalanced. Removing the 2.8 kW load from Phase C resulted in balanced grid-side currents increasing to 3 to 5 A per phase, accompanied by negative power flow at the grid side. Disabling the current balancing function restored the unbalanced condition, with Phase A at 17.4 A (regenerating), Phase B at 12.2 A, and Phase C at 0 A. The test results are shown in Figure 43.

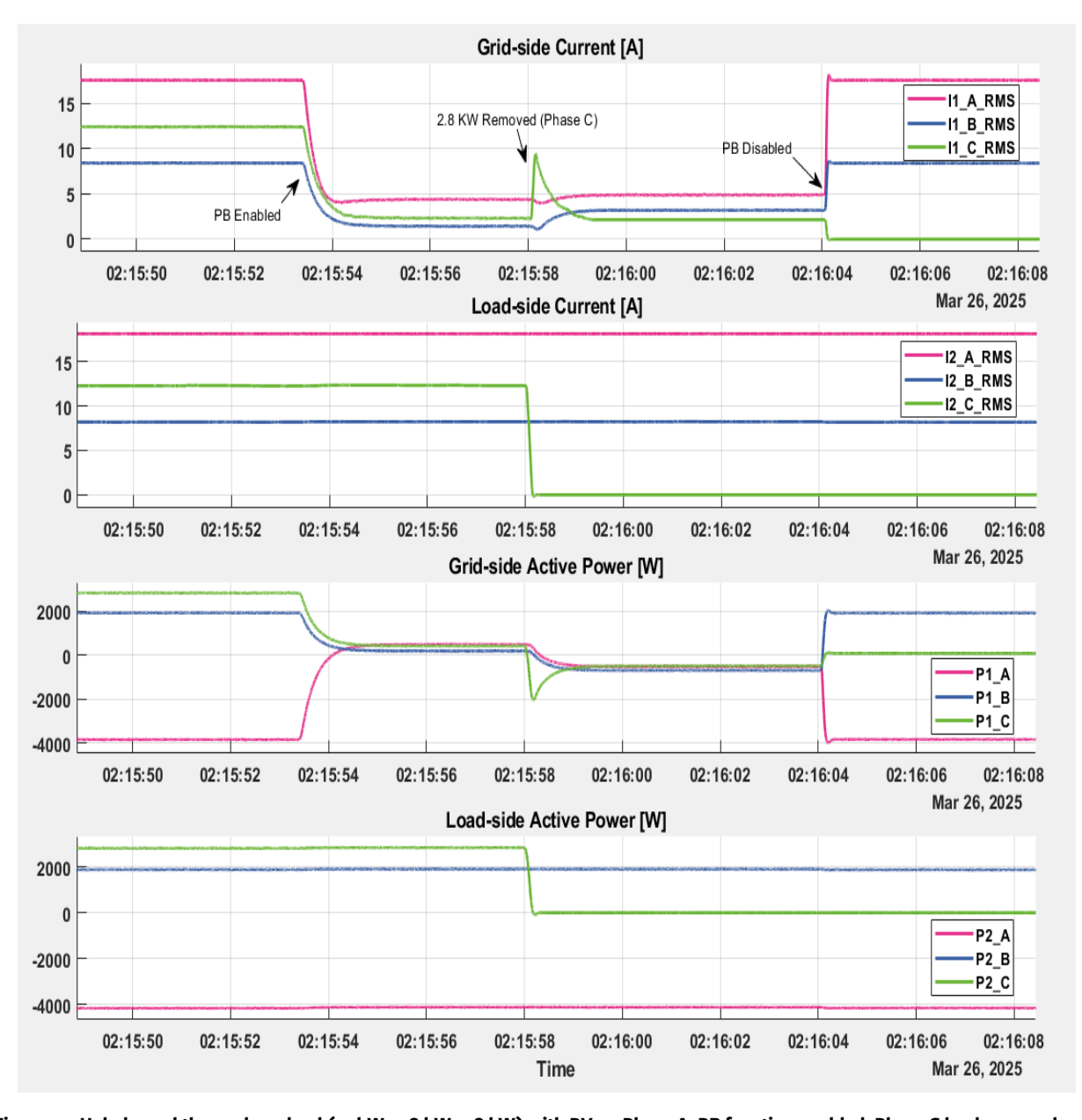


Figure 43. Unbalanced three-phase load (-4 kW, 2.8 kW, 1.8 kW) with PV on Phase A. PB function enabled, Phase C load removed, and PB disabled at the end.

9.4 Power Factor Correction Test (PFC)

The system was started, and a 0.08 H inductive load was applied to Phase A. Both load-side and grid-side measurements showed a power factor close to zero, with Phase A current at 8.5 A and Phases B and C at 0 A. After enabling the power factor correction (PFC) function, the load-side power factor remained near zero, while the grid-side power factor improved to unity. The grid-side currents dropped to nearly zero, indicating successful reactive power compensation. A 3 kW resistive load was then added in parallel on Phase A, resulting in a load-side power factor of 0.82 and a current of 15.5 A, while the grid-side power factor remained at unity with Phase A current measured at 13 A. Disabling the PFC function restored the uncorrected condition, with both load-side and grid-side power factors at 0.82, and Phase A current at 15.5 A. The test results are shown in Figure 44.

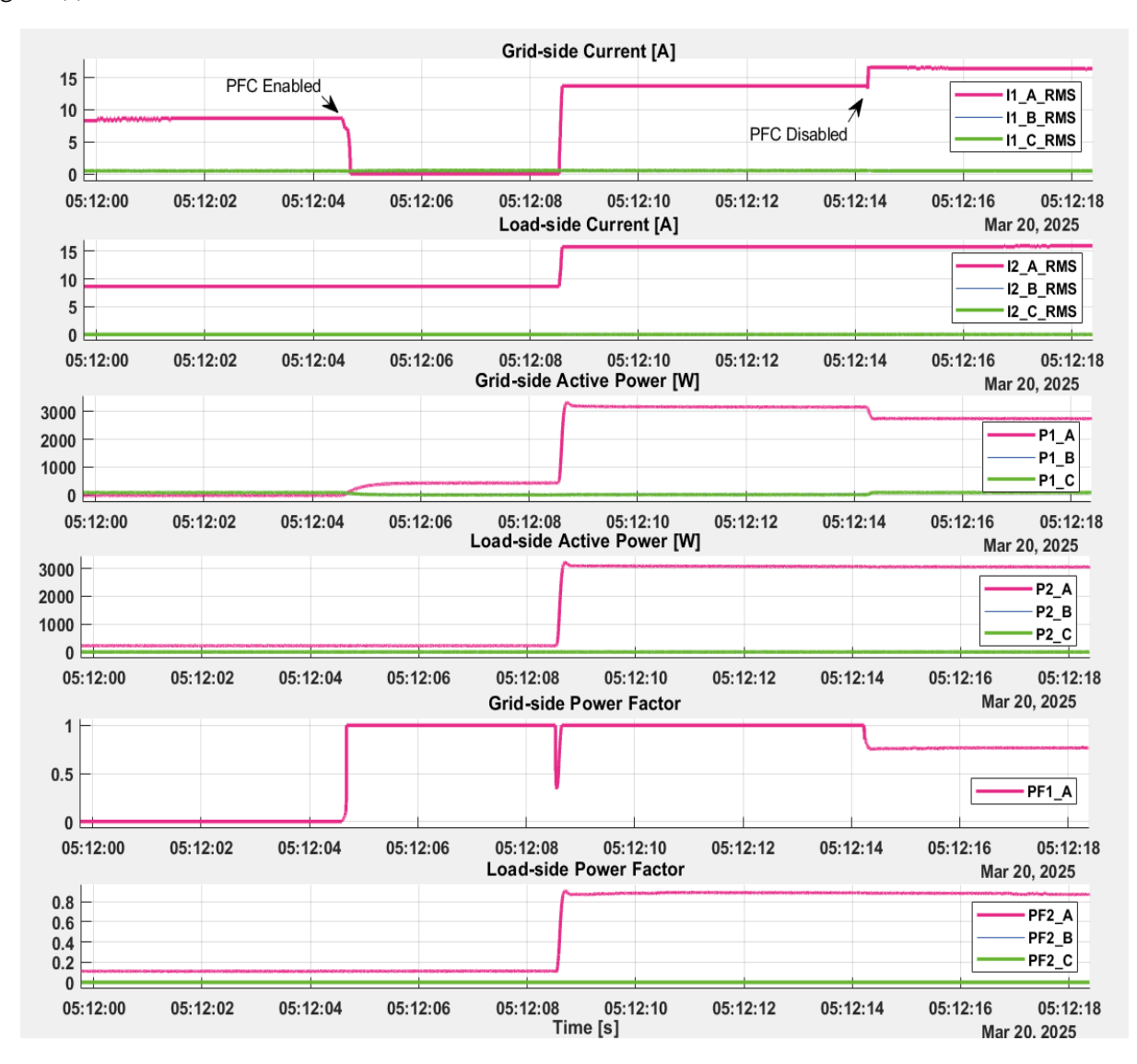


Figure 44. Single-phase inductive load (0.08 H) with a 3 kW resistive load added in parallel. PFC function enabled and disabled during the test.

9.5 Voltage Regulation Test (VR)

Voltage Regulation with Different Grid-Side Phase Voltages

The system was started, and balanced loads of 0.95 kW were applied to each phase. The grid simulator voltages were set to 207 V, 230 V, and 253 V for Phases A, B, and C respectively. Initial measurements confirmed that the load-side voltages followed the grid-side voltages. After setting the NEx voltage setpoints to 230 V on all phases and enabling the voltage regulation function, the load-side voltages were regulated to 230 V per phase, regardless of the unbalanced grid-side voltages. The loads were then increased to 3.8 kW per phase in 0.95 kW steps, with the NEx system maintaining 230 V on the load side. When the voltage regulation function was disabled, the load-side voltages returned to the grid-side conditions, measuring 207 V, 230 V, and 253 V on Phases A, B, and C respectively. The test results are shown in Figure 45.

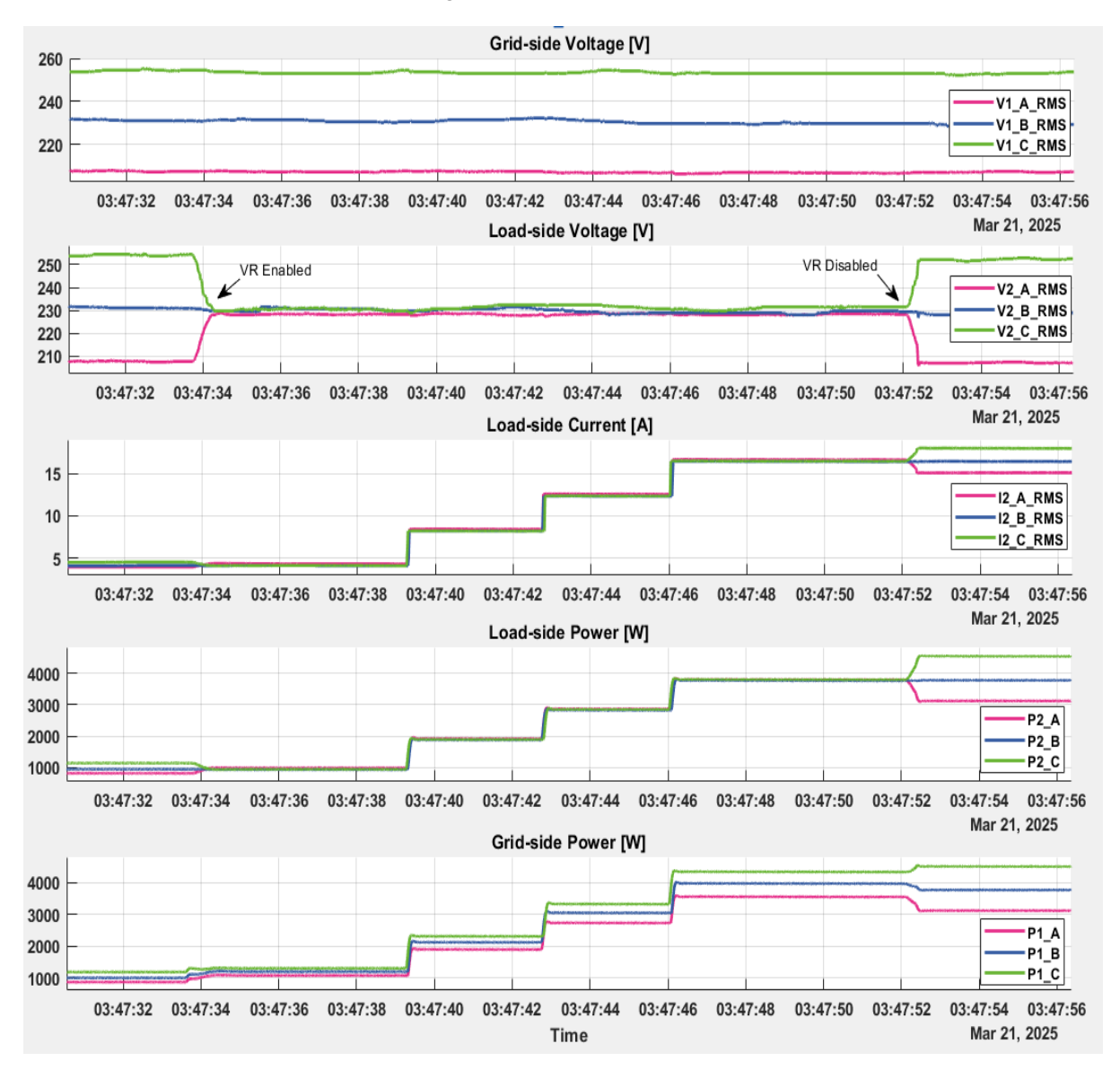


Figure 45. Load-side voltages regulated at 230 V with grid-side voltages set to 207 V, 230 V, and 253 V. VR function enabled and disabled at the end.

2. Voltage Regulation with Different Setpoints per Phase

The system was started, and balanced loads of 0.95 kW were applied to each phase. Both load-side and grid-side voltages were initially set to 230 V per phase. The NEx voltage regulation setpoints were then adjusted to 207 V, 230 V, and 253 V for Phases A, B, and C respectively. After enabling the voltage regulation function, the load-side voltages were regulated to these setpoints, while the grid-side voltages remained at 230 V.

The load on each phase was increased to 3.8 kW in 0.95 kW steps, and the NEx system maintained the set load-side voltages despite the load variation. When the voltage regulation function was disabled, the load-side voltages returned to 230 V for all phases. The test results are shown in Figure 46.

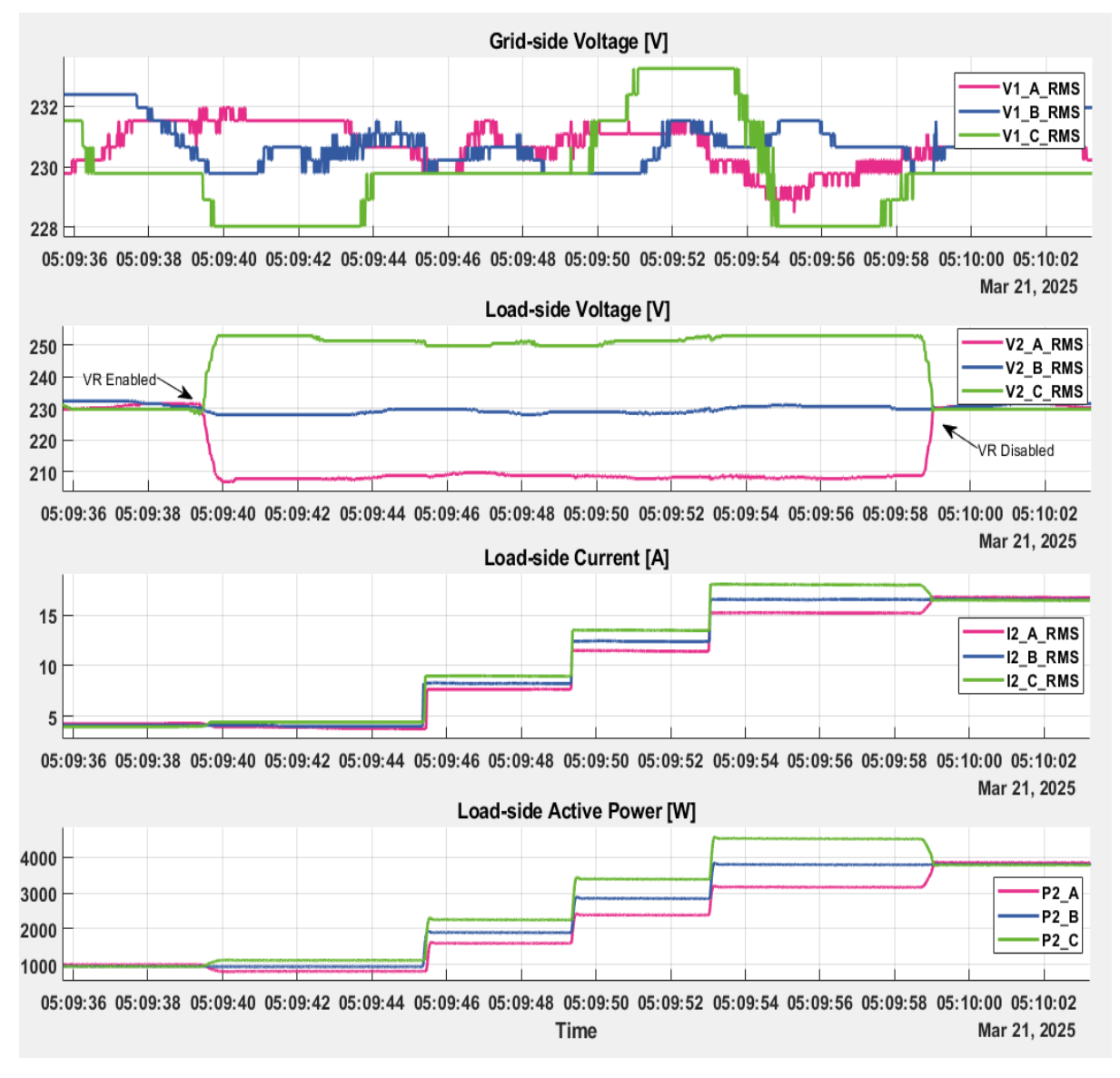


Figure 46. Load-side voltages regulated to 207 V, 230 V, and 253 V per phase. VR function enabled and disabled at the end.

3. Voltage Regulation Test under Grid Voltage Sag and Swell

The system was started, and balanced loads of 3.7 kW were applied to each phase. The grid simulator was set to 230 V per phase, and the initial load-side voltages matched the grid-side voltages.

A voltage sag (211.6 V) and a voltage swell (248.4 V) were consecutively applied at the grid side. The load-side voltages remained stable at 230 V after a short transient in each case, effectively compensating for the grid-side variations. The test results are shown in Figure 47.

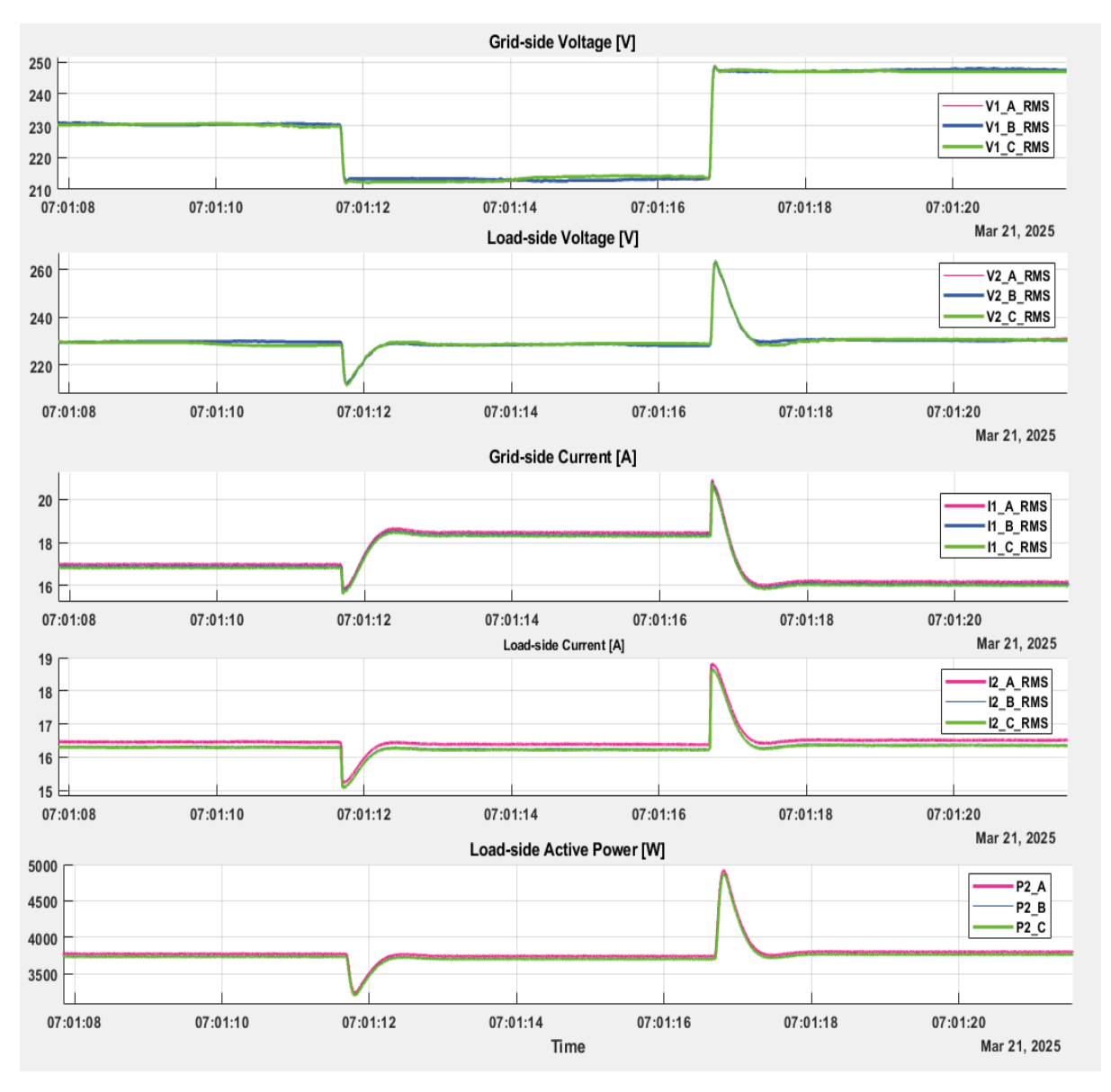


Figure 47. Load-side voltages regulated at 230 V during consecutive 8% grid voltage sag and swell events.

9.6 Multi-Function Tests

Phase Balancing and Voltage Regulation with Single-Phase Load under Unbalanced Grid Voltage

The system was started with the grid simulator voltage setpoints configured to 207 V, 230 V, and 253 V for Phases A, B, and C, respectively. A single-phase resistive load of 7.4 kW was applied to Phase B, resulting in an unbalanced current of 32 A on Phase B, while Phases A and C remained at 0 A.

After enabling the current balancing function, the grid-side currents became balanced at approximately 10.6 A per phase, while the load-side current remained unbalanced. Enabling the voltage regulation function further adjusted the load-side voltages to 230 V on all phases, regardless of the grid-side unbalance. The test results are shown in Figure 48.

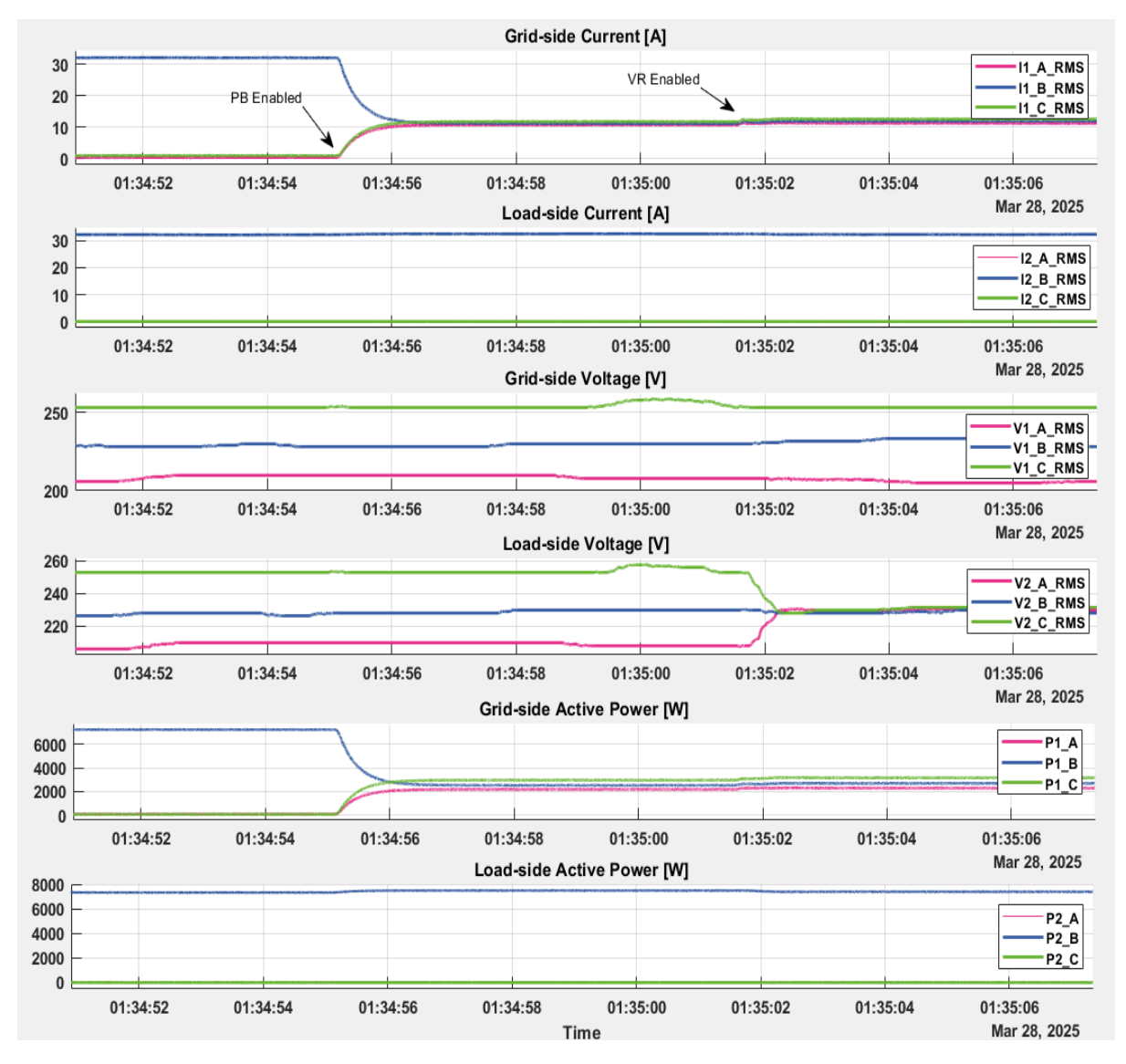


Figure 48. Phase balancing and voltage regulation with a single-phase resistive load under unbalanced grid voltages. PB and VR functions enabled during the test.

2. Phase Balancing, Voltage Regulation, and Power Factor Correction with Unbalanced Load under Unbalanced Grid Voltage

An unbalanced load was applied: a 0.08 H inductive load on Phase A, a 2.8 kW resistive load on Phase B, and a 5.7 kW resistive load on Phase C. The grid simulator voltage setpoints were configured to 210 V, 230 V, and 250 V for Phases A, B, and C, respectively. Initial measurements showed unbalanced grid-side currents of 8.3 A, 12.5 A, and 22.7 A.

After setting the NEx voltage regulation setpoints to 230 V and enabling the voltage regulation function, the load-side voltages were stabilized at 230 V per phase. Enabling the phase balancing function balanced the grid-side currents to approximately 15 A on Phase A and 12 A on Phases B and C. Finally, activating the power factor correction (PFC) function further adjusted the grid-side currents to 12 A on all phases, compensating for the inductive component on Phase A. The test results are shown in Figure 49.

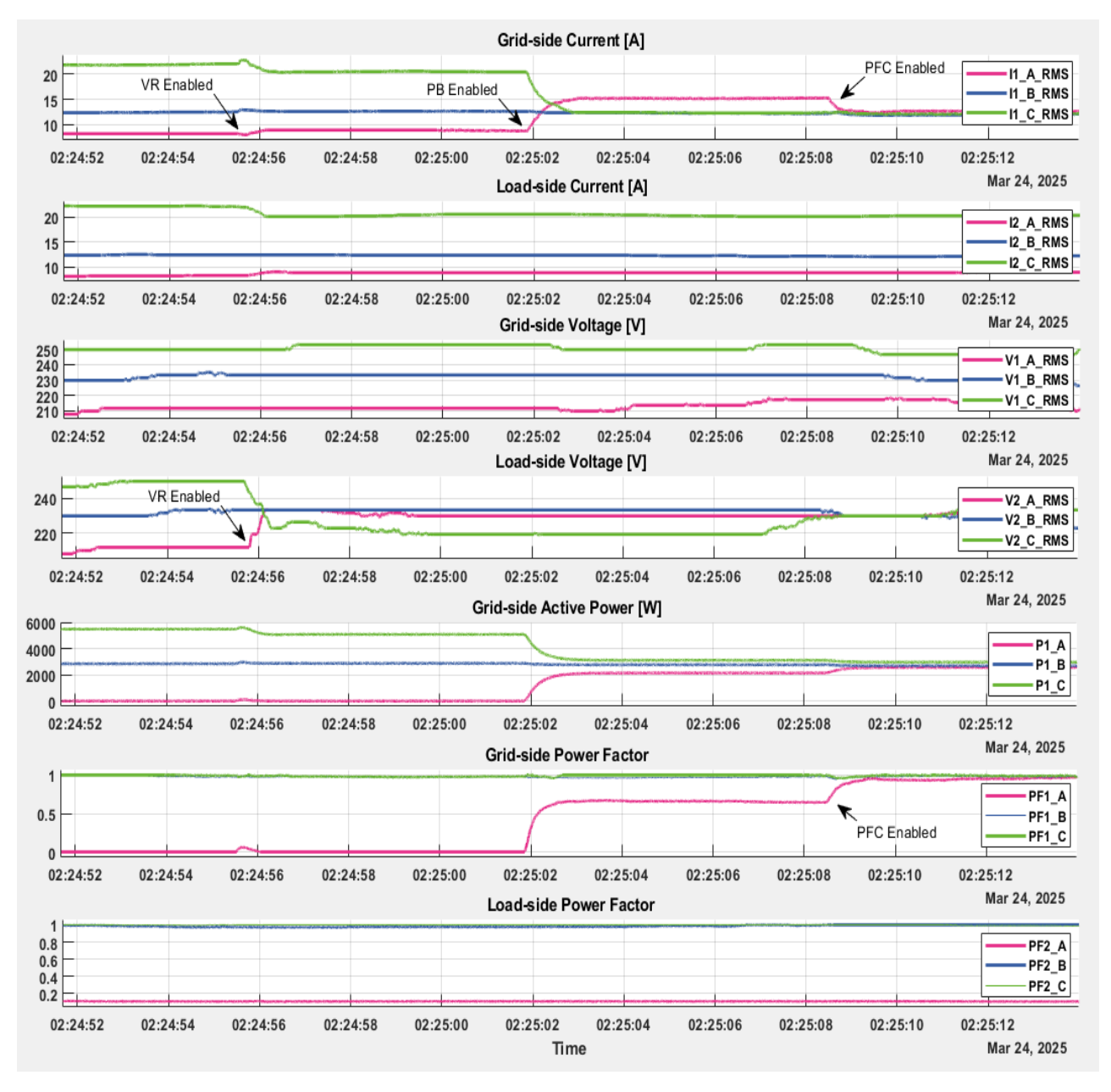


Figure 49. Combined phase balancing, voltage regulation, and power factor correction with unbalanced load under unbalanced grid voltages. PB, VR, and PFC functions enabled during the test.

9.7 NEx Operation Tests under Weak Grid Condition

A weak grid scenario was emulated to assess the NEx system's performance under low system strength and unbalanced conditions. The test simulated a 30 kVA substation connected to a 50 Hz, 11 kV feeder with an X/R ratio of 8.7 and a short-circuit ratio (SCR) of 3:1 (Rg = 0.2 Ω , Lg = 5.6 mH). The distribution transformer was modelled with 0.0427 Ω resistance and 0.849 mH inductance, resulting in a total grid impedance of 0.2454 Ω and 6.45 mH at the 0.4 kV base. The grid simulator voltages were set to 210 V, 230 V, and 250 V for Phases A, B, and C. A single-phase RL load (4.7 kW resistive and 0.16 H inductive) was connected to Phase A, creating unbalanced and inductive loading. After initial measurements confirmed the unbalanced condition, the NEx system's voltage regulation (VR), phase balancing (PB), and power factor correction (PFC) functions were sequentially enabled. This resulted in balanced grid-side currents, regulated load-side voltage at 230 V, and corrected power factor. The test results are shown in Figure 50.

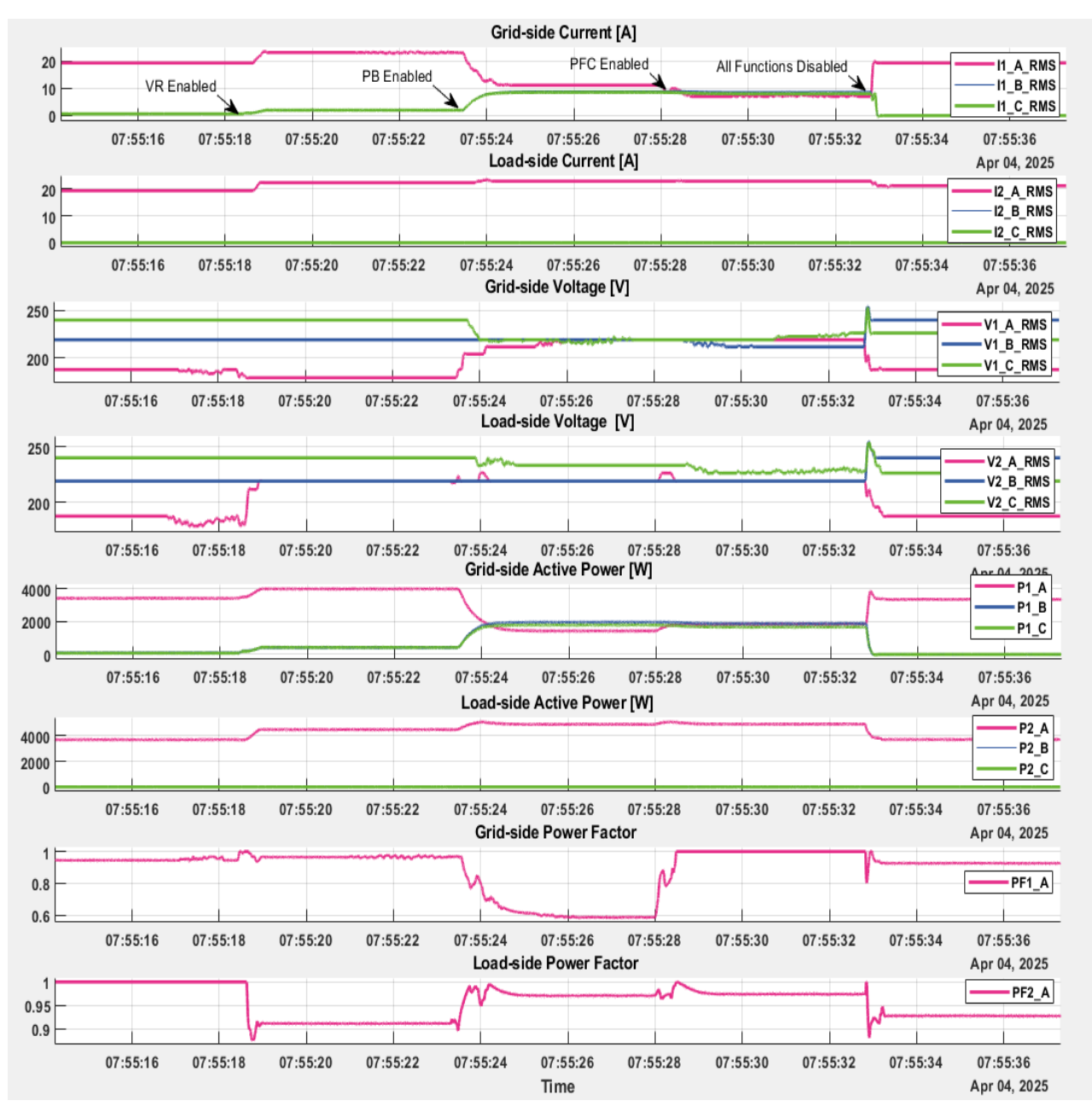


Figure 50. NEx operation under weak and unbalanced grid conditions with a single-phase RL load (4.7 kW resistive + 0.16 H).

10 Conclusion

The findings of this study provide a comprehensive insight into the challenges and potential solutions for enhancing hosting capacity in LV distribution networks amid rapidly increasing CERs. Through a dual approach involving simulation-based scenario analysis and experimental validation, the Network Exchanger was rigorously assessed for its ability to alleviate critical network constraints such as voltage violations, and thermal overloading.

Simulation results drawn from a high-fidelity, distribution model of a suburb in Queensland demonstrate that future CER uptake — particularly rooftop PV installations — will impose significant stress on distribution infrastructure. Voltage non-compliance, unfair customer curtailment, and widespread transformer and cable overloading are projected to emerge as systemic challenges in the coming decades under the Step Change scenario. While EV integration poses less of a voltage risk due to staggered charging behaviours, it still contributes to peak loading concerns, particularly for transformers.

To address these emerging issues, three technologies: STATCOMs, OLTCs, and NEx, were evaluated for their potential to mitigate operational constraints and improve hosting capacity in the year 2035. The comparative analysis revealed that traditional approaches such as deploying a single STATCOM offered limited network-wide benefits, especially in complex LV topologies. Distributing multiple STATCOMs along circuit ends improved performance but still fell short of fully resolving voltage issues. OLTCs, due to their ability to regulate voltage at the transformer level, showed greater promise. However, their inherent limitation in adjusting all three phases uniformly proved suboptimal in networks with significant unbalance, sometimes resulting in under-voltage conditions in specific phases. NEx, on the other hand, demonstrated better technical performance, eliminating all voltage violations in the evaluated areas while also improving current symmetry and power factor. Its phasespecific control, when deployed at the LV transformer, allowed for granular voltage regulation, enabling it to address both over- and under-voltage issues even in highly asymmetrical networks. It is important to note that the correct target voltages would have to be set at the voltage regulation point considering the full downstream network. Hence, it would be important to incorporate near real time measurement data from a limited number of critical nodes to enable a fully decentralized control by NEx. On the other hand, the behaviour of the downstream network could also be analysed by running a series of power flows by the DNSP to determine the appropriate target voltage. The current version of NEx enables a 10% buck or boost at the voltage regulation point on each phase. If the voltage violations of the network can be resolved by inducing a voltage change near the transformer within this range, NEx would be able to resolve all voltage issues in the network. This was the case in the investigated LV areas, as all voltage issues were resolved with the integration of NEx.

Notably, NEx also contributed to lowering transformer loading particularly in cases where higher level of unbalance was recorded. This was achieved through its ability to equalize phase currents, reduce reactive current demand from inverters due to reduction in voltage levels, and actively supply or absorb reactive power to maintain unity power factor. These features collectively reduce thermal stress on transformers and cables, potentially deferring capital-intensive network augmentations. However, replacement or augmentation of cables and transformers would be required if the thermal limits are exceeded by a significant margin.

Experimental validation under workstream 2 further substantiated NEx's real-world effectiveness. Tests under conditions—such as regenerative loading, weak grid operation, and unbalanced demand—confirmed that NEx consistently maintained operational stability. Its integrated functionalities—phase balancing, voltage regulation, and power factor correction—worked in harmony to enhance power quality at the grid interface while preserving customer-side voltage levels.

Economically, NEx yielded the highest annual value when assessed via the CECV metric, which was closely followed by OLTCs. While CECV does not capture the full spectrum of network and customer benefits—such as improved power quality, reduced complaints, and asset lifespan extension—the metric still clearly positions NEx as an advantageous investment among the technologies considered.

In conclusion, the NEx system emerges as a scalable solution capable of addressing the challenges facing LV networks under high CER uptake. Its impact on voltage regulation and thermal loading makes it a highly compelling candidate for trials and deployment in Australian distribution networks seeking to balance reliability, equity, and sustainability in the transition to a decarbonised energy future. It provides benefits to customers such as reduced CER curtailment due to increased hosting capacity, thus improving fairness in CER penetration, and provides benefits to DNSPs through reduced customer complaints about voltage issues. This work also opens up new areas of research, such as field trials to evaluate the performance of NEx on constrained feeders, integration of NEx with DOEs, and long-term reliability studies for interested researchers.

References

- [1] L. O'Neil, L. Reedman, J. Braslavsky, T. Brinsmead, C. McDonald, A. Ward and B. Williams, "Analysis of the VPP dynamic network constraint management.," 2021.
- [2] R. Razzaghi, E. Burstinghaus, Y. Gerdroodbari, M. Hibbert and J. Liu, "Investigation into Voltage Management Technologies for Future Australian Suburban Distribution Networks. Prepared for RACE for 2030 CRC.," 2023.
- [3] Australian Energy Market Operator, "Compliance of Distributed Energy Resources with Technical Settings: Update," 2023.
- [4] P. Pillay and M. Manyage, "Definitions of voltage unbalance," *IEEE Power Engineering Review*, vol. 21, no. 5, pp. 50-51, 2001.
- [5] A. T. Procopiou, M. Z. Liu, W. Nacmanson and L. Ochoa, "Advanced Planning of PV-Rich Distribution Networks Deliverable 4:Non-Traditional Solutions," 2020.
- [6] Australian Energy Market Operator, "2024 Integrated System Plan," 2024.
- [7] P. Graham, C. Mediwaththe and D. Green, "Electric vehicle projections 2024," CSIRO, Australia, 2025.
- [8] P. Graham and C. Mediwaththe, "Small-scale solar PV and battery projections 2024," CSIRO, Australia, 2024.
- [9] "Australian Bureau of Statistics," [Online]. Available: https://www.abs.gov.au/statistics.
- [10] "Australian Bureau of Statistics," [Online]. Available: https://www.abs.gov.au/statistics/industry/tourism-and-transport/transport-census/latest-release.
- [11] W. J. Nacmanson, J. Zhu and L. N. Ochoa, "Milestone 8: EV Management and Time-of-Use Tarriff Profiles," The University of Melbourne, 2022.
- [12] C.-Y. Lee, "Effects of unbalanced voltage on the operation performance of a three-phase induction motor," *IEEE Transactions on Energy Conversion*, vol. 14, no. 2, pp. 202-208, 1999.
- [13] M. M. Haque and P. Wolfs, "A review of high PV penetrations in LV distribution networks: Present status, impacts and mitigation measures," *Renewable and Sustainable Energy Reviews*, vol. 62, pp. 1195-1208, 2016.
- [14] J. Braslavsky, F. Geth, C. McDonald, A. Ward and S. West, "Closed-loop voltage control in a limited-visibility environment," CSIRO, Newcastle, Australia, 2021.

APPENDIX A - NEx QDSL Models

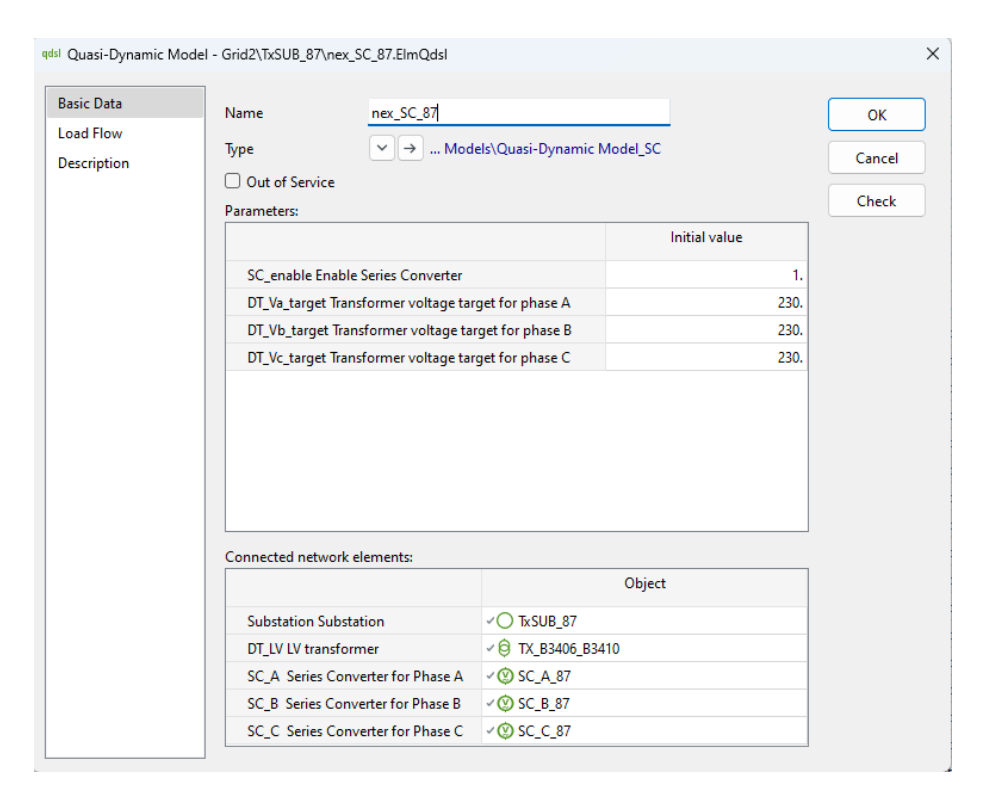


Figure 51. Overview of the QDSL model developed for the series converter.

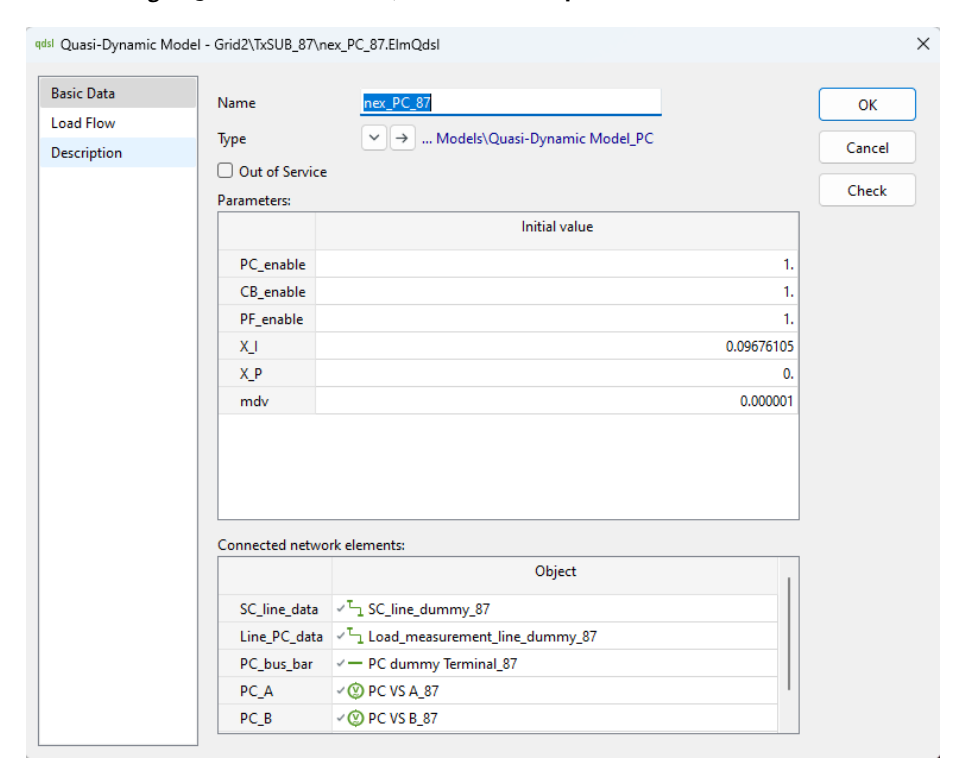


Figure 52. Overview of the QDSL model developed for the parallel converter.

APPENDIX B – Transformer current and power factor data

Table 13. Transformer currents in per unit of each phase at noon in spring under high solar conditions.

	Transformer Current (p.u)														
LV area	BAU			STATCOM			Multiple STATCOM			OLTC			NEx		
	Phase A	Phase B	Phase C	Phase A	Phase B	Phase C	Phase A	Phase B	Phase C	Phase A	Phase B	Phase C	Phase A	Phase B	Phase C
А	0.498	1.120	0.896	0.526	1.155	0.921	0.676	1.280	1.047	0.609	1.168	0.895	0.796	0.795	0.795
В	1.095	1.104	1.500	1.151	1.138	1.546	1.311	1.258	1.679	1.301	1.088	1.503	1.216	1.216	1.215
С	0.821	1.475	0.402	0.954	1.527	0.446	1.068	1.566	0.478	0.990	1.540	0.444	0.876	0.878	0.878
D	1.342	2.167	1.679	1.394	2.192	1.709	1.480	2.244	1.761	1.492	2.208	1.657	1.632	1.632	1.632
E	1.224	1.264	0.523	1.399	1.294	0.595	1.489	1.333	0.677	1.507	1.333	0.561	1.014	1.014	1.014
F	0.976	1.823	0.851	1.104	1.852	0.874	1.105	1.852	0.874	1.272	1.897	0.924	1.240	1.242	1.242

Table 14. Power factor of LV terminals of the transformer in each phase at noon in spring under high solar conditions.

	BAU			STATCOM			Multiple STATCOM			OLTC			NEx		
LV area	Phase A	Phase B	Phase C	Phase A	Phase B	Phase C	Phase A	Phase B	Phase C	Phase A	Phase B	Phase C	Phase A	Phase B	Phase C
А	0.986	0.885	0.870	0.961	0.873	0.851	0.816	0.823	0.772	1.000	0.997	0.998	1.000	1.000	1.000
В	0.989	0.916	0.897	0.976	0.896	0.883	0.919	0.824	0.839	0.999	0.991	0.976	1.000	1.000	1.000
С	0.809	0.929	0.991	0.774	0.910	0.905	0.745	0.895	0.849	0.959	0.987	0.997	1.000	1.000	1.000
D	0.971	0.935	0.924	0.958	0.929	0.910	0.927	0.915	0.885	0.999	0.997	0.997	1.000	1.000	1.000
E	0.926	0.953	0.945	0.904	0.934	0.846	0.876	0.907	0.754	0.998	0.999	1.000	1.000	1.000	1.000
F	0.971	0.960	0.998	0.938	0.951	0.980	0.938	0.950	0.980	0.994	0.995	1.000	1.000	1.000	1.000



www.racefor2030.com.au



